2-1-2015

Fabrication of cellulose acetate /citric acid composite electrospun nanofibers and their antibacterial activities

Mohamed Adly Faried

THE AMERICAN UNIVERSITY IN CAIRO
الجامعة الأمريكية بالقاهرة

School of Sciences and Engineering

"Fabrication of Cellulose Acetate /Citric Acid Composite Electrospun Nanofibers and their Antibacterial Activities"

A Thesis Submitted to

The Biotechnology Master's Program

In partial fulfilment of the requirements for

The degree of Master of Science

By:

Mohamed Adly Saied Faried

Under the supervision of:

Dr. Wael Mamdouh (Supervisor)

Department of Chemistry, The American University in Cairo

December 28th, 2015

The American University in Cairo

"Fabrication of Cellulose Acetate /Citric Acid Composite Electrospun Nanofibers and their Antibacterial activities"|

A Thesis Submitted by

Mohamed Adly Saied Faried

To the Biotechnology Graduate Program

December 28th, 2015

In partial fulfillment of the requirements for

The degree of Master of Science

Has been approved by

Thesis Committee Supervisor/Chair

_____

Affiliation _____

Thesis Committee Reader/Examiner _____

Affiliation _____

Thesis Committee Reader/Examiner _____

Affiliation _____

Thesis Committee Reader/External Examiner

_____

Affiliation_____

_____ _____ _____ _____

Dept. Chair/Director Date Dean Date

Acknowledgements

I would like to thank my supervisor, **Dr. Wael Mamdouh**, for his support during this research work. I've learnt too much from him. His limitless support and close guiding was a cornerstone to accomplish this work, without which it wouldn't be done at this level of professionalism and perfection.

I would like also to thank all my professors in AUC during this program for their great effort in teaching us. I'm proud being a student of you. I'd like to specially thank **Dr. Rania Siam** for her endless support during the whole program. "First impression lasts" and if I'm proud of being an AUC student, a major part of this is because you were my first impression about AUC.

I also like to thank my colleagues and research group for their support and the time we spent together. Special thanks for **Walaa Wahby,** for her time & support in this research work.

I'd like to thank **Rami Wasfi** for helping me in the SEM imaging**, Mr. Mahmoud AbdelMoez**, **Ahmed Omaia** for the FTIR experiments and **Mohamed Rabie**e for the antimicrobial assessment.

My deep thanks for all my family, specially my father **Mr. Adly Saied** and my mother **Mrs. Samia Hassan**. I wouldn't achieve any good thing in my life without your encouragement, support and prayers. I still remember the little stories you kept buying me to make me like reading and learning. Grown as me, those little stories are now references and textbooks. Not only I and my stories have grown, my love to you and my honor you're my parents is the ever growing inside me.

I would also like to thank my beloved wife **Amira Hamdy** for her support and understanding of this period of my life. I apologize being a too busy husband with full loaded agenda that has too limited time to spend with you and with our kids. I wish to enjoy our time together soon. This is extended to my cute daughter, **Roqayyah,** and my brave son, **Hamzah.** I know you are missing your dad and missing the play zones, too. When you grow and read this, I

want you to know I'm trying doing my best for a better future for you and your generation. I wish you too, will keep it up.

I would like also to dedicate this work for youth people in Egypt and everywhere who strive for shaping a better future for their countries and the whole humanity and I'm fully confident they'll do.

Last but not least, my deep thanks to Allah the Almighty for all his blessings on me and all are from him. Without your grace I can't ever do anything or achieve anything. I wish this work will be for the welfare of his creatures and that he accepts it.

Abstract

In an attempt to develop novel natural nanofibers with enhanced antimicrobial activities, polymer composites and nanomaterials play a vital role and exhibit superior properties. Among the different types of nanomaterials, nanofibers have attracted a lot of attention in various fields due to their large surface area per unit mass and advanced mechanical performance. Nanofibers are potential candidates to be used in many fields such as drug delivery systems, nano-sensors, filtration media, and medical applications, etc.

Among theses applications is the use of these nannanofibers in wound management. The development of novel approaches that can enhance wounds healing is always in focus of research. Here in our research, we're trying to develop an effective, safe and economic composite nanofibers with an antimicrobial activity that can have an application as a novel wound dressing that can enhance healing. The main objectives of this thesis are: (i) to prepare and optimize the fabrication of Cellulose Acetate (CA) nanofibers by Electrospinning technique, (ii) to add Citric acid (CIT) as an antimicrobial material to the formed electrospun CA nanofibers and (iii) to finally investigate a possible enhancement in the antibacterial activity of the electrospun composite CA/CIT nanofibers against two different bacterial strains; *Escherichia coli (E. Coli)* and *Staphylococcus aureus (S. aureus).*

In this study, electrospinning technique was used and the experimental parameters were optimized to fabricate uniform CA electrospun nanofibers as well as CA/CIT composite nanofibers to be tested for their antimicrobial activities.

Electrospinning parameters (such as applied voltage, and solution flow rate, distance from the spinneret tip-to-the collector and the solvent system) of CA and CA/CIT blend solutions were varied to be electrospun to choose the most acceptable electrospinning conditions. The most uniform nanofibers were obtained with 5% (w/v) for CA dissolved in acetone at voltage 15 KV, at a tip-collector distance of 5 cm and a solution flow rate of 5mL/hr. Thereafter, these parameters were used with CA/CIT blend solution (5% CA and 10% CIT in acetone) in order to obtain uniform and bead free electrospun CA/CIT composite nanofibers.

After successful preparation of electrospun CA and CA/CIT composite nanofibers, full characterization of the morphology and chemical structural characteristics by using scanning electron microsopy (SEM) and Fourier Transform Infrared (FT-IR) spectroscopy were carried out.

After characterization of the produced CA and CA/CIT Electrospun nanofibers, they were tested for their antibacterial activity with *E. coli* and *Staphylococcus aureus* (*S. aureus)* bacteria, by the dynamic contact method.

Amazingly, the negative control (E.coli) showed an increase in the bacterial growth from zero to 48 hours by 26.5% (i.e. from 1.06 x 10^8 to 2.8 x 10^9 CFU), respectively, while on the other hand, the electrospun CA nanofibers showed only 2.2% increase in the bacterial growth at the same time interval (from 1.09 x 10^8 to 2.4 x 10^8 CFU), respectively.

Similarly, the negative control (S. aureus) showed an increase in the bacterial growth from zero to 48 hours by 28% (i.e. from 1.09 x 10^8 to 3.08 x 10^9 CFU), respectively, while on the other hand, the electrospun CA nanofibers showed only 2.1% increase in the bacterial growth at the same time interval (from 1.1 x 10^8 to 2.34 x 10^8 CFU), respectively.

Moreover, CA/CIT electrospun composite nanofibers showed much higher antibacterial activities (i.e. lower growth rate) than CA electrospun nanofibers and also the negative control against both bacterial strains. So, in case of E-coli, the CA/CIT electrospun composite nanofibers showed only 1.5% increase in the bacterial growth at the same time interval (from 1.3 x 10^8 to 1.98 x 10^8 CFU), respectively.

Similarly, in case of S-aureus, the CA/CIT electrospun composite nanofibers showed only 1.46% increase in the bacterial growth at the same time interval (from 1.15 x 10^8 to 1.69 x 10^8 CFU), respectively.

These results open new avenues for fabricating antibacterial products from semi synthetic materials with superior biomedical activities.

Additionally, trials to electrospin other composites of CA, namely CA/CS & CA/CS/CIT were done, however no nanofibers could be obtained.

Table of Contents

List of all Abbreviations

AFM: Atomic-force microscopy

BSA: bovine serum albumin

CA: Cellulose Acetate

CAB: cellulose acetate butyrate

CDC: centers for disease control and prevention

CIT: Citric acid

CS: Chitosan

CNs: Cellulose nanocrystals

DBC: dibutyryl chitin

DEAE: diethylaminoethyl

DCM: Dichloromethane

DMAc: Dimethylacetamide

DMF: Dimethylformamide

E. Coli: *Escherichia coli*

FTIR: Fourier Transform Infrared spectroscopy

GM-CSF: Granulocyte-Macrophage Colony-Stimulating Factor

HAI: healthcare associated infections

HIV: Human immunodeficiency Virus

HUVECs: human umbilical vein endothelial cells

H-PURET: hydrolyzed poly [2-(3-thienyl) ethanol butoxy carbonyl – methyl urethane]

KV: Kilovolt

MIC: Minimum inhibitory concentration

ml: Milliliter

MRSA: methicillin resistant S. aureus

nm: nanometer

PAN: Polyacrylonitrile

PBA: poly (Butyl acrylate)

PBS: Poly (butylenes succinate)

PDLA: Poly D- lactide

PEG: Polyethylene glycol

PEO: polyethylene oxide

PET: polyethylene terephthalate

PEU: polyester urethane

PHMB: polyhexamethylene biguanide

PMMA: poly(methacrylic acid)

POSS: polyhedral oligomeric silsequioxane

PS: polystyrene

PU: polyurethane

PVA: Polyvinyl alcohol

PVC: polyvinyl chloride

PVP: Polyvinyl pyrrolidone

QCS: quaternary ammonium derivatives of chitosan

SED: Secondary electron detector

SF: Silk fibroin

SHM: sodium hypophosphite monohydrate

SEM: Scanning Electron Microscopy

SLPF: silk like polymer fiber

SSI: surgical site infections

S. aureus: *Staphylococcus aureus*

TDD: transdermal drug delivery

THF: Tetrahydrofuran

UV-Visible spectroscopy: UltraViolet-Visible spectroscopy

WHO: World health organization

ZPD: Zero path difference

ZnO: Zinc Oxide

List of Figures

List of Tables

List of Equations

Chapter 1 **General Introduction and Literature Review**

Chapter 1: General Introduction and Literature Review

1.1 Wounds

Every day many people get injured, from simple injuries in kindergartens to life threatening ones. According to the WHO, 1.3 million people died in the year 2012 accounting for 2.2 % of total morbidity and ranked among the ten top causes of death because of road injuries which is simply a type of wounds (Figure 1.1).

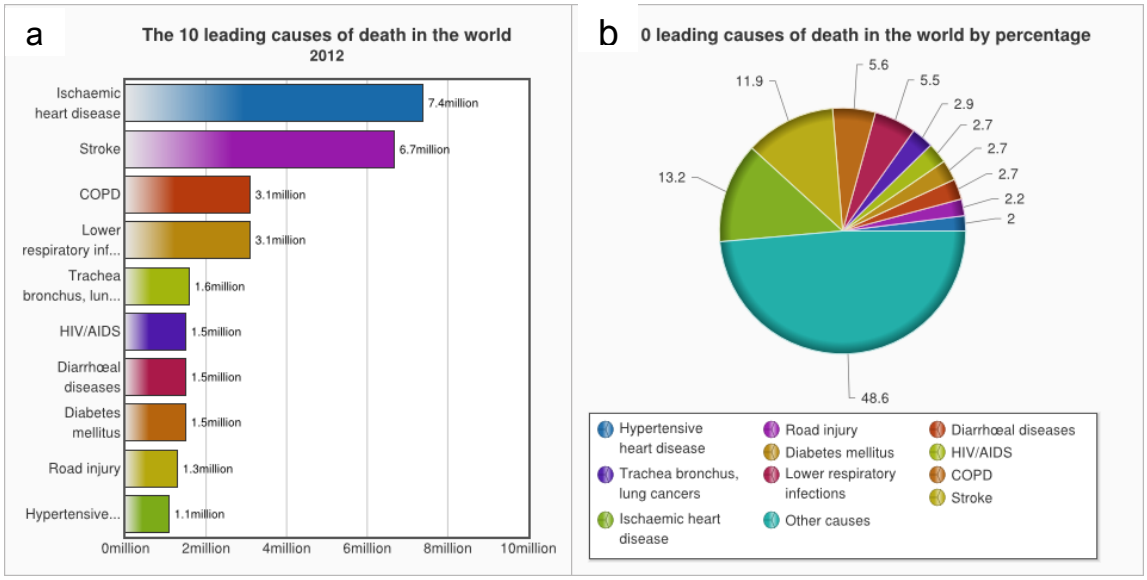

Figure 1-1 The top leading causes of death in the world a. by number & b. by percentage**. (1)**

1.1.1 Wounds classifications

Wounds are defined as: " a breakdown in the protective function of the skin; the loss of continuity of epithelium, with or without loss of underlying connective tissue (i.e. muscle, bone, nerves), following injury to the skin or underlying tissues/ organs caused by surgery, a blow, a cut, chemicals, heat/ cold, friction/ shear force, pressure, or as a result of disease, such as leg ulcers or carcinomas."(2)

Wounds can be classified into different classes based on different factors. First, based on healing nature, they can be classified into acute and chronic wounds. In acute wounds, healing occurs completely within 8-12 weeks leaving minimal scars. (3) However, in chronic wounds, they last

for more than 12 weeks and are not completely healed, and they usually reoccur again. (4) Wounds can also originate from various causes, as for example, mechanical wounds such as abrasions, or penetrations of sharp objects as knives or bullets, or even due to surgical operations. Burning injuries, on the other hand, result from chemical corrosives (chemical burning), electricity or resulting from hot objects touching the skin. The number of affected layers is also used as a classification tool (5, 6) (as shown in Figure 1.2). For example, superficial wounds represent a type of wounds in which only epidermis is affected. Deeper wounds reaching to lower dermal layers with involvement to blood vessels, hair follicles and skin glands are described as partial thickness wounds. While full thickness wounds are those going even deeper to affect the lower fat or deeper tissues layers.

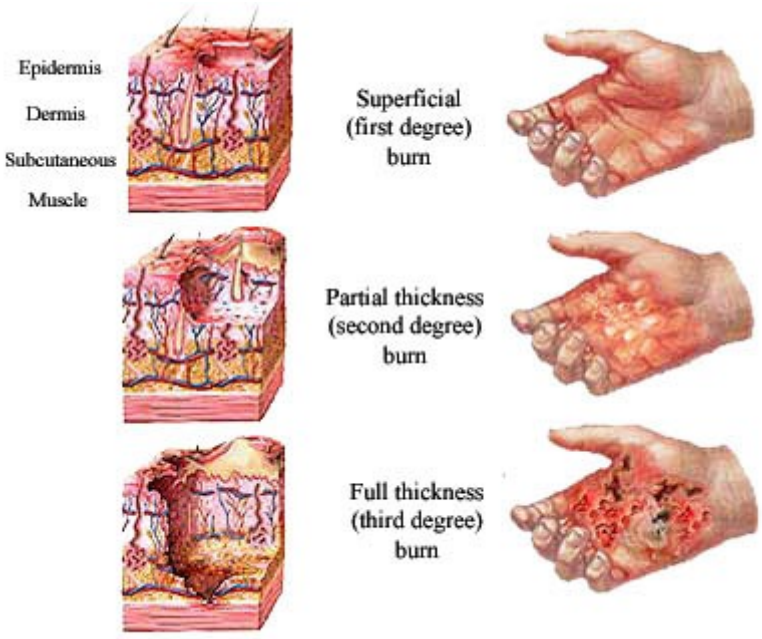

Figure 1-2 Superficial, partial thickness and full thickness wounds. (7)

Another system of classification is based on the wound color in which severity varies with each color. (8) The worst case is the wound appears in black color with black necrotic remnants of blood and skin. On the other hand, wounds appear in yellow color are less severe and represent an indication of infection. The least of severity is the wound appears in red color, which represents a good indication of wound healing. Many other systems of classification also exist and are specific to certain cases, and they all work as a guide for required type and degree of medical care.

A major complication of wound is wound infection. Infection can be defined as: "invasion and multiplication of microorganisms in body tissues, especially that causing local cellular injury due to competitive metabolism, toxins, intracellular replication or antigen – antibody response. (9) Microorganisms are everywhere, on our skin, in air, on sand and objects causing the contamination of the wound which is no way avoidable. Once the skin is broken by wound, the body loses its barrier and the microorganisms find their easy way to the body. The fate depends on both the microorganism and the host. For the microorganism, this varies with its pathogenicity, which means the ability of microorganism to cause disease. (10)

The degree of effects of the disease caused by microorganism defines the other important factor related to microorganism, which is viruelnce. By increasing the pathogenicity and virulence, the outcome is expected to be worse. The ability of micororganism to invade and penetrate as well as to secrete toxins that affect the host is crucial factor in its pathogenicity and virulence. For example, *Pseudomonas aeruginosa* has an outer capsule that protects it from immune cells and makes it more capable of multiplying inside the host and causing serious drawbacks (10). (Figure 1.3) On the other hand, alpha exotoxin secreted by *Clostridium perfringens* can cause very serious gas gangarene.(Figure 1.3) After wound, invasion of the bacteria to the muscular layers occurs, where it keeps multiplying and secreting its toxins. The toxins cause gases formation and destruction of surrounding tissues leading to a life threatening medical condition. (11)

The host status is the second determinative factor of the fate of contamination. Immunocompromized patients are more susceptible for severe implications by wound infections than normal persons. There are various reasons for decreased immunity. Disease like Human immunodeficiency Virus (HIV) and diabetes can cause weakening in immunity. Special ages such as neonates, pediatrics and elder geriatric populations are also more labile. People on therapies that affect their immunity such as those in case of transorgan patients are also on a higher risk than normal population. (10)

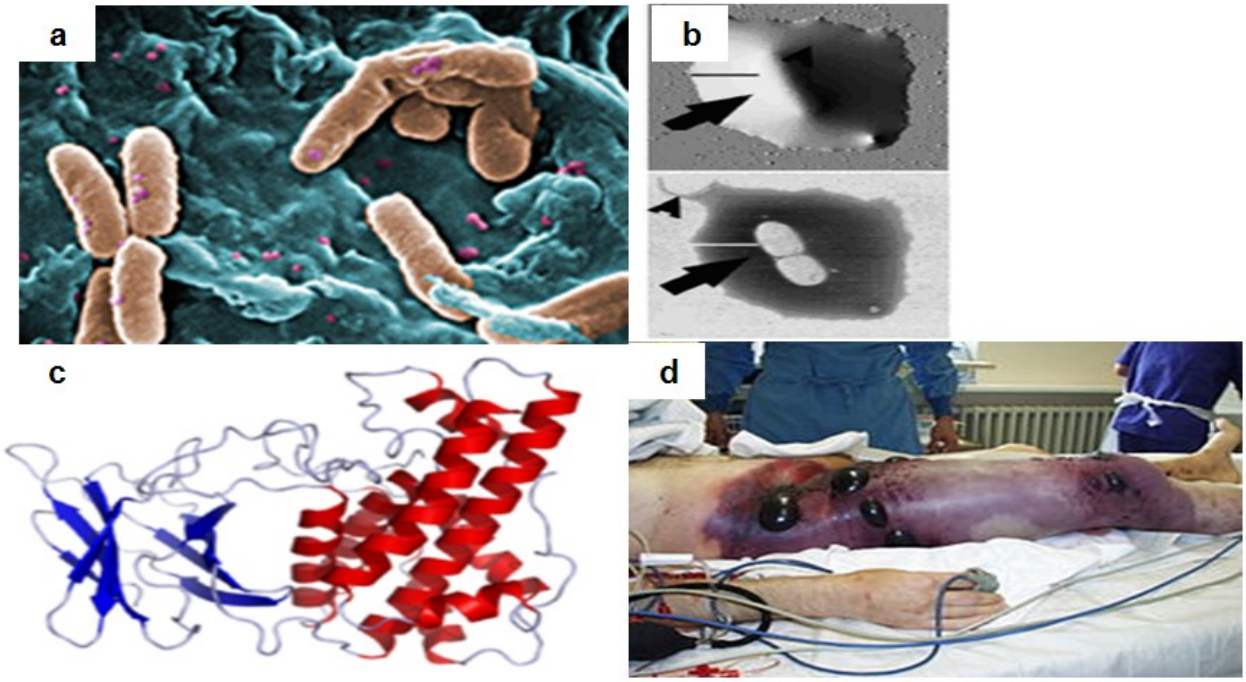

Figure 1-3 a) *Pseudomonas aeruginosa* (12). b) AFM image of capsule structure of *P. aeruginosa*. (13) C) crystal structure of alpha toxin (14) secreted by *Clostridium prefrengins* the causative agent of gas gangrene shown in d.(15**)**

Based on the interaction of invading microorganism and defending host, the fate can be one of three things; contamination, colonization and infection. (10)

Contamination: in which all wounds will be contaminated as mentioned before, however, if the microorganism failed to persist and multiply, it will be completely destroyed, and will not affect the wound and its healing.

Colonization: It happens when the microorganism is capable of a little degree of growth that is not high enough to cause an infection.

Infection: This happens when the microorganism is capable of growing and multiplying, leading to host cellular damage and negatively affecting the wound healing process. (10)

1.1.2 Wound healing

The objective of the wound healing process is the restoration of the integrity of the broken skin and the regeneration of the damaged tissues. It proceeds through various biological actions that can generally be described as haemostasis, inflammation, migration, proliferation and maturation (as shown in Figure 1.4). (16)

Directly after the wound occurs, the blood floods out from injured blood vessels, flushing and cleaning the wound from microorganisms. However, to avoid excessive bleeding, the body works to "plug" the site of cutting and to prevent further loss of blood in the step of “heamostasis” (Figure 1.4a). At first, the platelets in the blood attach to the site of cutting and binds to each other to form a primary clot. Meanwhile, a set of enzymes that are collectively known as the clotting factors, are triggered and work to stop the bleeding in cooperation with platelets. This is mainly mediated by polymerization of a soluble protein known as fibrinogen into a fibrous protein called fibrin. The fibers of fibrin work as a network covering the wound and over which further blood platelets are attached and linked to ensure complete closure of the wound cutting site. (16)

Simultaneous to haemostasis step, the inflammatory step occurs. The latter involves dilatation of the vessels by the effect of physiological chemical compounds histamine and serotonin to allow the passage of phagocyte immune cells to enter to the site of injury. They work to "clean" the site by removing the dead cells (also known as necrotic) through engulfing them. (16)

To add further thickening of the clot and to replace the damaged cells, movement of the surrounding epithelial cells to the site of wound occurs and this step is so called “the migration” (Figure 1.4b). (16)

Together with the restoration of the damaged cells, the body works to restore the damaged circulatory vessels on the wound site. This occurs by growth of the blood and lymphatic vessels into the wound site in the step known as “proliferation” (Figure 1.4c). This step also involves further enforcement of the wound regenerating site by the synthesis of collagen, which works to bridge the wound. (16)

Further strengthening and thickening processes last from a few months up to two years in order to restore the pre injury status and normal skin layer formation and is known as the "maturation step" (Figure 1.4d). (16)

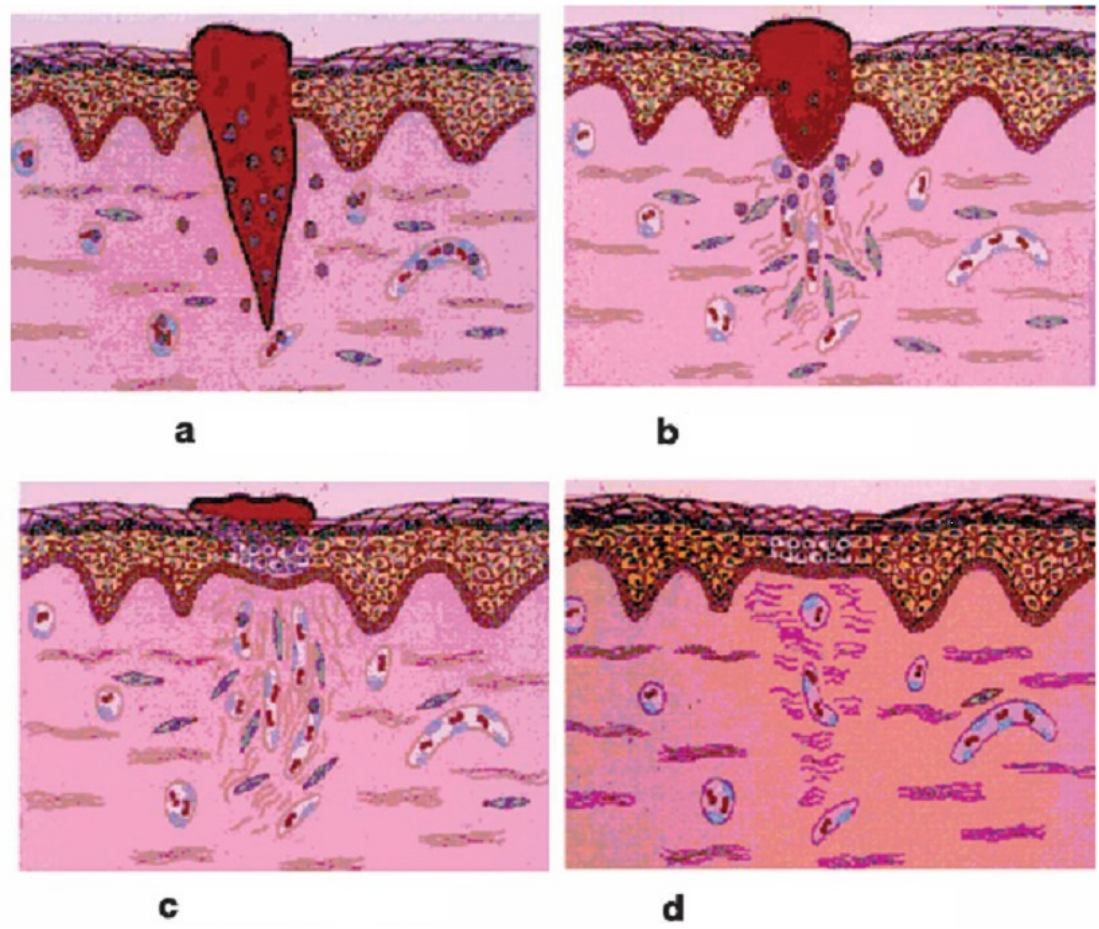

Figure 1-4 The wound healing steps: a) haemostasis and inflammation. b) migration. c) proliferation and d) maturation. (16)

1.1.3 Wound healing management

As wounds vary as mentioned earlier in the wound classification section, the ways to manage them vary too. However, at first, proper cleaning of the wound and removal of any debris or foreign materials should be done. A number of tools are in use to ensure better management of wound healing process. For example, topical preparations are used in liquid form and semi solid form that exert longer contact time with the wound and so exhibit a longer effect. The main purpose of these preparations is to clean and disinfect the wound. Preparations such as povidone

iodine and silver containing formulations such as silver sulphadiazine and silver nitrate are commonly used. (17, 18, 19). On the other hand, formulas in powder form also exist; an example is bacitracin topical formulation. As an advantage of the powder formulas, they are more easily applied to the wound without the need for rubbing it as with semisolid preparations for example. This is of great value to avoid painful application to the injured area (20).

1.1.3.1 Types of wound dressings

A cornerstone of the wound management is the use of wound dressing. Major functions of wound dressing include their use for cleaning the wound, absorbing the blood and extra materials existing at the wound site, preventing wound infection by preveting access of bacteria into the wound, in addition to other functions according to the type of the wound and the type of wound dressing. (21)

Wound dressing can be classified into different classes also by using different systems. One way to classify them is based on the degree they're in contact with the wound. Those which are in direct contact with the wound are classified as “primary dressings”, while those cover the primary one and not in direct contact with the wound are classified as “secondry dressings”. (22)

Another way of classification is based on the function that the dressing performs. In this regard, they can be antibacterial, absorbent, occlusive, etc. (21).On the other hand, the material of the dressing is also used as a classification method. They are then classified as hydrogels, collagen, etc. (23) The most commonly used dressings includes gauzes, cotton, wool and bandages; composed of either natural or synthetic material. An example of the natural materials of bandage is cellulose and cotton wool, while polyamides are examples of synthetic materials. (24, 25)

1.1.3.2 Approaches of enhancing dressings

Various approaches to enhance the performance of wound dressing have emerged in the past few years, particularly; at the level of new materials that have better properties and can lead to better wound healing have been reported. These for example include the use of hydrocolloids, hydrogels, or alginates (as shown in Figure 1.6).

Hydrocolloids (Figure 1.6b) are made of materials that have the ability to form gel in combination with other materials that work as adhesives and elastomers. These materials include carboxymethylcellulose (CMC), pectin & gelatin. (26) Upon contact with wound exudates, a gel of the material is formed accompanied with a change in its physical structure and making it more permeable to water and air. (27)They have little degree of pain when removed from the wound area and are, therefore, advantageous in the treatment of wound of children in particular.(28) However, the left behind fibers in wound area together with its low permeability of water vapor that cause decrease in supplied oxygen to the healing wound are considered as disadvantages of its use. (29)

On the other hand, hydrogels are made from synthetic polymers that are cross-linked to each other while entrapping large volume of water within its matrix (Figure 1.6a). The materials used in their fabrication include poly(methacrylates) and polyvinyl pyrrolidine (PVP). (30) They are characterized by their non-reactivity to biological material, their good permeability to nutrients and their low irritability. (31) Being non-adherent and giving a cool sensation to the skin, they are highly comfortable to the patients.(32) However, their low ability to absorb exudates and the resultant accumulation of fluid that enhances microbial growth are considered main limitations to their use. Another disadvantage also is their low mechanical strength leading to non-easy handling by the patients. (33)

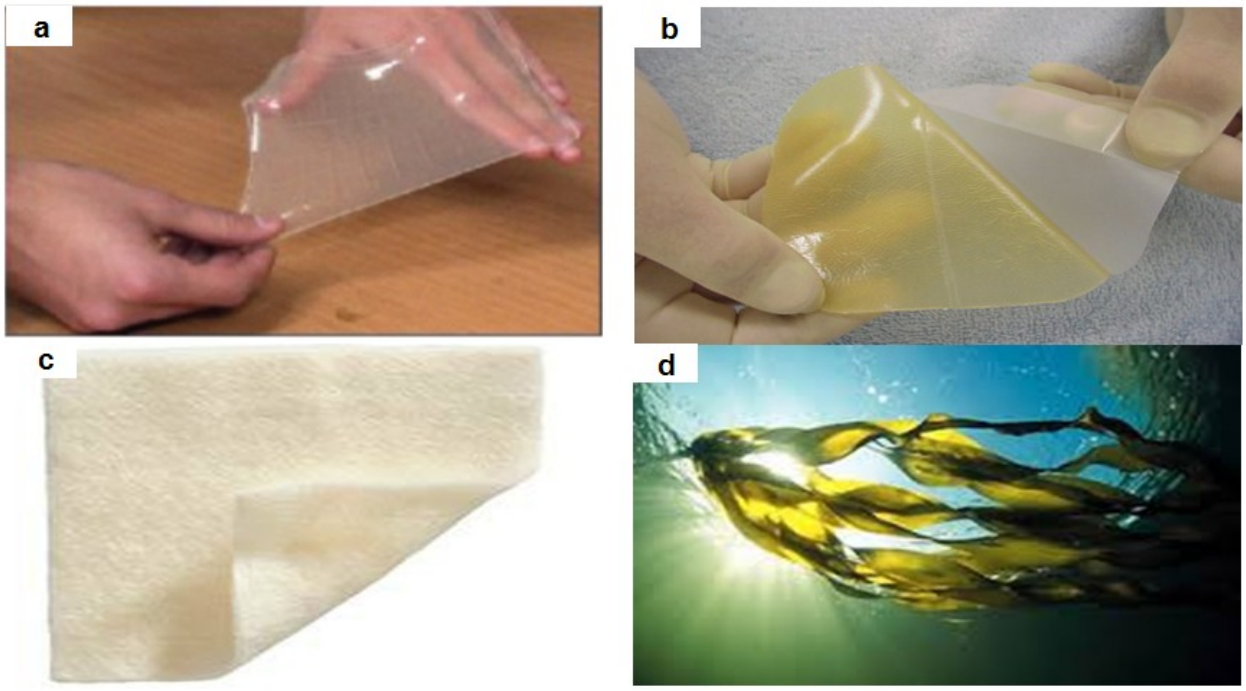

Figure 1-5 New materials in wound dressings. a) Hydrogel. (34) b) Hydrocolloid. (35)c) Alginate (36) and d) Seaweed from which alginic acid is obtained. (37)

Alginates (Figure 1.6c) are also a new type of materials used to enhance the performance of dressings in wound healing. They are composed of calcium and sodium salts of aliginic acid. They are characterized according to their high absorbing ability as they form a gel material upon exposure to wound exudates. This prevents microorganisms attaining their optimum moisture condition and protecting the wound from infection accordingly. The role of calcium has been addressed by many researchers (38, 39, 40, 41). The calcium ion was proposed to exert a pharmacological action enhancing the wound healing. It was suggested that it has a role in heamostasis step and in activation of macrophages and fibroblasts. Among the advantages of its use is the biodegradability, ease of removal and good solution retainability have been reported. (42) However, being dependant on moisture conditions, it has been reported that they are not suitable for dry wounds and where high necrotic tissue exist as it can lead to dehydration and retard the wound healing.(43)

Moreover, the use of a medicated dressing that can deliver a local wound healing drugs is another important approach.

The drugs used include antibacterial drugs (44, 45, 46), growth factors (47) and supplements (48). The role of antibacterial loaded dressings to prevent infection and treating it if any is obvious and clear. Those include growth factors as a loaded drug target the underlying physiological healing process. This leads to enhancing the formation of new blood vessels instead of the damaged ones (angiogensis), enhancing cells proliferation and migration for better healing. (47, 49) As an example is the use of granulocyte-macrophage colony-stimulating factor (GM-CSF). It is found to play a major role in wound healing and its deficiency leads to delayed and improper healing of the wounds. (50) The Supplements loaded dressings on the other hand is another way, which provide the wound with the required vitamins and minerals that affect the wound healing process.(48) These include Vitamins C, A and E, in addition to zinc and copper. The role of vitamin C, for example, is well known in helping of collagen synthesis, and in enhancing the immunity. (51) While the antioxidant and anti inflamatory role of Vitamin E makes it useful in wound treatment. (52)

1.2 Nanotechnology and Nanomaterials

Nanotechnology is a multidisciplinary science with wide range of applications that affects almost every field of life. The term "nano" refers to a scale of measuring where 1 nanometer equals to 10-9 meter. (Figure 1.7) The materials at the nanoscale have unique properties regarding the extremely high surface area. Additionally some other properties are acquired based on the material's type that differs in the nanoscale than in bulk such as electric, optical and magnetic properties.

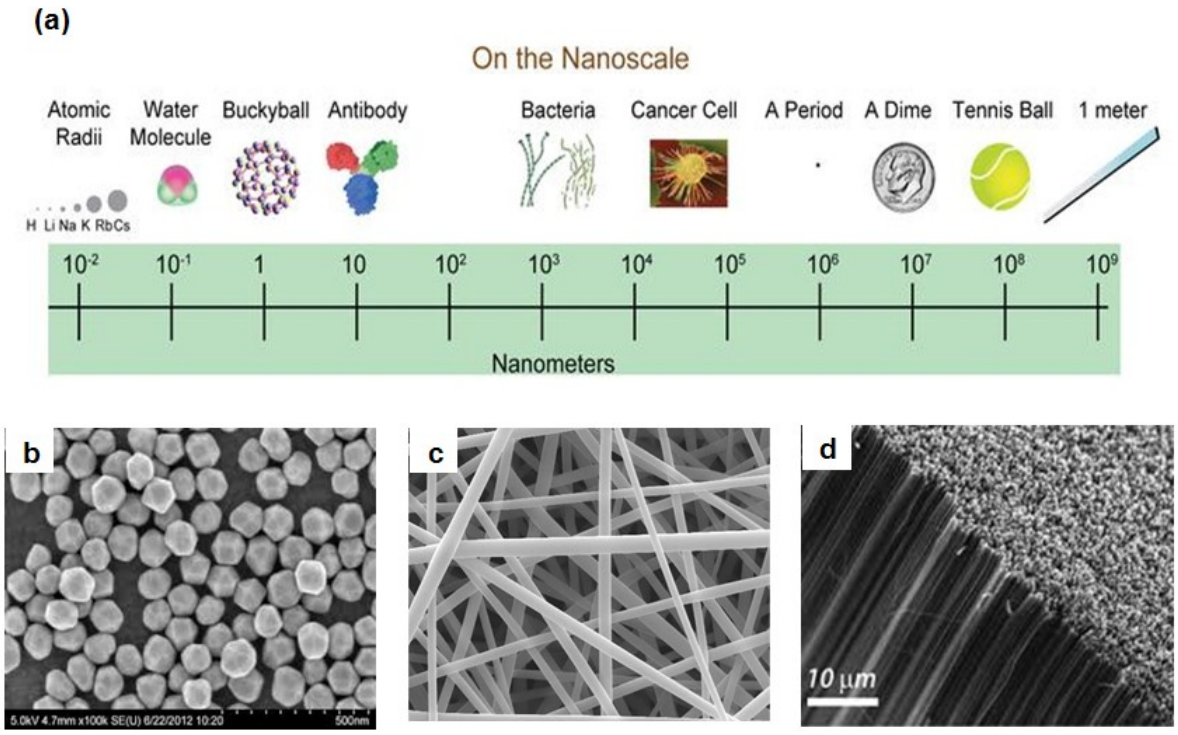

Figure 1-6 a) Illustration of the scale of materials (53) .b) c, and d) Different forms of nanomaterials ranging from nanpoarticles, nanofibers and nanotubes, respectively. (54, 55, 56)

Nowadays, a large number of publications have been reported on the study of new nanomaterials and their properties at the nanoscale and also to fabricate new materials with new properties that can have beneficial applications (as illustrated in Figure 1.8). The applications of Nanomaterials in many fields are countless such as chemical and catalysis applications, drug delivery and medical applications, optical and magnetic applications, sensors applications and many others. (57)

1.2.1 Applications of nanomaterials

There are various forms of nanomaterials, for example, they can exist as nanoparticle; aggregates, nanotubes; and nanofibers. (Figure 1.7) They can even have many other forms and all depends on the used material and the method of synthesis or fabrication.

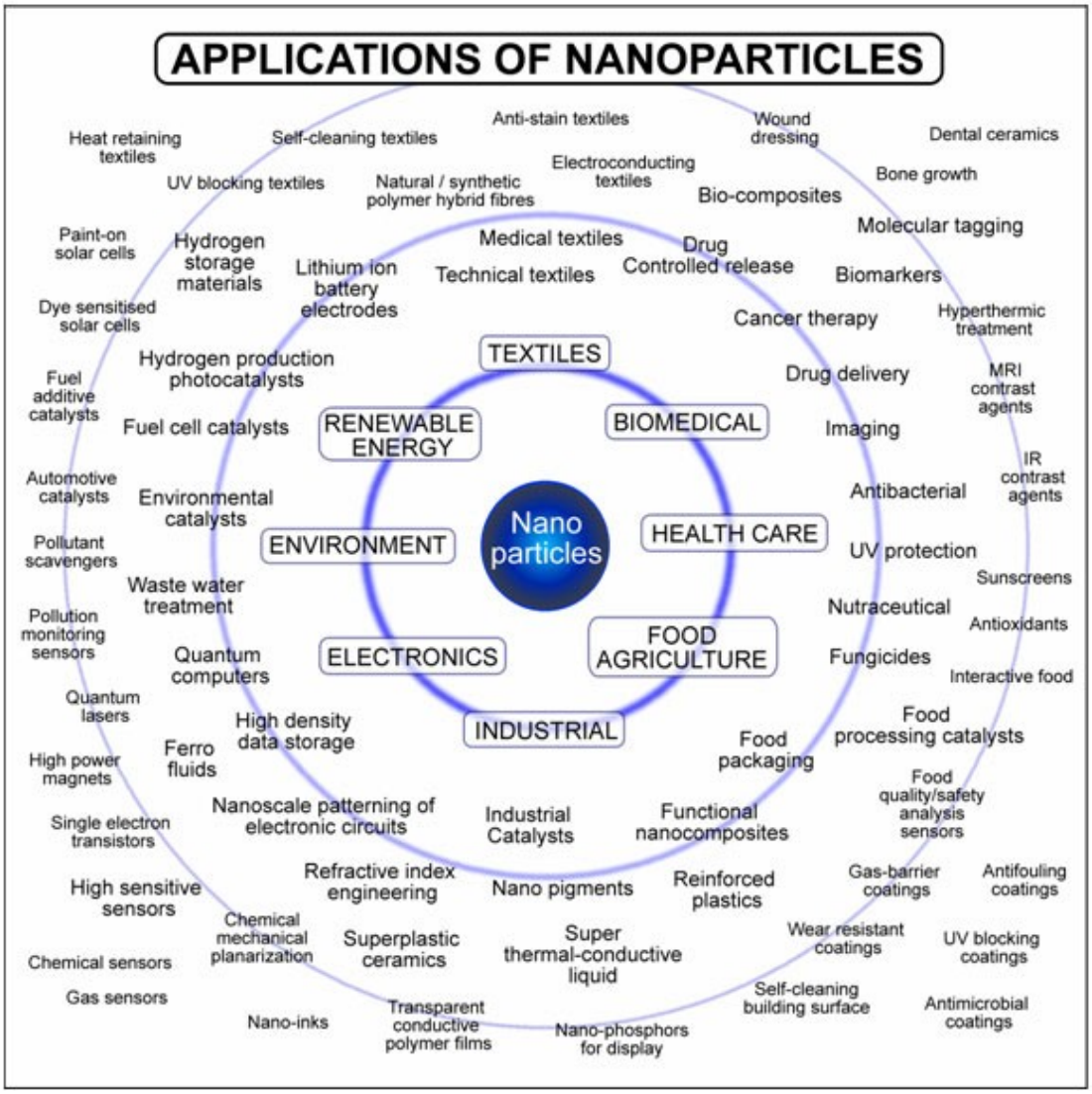

Figure 1-7 Some of the applications of Nanotechnology in various fields. (57)

1.2.2 Fabrication of Nanomaterials

To synthesise a nanomaterial, two common approaches have been proposed. One is known as "top-down" approach in which a material is broken down until it is in the nanoscale. The second approach is known as "the bottom-up" approach in which assembly or aggregation of atoms and molecules together to form a structure in the nano-range occur.(58) The methods of the later approach include, but not limited to, Sol- Gel technique in which a precipitation of material is induced with controlling the growth of the particle size to be in the nanoscale. (59) In addition, another method includes the use of surfactant as soft mold into which aggregates of the material of interest is contained and formed in the nano-range. (59) Furthermore, hard templates are also used and by further deposition of the material inside the mold, a nanomaterial with the complementary shape of the used mold is then formed. These various methods can all obtain different nanomaterials of different sizes and shapes. (59)

Nanofiber is an important class of nanomaterials, in which a thin film in the nanoscale is formed. A wide variety of nanofibers have been developed and reported in a wide range of applications for example in textile industry, filtration and biomedical applications. In order to obtain nanofibers, number of methods have been used such interfacial polymerization (60), melt spinning (61), solution spinning (62), chemical vapour deposition (63), template synthesis (64) & Centrifugal Spinning (65) among which the use of Electrospinning technique has been reported to have many advantages as will be discussed below.

1.3 Electrospinning technique

Electrospining technique has been reported to be highly effective method to fabricate nanofibers. The main parts of the electrospinner setup are shown in Figure 1.9 and include: i) A syringe pump, ii) a plastic or glass syringe, iii) high voltage generator, and iv) stationary plate or rotating drum collector. First, the polymer of interest is fed into the syringe which is installed in the syringe pump, then the needle of the syringe is connected by a crocodile wire to the high voltage generator, and the distance from the spinneret tip to the plate or rotating drum collector is adjusted. (66)

The solution flow rate of the polymer solution can be controlled through the syringe pump. The high voltage power supply connected to the needle of the syringe leads to charging of the polymer material. At a critical point, the electric repulsion forces exceeds the surface tension forces between the polymer molecules leading them to be ejected out of the syringe to an oppositely charged plate or rotating drum collector into which the other terminal of the high voltage power source is connected. This is known as the Taylor cone effect. The travelling polymer solidifies in its way in air due to rapid evaporation of the solvent leaving the polymer in a form of a very thin fiber in the nano-range to be deposited on the collector. (66)

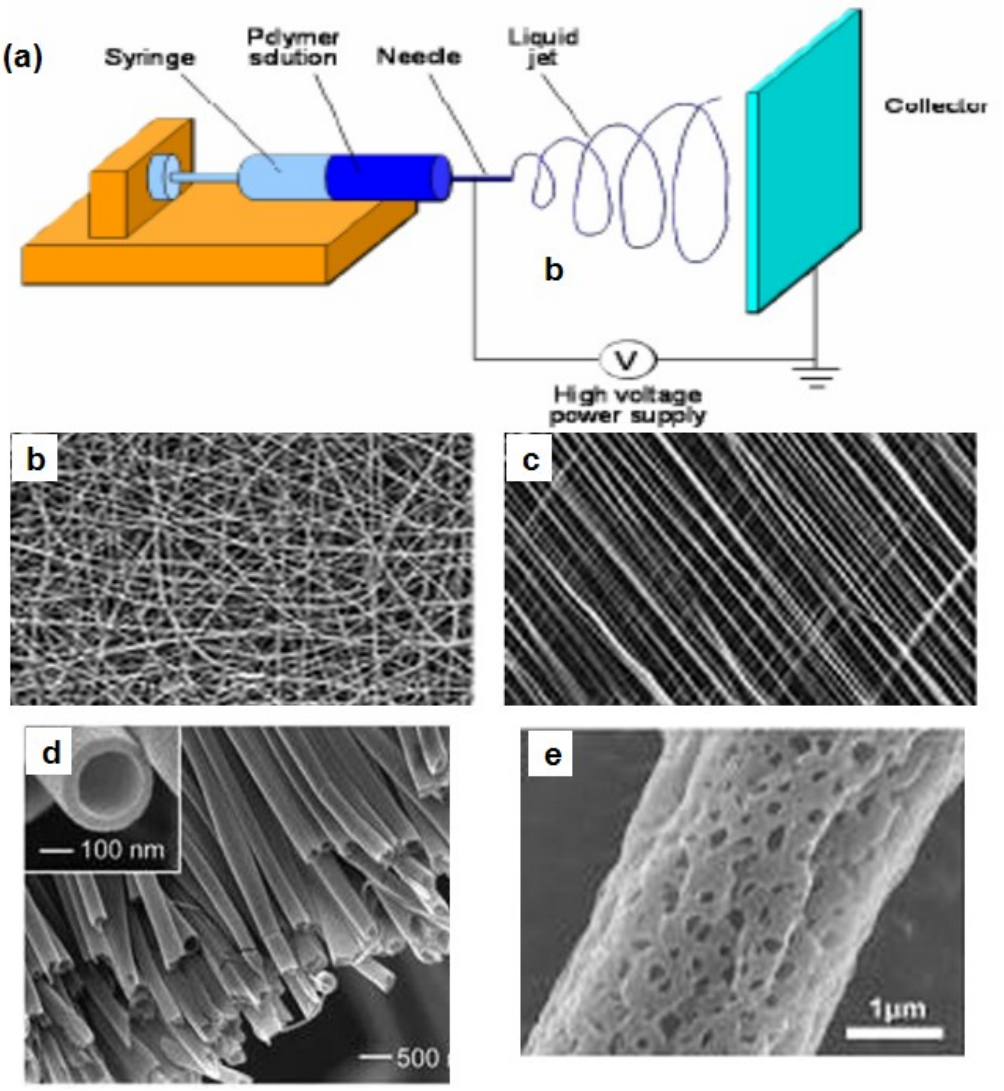

Figure 1-8 a) schematic illustration of the main components of the Electrospinner setup. (66), Various forms of electrospun nanofibers; b, c) non-woven versus aligned (68) , d) hollow fibers (67) & e) porous fibers. (67)

Due to the simplicity of this technique, more options have been added by many researchers depending on the desired conditions. For example, a heating chamber and heating spinneret could be implemented into the setup when heating of the polymer solution to be electrospun is required. Moreover, a circulating (rotating) drum collector instead of a stationary plate type could also be used in order to obtain more aligned nanofibers instead of mesh structures. In addition, a particular spinneret that allows co-axial electrospinning of more than one polymer solution at the same time could also be used that leads to the formation of a nanofiber surrounding another one inside. This helps in spinning low spinnable polymers and can also be used in the formation of hollow nanofibers by further removal of the inner fibers leaving the outer in a hollow tube like fiber. (67)While in its way from the needle apertures to the collector, the polymer is subjected to three main forces; a) the repulsion forces between the polymer molecules due to the charges applied by the high voltage power supply, b) the attraction forces with the oppositely charged collector and c) the surface tension forces intrinsic of the polymer. The combinations between these three forces play a major role in controlling the fiber's features. (69)

Generally, some factors have been reported to affect the morphology of the electrospun nanofiber. These can be categorized into (i) process parameters and (ii) polymer solution parameters. (69)

1.3.1 Process parameters that affect the morphology of electrospun fibers

These parameters are related to the setup of the electrospinning process and can be summarized into:

- Applied voltage
- The distance between the needle aperture and the collector.
- Polymer solution flow rate
- The chamber environmental conditions.

Each of these parameters is discussed in details in the following section.

1.3.1.1. Effect of voltage

The applied voltage has been reported to be one of the most important factors which affects the charging of the polymer particles, as well as the charge of the collector plate, hence it has great effect on the fiber's morphology. Generally, increasing the applied voltage leads to higher flow and deposition of the electrospun nanofibers on top of the collector.

Megelski *et al.* investigated the effect of applied voltage on the diameter of the formed nanofibers of polystyrene (PS). It was observed that the PS fiber size decreased from about 20 μm to 10 μm upon increasing the applied voltage from 5KV to 12KV (70). Buchko *et al*. also reported on the same observation while working on silk like polymer fiber with fibronectin functionality (SLPF) as shown in Figure 1.10. (71)

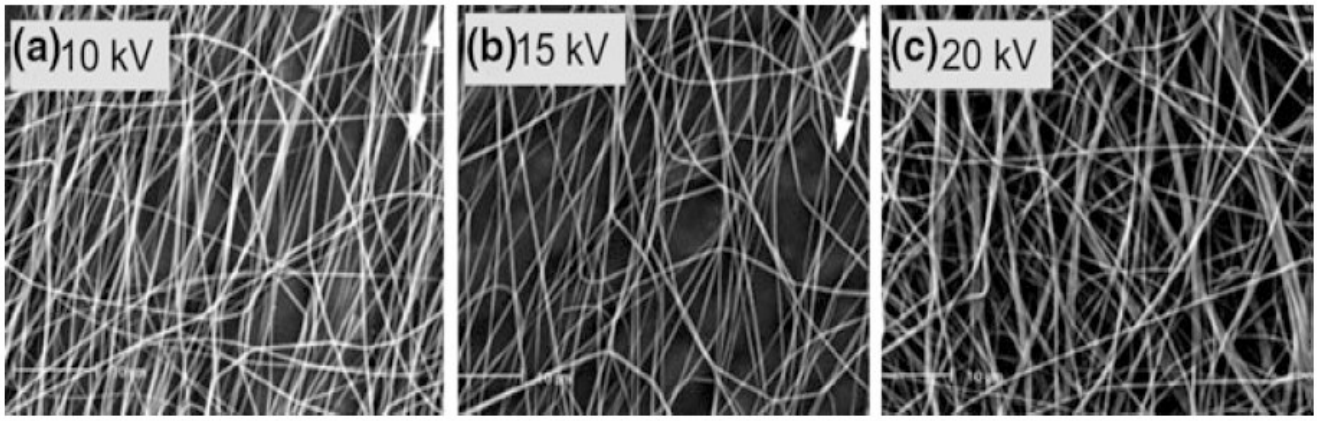

Figure 1-9 SEM images of electrospun SPLF fibers at different applied voltages, where the average diameter decreases from 344 to 331 then to 323 nm with increasing applied voltage from 10 to 15 then to 20 KV (72)

1.3.1.2. Effect of distance between the needle aperture and the collector

As the distance between the needle and the collector will affect the time for the ejected material to be deposited on top of the collector, and the time required for the solvent to evaporate, it has been reported to affect the morphology of the electrospun fibers. The distance between the needle and the collector will determine how much "stretching" the fibers will undergo, and it is also expected that with constant amount of material - i.e. constant flow rate-, it is expected to have thinner fibers with longer distance and thicker fibers with shorter distances. Not only

thicker, but as mentioned before, it can lead to beads formation in the formed fibers. The other point addressing the time available for solvent to evaporate will accordingly lead to whether a dry fibers can be obtained with longer distance (longer time to evaporate) or wet fibers with shorter distance (shorter time to evaporate), as has been demonstrated in the work of Buchko *et al.* (71) and Megelski *et al*(70). Buchko *et al*. reported the formation of wet and beaded fibers of SLPF, regardless of the concentration of the materials they prepared when shorter distance was used. The same observation of beaded fibers was also reported by Megelski *et al* with PS when shorter distance was used as shown in Figure 1.11.

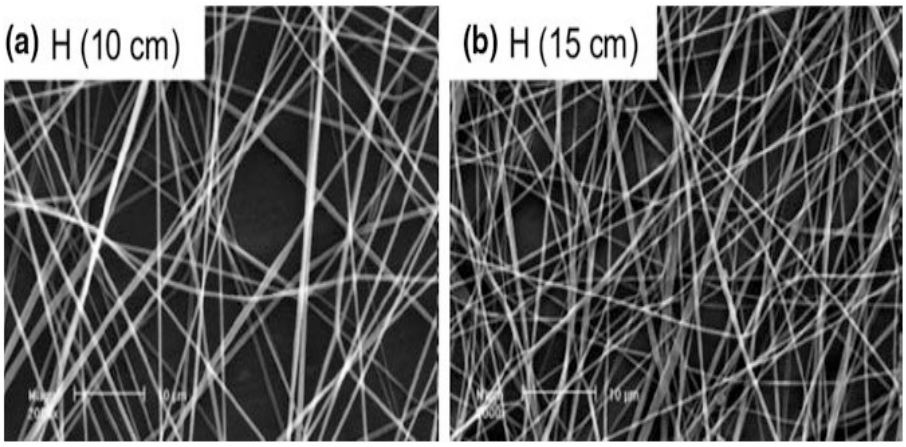

Figure 1-10 SEM images of electrospun SPLF fibers at different needle- collectore distances, a) at 10 cm & b) at 15 cm, where average thicker fibers (438 nm) obtained in shorter distance than thinner (368 nm) with longer one (72).

1.3.1.3. Effect of flow rate

The syringe pump is considered as another essential component of any Electrospinner setup. This is mainly because it allows the flow of polymeric solutions through the needle to be ejected (at certain applied voltage) to reach the plate collector. It is worth mentioning that the flow rate of the polymer solution determines how much flow of material would reach to the critical zone of the needle aperture. This would accordingly expose either more or less material to the applied voltage as the flow rate increases or decreases, respectively.

On the other hand, as discussed under the effect of distance, that if at a constant distance i.e constant "stretching of material", the existence of more material will lead to thicker fiber, and

thinner one will be obtained if less materials exist. Hence, there is a critical role of the flow rate as it affects how much material will exist at needle tip. Higher flow rate will make more material available at the spinneret and so a thicker fiber. The opposite is also true with lower flow rate. The above-mentioned work of Megelski *et al.* on PS, showed that increasing the flow rate had led to an increase in fiber diameter. It was also observed that bead-like structures exist in fibers with increasing the flow rate as shown in Figure 1.12. (70)

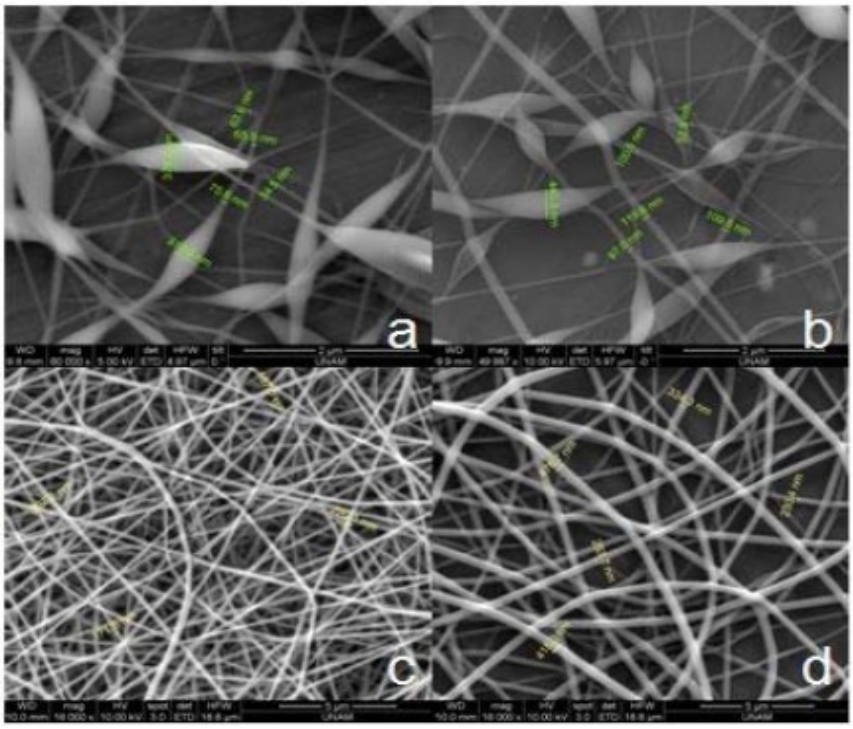

Figure 1-11 SEM images of electrospun PS fibers at different flow rates, where the absence of beads and change in fiber diameter observed with decreasing the flow rate a) at 10 mL/hr b) at 6 mL/hr c) at 1.6 mL/hr and d) at 1.1 mL/hr (73)

1.3.1.4. Effect of environmental conditions

Temperature, humidity, vaccum or gaseous environment inside the Electrospinner chamber have been reported to have a noticeable effect on the morphology of the formed electrospun fibers. Relatively high humidity (more than 60%) would decrease the drying of the fiber as was observed during the work of Baumgarden *et al.* on acrylic fibers. (74)

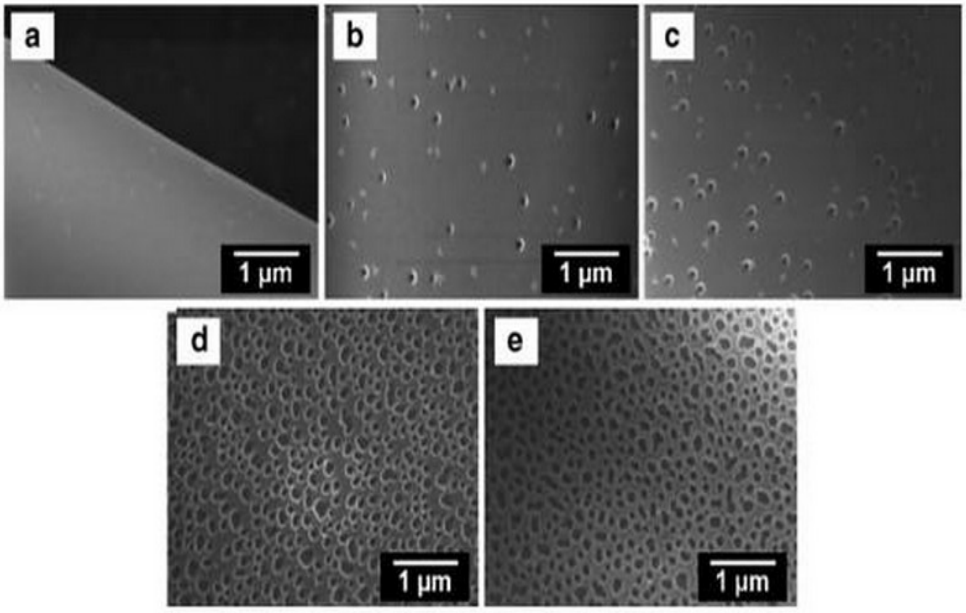

Figure 1-12 SEM images showing the effect of variable humidity levels on the porosity of the Polystyrene (PS) fibers, where the porosity increased with the increase of humidity a) < 25 % , b) 31–38 %, c) 40–45 %, d) 50–59 % & e) 60–72 %. (75).

1.3.2 Polymer solution parameters that affect the morphology of the electrospun fibers

These parameters are related to the solution itself that is used for electrospinning. They are:

- Polymer solution concentration
- Polymer solution conductivity
- Polymer solution solvent volatility

1.3.2.1 Polymer solution concentration

The concentration of the polymer solution was reported to affect the morphology of the formed electrospun nanofibers. It is expected to have thicker fibers with higher concentrations as was observed in the work on polystyrene (PS) solution by Megelski *et al*.(70) In addition to his work on polyethylene oxide (PEO), Dietzel *et al* observed the relationship between the concentration of the solution to be electrospun and the diameter of the electrospun fibers. (76) The concentration has its effect on the morphology of the formed fibers through two important

factors during the electrospinning process. First, is its effect on the surface tension of the solution. Variation of the concentration will lead generally to changes in the surface tension of the solution. The surface tension would resist the effect of the applied voltage as it increases the solution's tendency to aggregate into droplets rather than elongation to fibers. The second factor is related to the viscosity of the polymer solution. As the concentration varies, the viscosity will vary, too. And as the viscosity will affect the flow rate of the solution - which on turn would affect spinability as discussed before – one can deduce that changing viscosity will affect solution spinnability. The effect of viscosity of PEO solution on the morphology of the formed fibers was illustrated by Doshi & Reneker. (77)

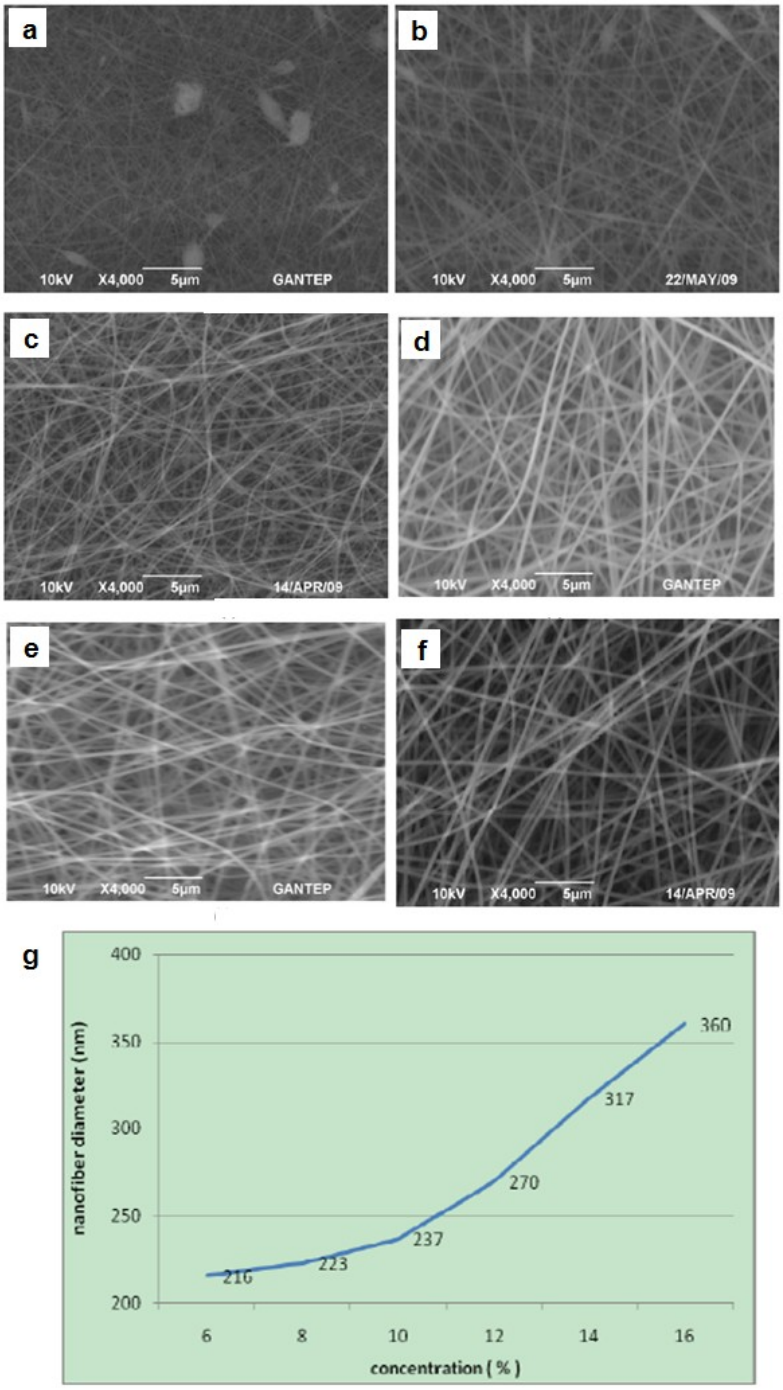

Figure 1-13 SEM images of Polyacrylonitrile (PAN) electrospun nanofibers from different solution concentrations a) 6%, b) 8%, c) 10%, d) 12%, (e) 14%, f) 16%. (78). (g) graphical illustration showing increase of fibers diameter with increasing concentration

1.3.2.2 Polymer solution conductivity

The conductivity of the polymer solution was reported to determine the amount of charges on the molecules and accordingly the degree to which it would be affected by the applied voltage. A highly conductive solution would therefore be highly affected by the applied voltage. More "stretching" of the fibers accordingly would occur and thinner fibers would be obtained as shown in Figure 1.15. The effect of ions on the fiber morphology and diameter was observed in the work of Zong *et al* on Poly D- lactide (PDLA) electrospun fibers. (79)

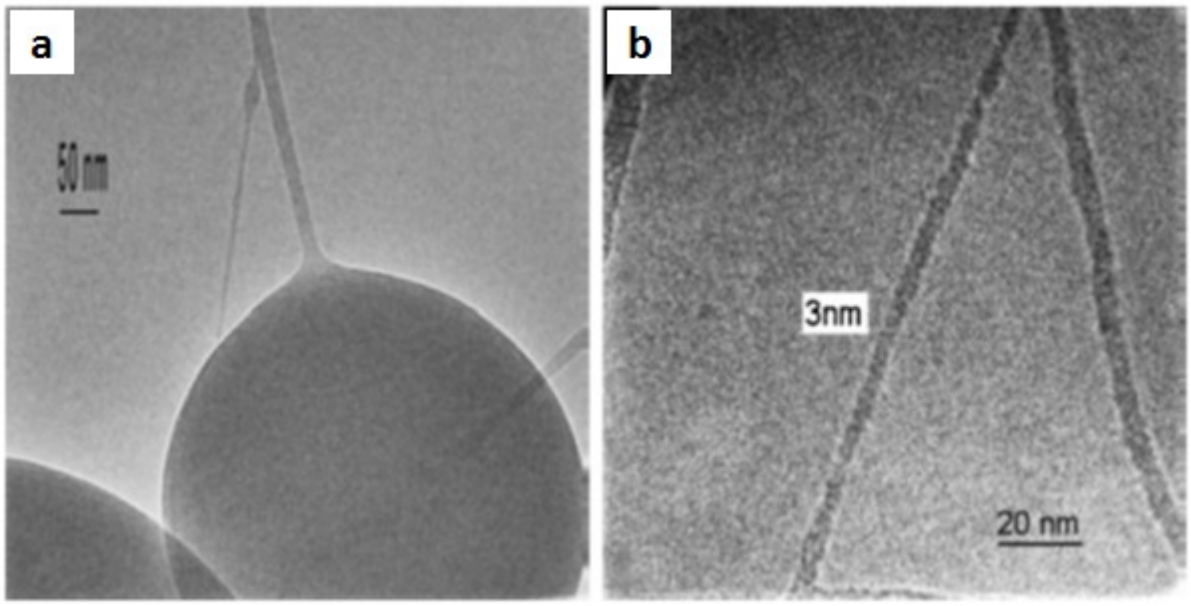

Figure 1-14 SEM images showing the effect of increasing solution conductivity by addition of pyridine to the electrospinning solution of nylon in formic acid, as thin fibers with no beads observed with pyridine addition (b) from only formic acid with beads structures (a) **(80)**

1.3.2.3 Polymer solution solvent volatility (effect of solvent)

The type of solvent used was reported to determine its volatility, the factor which would affect the solidification and fiber formation of the polymer during the electrospinning process. On his work on polyvinyl chloride (PVC), Lee *et al* observed the effect of solvent on the morphology and the diameter of the formed fibers. (81) This was enforced with the study of Megelski *et al*. on the effect of the physical properties of the solvent used on the formed fibers during his work on PS using variable THF/ DMF ratios as shown in Figure 1.16. (70)

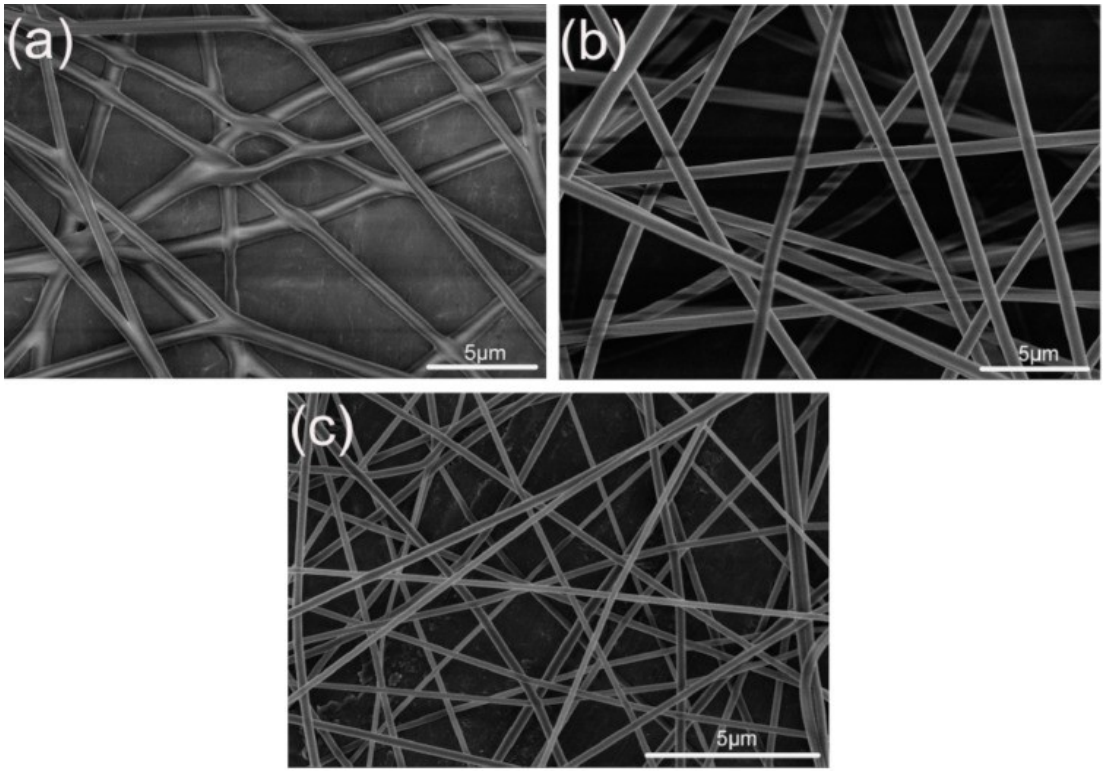

Figure 1-15 SEM images showing the effect of solvent volatility on diameter & morphology of formed PS nanofibers. a) Only Ethanol used as solvent where crosslinking due to delayed evaporation of solvent appears as well as having fibers with average diameter of 500 nm b) Ethanol/chloroform system used and the disappearance of crosslinking is clear and thicker fibers with average of 800 nm are obtained c) Ethanol/DMF system is used and thinner fibers of diameter average of 170 and with no crosslinking are obtained. (82)

Many polymers attracted researchers to use them in elecrospinning technique based on their unique properties. One of these polymers is cellulose acetate. In next section we will demonstrate some of its properties and applications as a polymer for electrospinnig.

1.4 Cellulose Acetate

Cellulose:

Cellulose is a natural occurring polysaccharide polymer. Knowing that it forms a major material in plants' cell wall, accounting for 40-50 % of the composition of wood and 90 % of cotton, one can easily know it is the most abundant polymer on earth. (85) Chemically, it is composed of repeated molecules of D- glucose monomers. (83) It is hydrophilic, biodegradable material that has wide chemical derivations through various modifications to its skeleton. (85) Cellulose and its derivatives have been used in wide applications in various fields such as textile industry, filtration membranes, pharmaceutical applications, coating & building material. The chemical structures of cellulose and cellulose acetate are depicted in Figure 1.17.

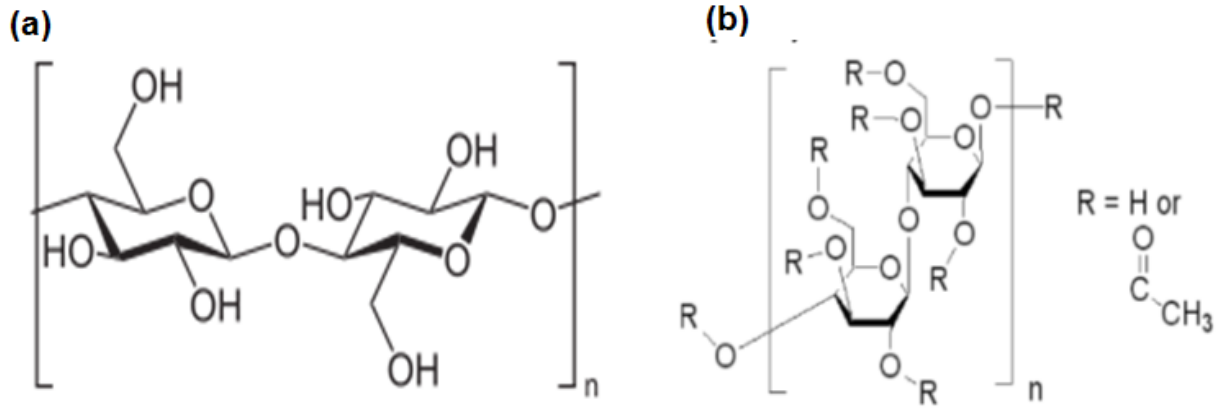

Figure 1-16 Chemical structure of cellulose (a) (83) & Cellulose acetate (b) (84)

1.4.1 Electrospinning of Cellulose Acetate

Cellulose acetate (CA) is an acetate ester derivative of cellulose. It is readily soluble in various solvents that make it suitable for electrospining experiments such as acetone, acetic acid, dimethylacetamide, dimethylformamdie, trifluroethylene, dichloromethane, chloroform and methyl acetate. (86) It is also the most important derivative used to prepare nanofibers of cellulose by electrospinning.

1.4.1.1 Electrospinning of CA – polymers mixtures

Not only mixtures of solvents in electrospinning of CA are of interest to researchers, mixtures of polymers with CA have raised their interest too. Various materials of various characteristics and properties were prepared with electrospinning by using different types of polymers with CA. Examples are polyvinylpyrrolidone (PVP) (Castillo- Ortega *et al*.) (87), polyurethane (PU) (*Tang et al.*) (88), Polethylene glycol (PEG) (Chen *et al.*) & silk fibroin (SF) (Zhou *et al.*) (88). Some examples are illustrated in Figure 1.20

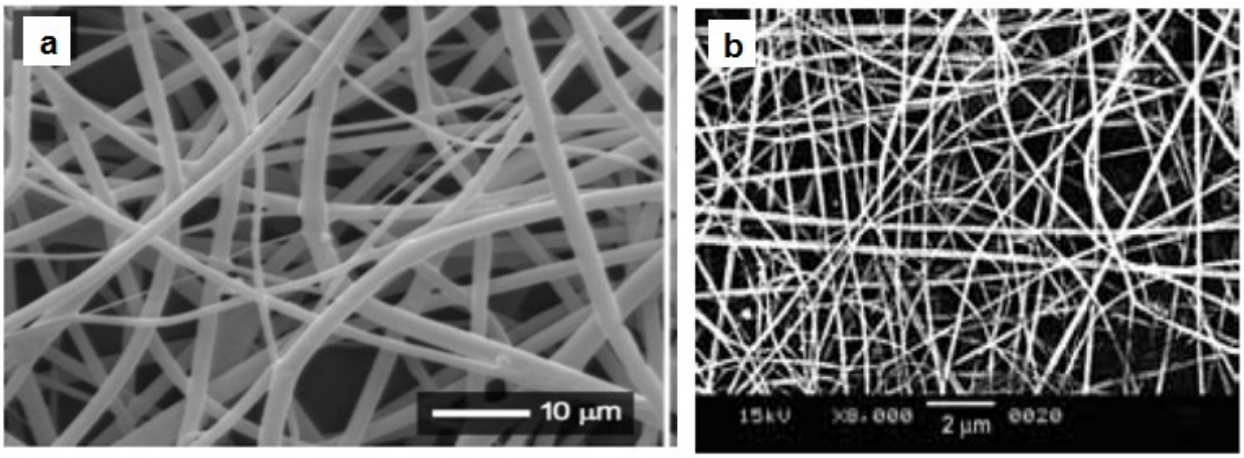

Figure 1-17 SEM images of electrospun CA fibers with other polymers a) With Polyethylene glycol (PEG) b) with silk fibrin (SF) (88)

1.4.2 Biomedical applications of CA nanofibers

The electrospun fibers of CA have been used in many biomedical applications. These include: (i) bioactive materials immobilization, (ii) scaffolds for cell culture and tissue engineering, (iii) nutraceutical applications, (iv) biosensor applications, (v) antimicrobial mat, (vi) bioseparation and (vii) bioremediation as shown in Figure 1.11 and will be described below.

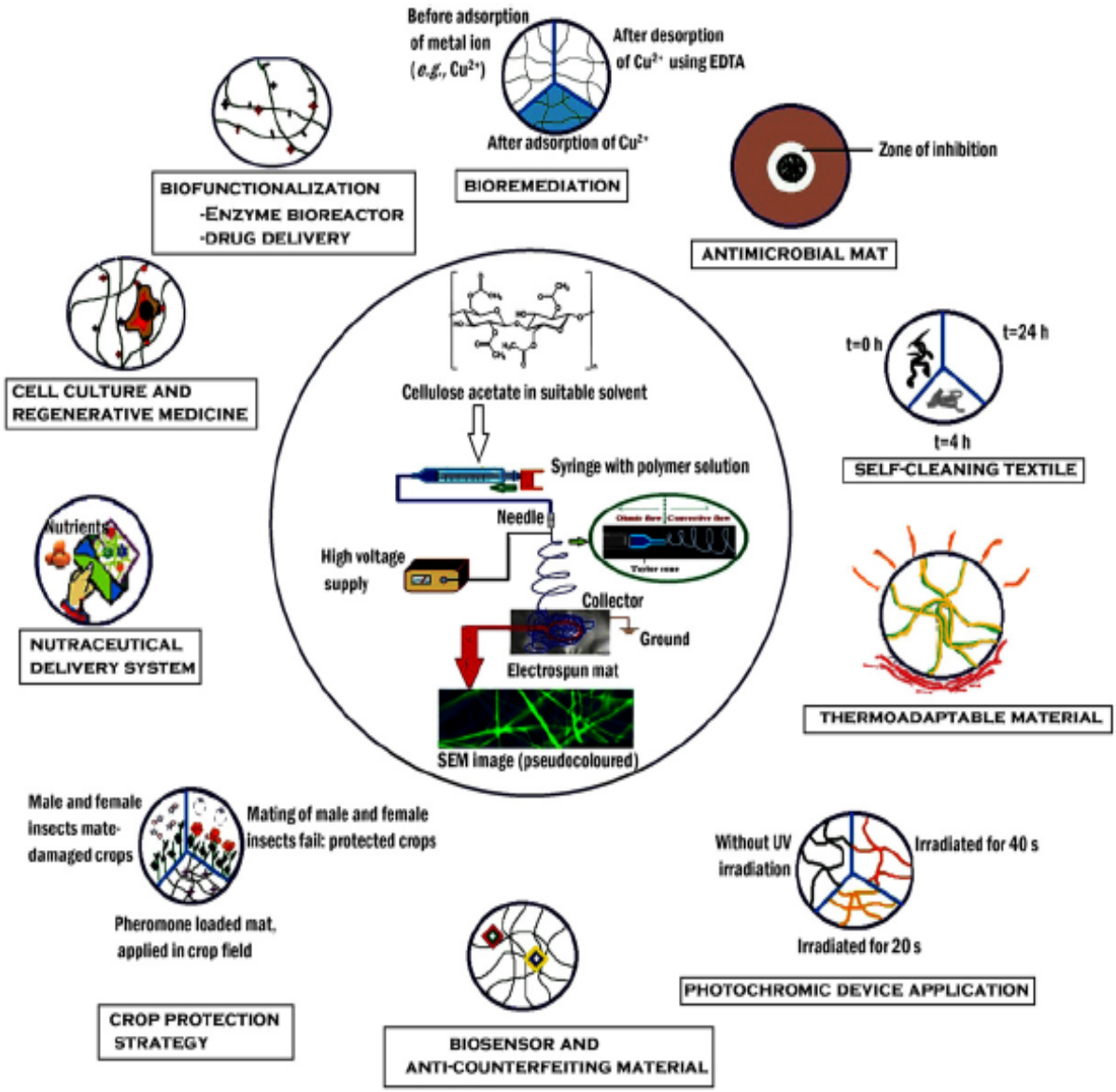

Figure 1-18 Biomedical applications of CA electrospuun fibers.(163)

1.4.2.1 Bioactive material immobilization

CA nanofibers were used extensively with wide range of bioactive materials for different applications. For example, Taepaiboon *et al.* reported on the immobilization of Vitamin A and Vitamin E on CA nanofibers produced by electrospinning. (164) A characteristic gradual release of Vitamins was observed instead of usual sharp release from non-electospun CA.

On the other hand, as an example of very interesting bioactive materials which is enzyme, Huang *et al.* reported on the immobilization of Candida rugosa lipase with significant increase in its thermal stability in comparison with its non immobilized free form. (165)

Drug loading is another interesting application of the bioactive materials immobilization with CA electrospun nanofibers. This can be applied for both local and systemic drug release. In local drug release or topical drug release, it has great value of effective focused drug release at low concentration of the drug. (170) This is of special importance for effective wound healing applications. Regarding the systemic drug release, this can be described under the highly growing concept of transdermal drug delivery (TDD). The major advantage of this route of drug delivery is the avoidance of the obligatory pathway through liver that is accompanied with normal oral route of drug administration.(171) As the liver contains many metabolic enzymes that act on administered drugs and accordingly affecting their bioavailability (effective reaching drug concentration to blood). This effect is known as hepatic effect. (172) As mentioned before, the absorption through the transdermal drug delivery route does not pass on liver and accordingly avoids the hepatic effect. Examples for research work on transdermal drug delivery medications using CA electrospun fibers include what was reported by Tungprapa *et al.* for the loading of Naproxen, indomethacin, ibuprofen and sulindac. (96) Castillo- Ortega *et al.* also reported on the use of electrospun CA and PVP for the loading of amoxicillin. (97). Known for their effective wound healing enhancement aided by their anti-inflammatory, antimicrobial and antioxidant effect, Alkannin, shikonin (A/S) the naturally occurring materials were also loaded on electrospun CA for wound healing applications as proposed by Kontogiannopoulos *et al* (98). Still in approaches of better wound healing applications, Liu *et al*. reported the use of electrospun CA/ polyester urethane (PEU) with the polyhexamethylene biguanide (PHMB)

which is used as a disinfectant.(99) Other work for the loading for Chlorohexidine (100) , N-halamine (101) were also reported.

1.4.2.2 Scaffolds for cell culture & tissue engineering applications

The suitability of Cellulose and its derivatives in the use as scaffolds for tissue engineering has been reported. This can be attributed to its advantages such as biocompatibility (102), suitable mechanical and stability properties (103, 104). For the work with electrospun CA nanofibers, Rodriguez *et al*., reported on the use of saponified electrospun CA mat with Calcium phosphate crystals and its growth as a way that could be extended in the application of bone healing (Figure 1.26) (105). Rubenstein *et al*., also reported on the use of electrospun CA and chitosan as scaffolds for the growth of human umbilical vein endothelial cells (HUVECs). (106) On the other hand, Dragulescu- Andrasi *et al.* reported on the use of modified electrospun CA for growing human marrow stromal cells (hMSC) (107). Also Gouma *et al*. reported on the use of electrospun CA with hydroxyapatite nanoaggregates for the growth of human osteoblast (108). Moreover, the use of CA derivatives was also reported. For example, the use of cellulose acetate butyrate (CAB) for growing Schwann cells and the use of methylacrylated cellulose acetate butyrate for growing 3 T3 (fibroblast cell line) were reported by Huang et al. (109) & Cakmakci et al.*(*110*)* respectively.

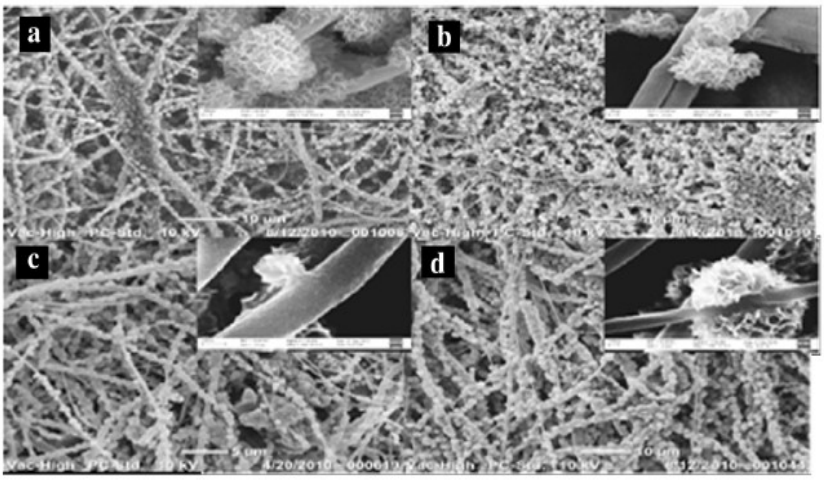

Figure 1-19 SEM images of regenerated Cellulose scaffolds from CA electrospun nanofibers at different regerneration time & treatment conditions showing minerlization & crystal growth of calcium phosphate (105)

1.4.2.3 Biosensor applications

With its high surface area/volume ratio, the fixation of biosensors on electrospun fibers could allow for highly sensitive detection of materials of interest. For example, Wang *et al*., reported on the use of electrospun CA nanofibers for fixing of hydrolyzed poly [2-(3-thienyl) ethanol butoxy carbonyl – methyl urethane] (H-PURET). It is used as a florescent probe for highly sensitive detection of methyl viologen and cytochrome c. The fixation of H-PURET on CA nanofibers allows greater exposure to analyte and so higher detection ability at very low concentrations. (Figure 1.27) (111)

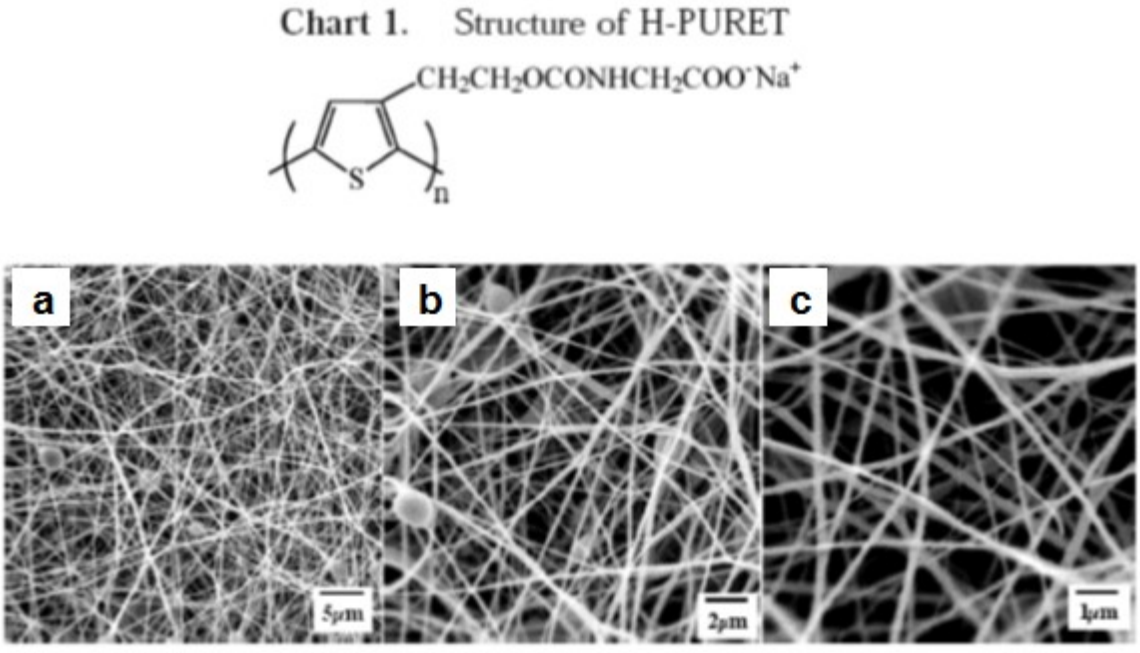

Figure 1-20 Chemical structure of hydrolyzed poly [2-(3-thienyl) ethanol butoxy carbonyl – methyl urethane] (H-PURET) and (a, b and c) SEM images of CA nanofibers loaded with it for highly sensitive analytes detection (111)

1.4.2.4 Antimicrobial mats

The use of electrospun fibers with integrated antimicrobial activities has attracted a lot of attention recently due to the versatility of applications in various fields such as medical, food, textile and packaging. Son *et al.* reported on the incorporation of silver and zinc oxide (ZnO) nanoparticles, which exhibit antimicrobial effect on their own, with CA electrospun nanofibers with the purpose of enhancing the antimicrobial effect of the overall composite. (112) Their results revealed an antibacterial effect of the composite against both Gram +ve and Gram –ve bacteria represented by *S. aureus*, *E. Coli*, *K. pneumoniae* and *P. aeruginosa*. On the other hand, based on its known antibacterial effect, ZnO was also used by Anitha *et al.* with electrospun CA fibers. The fibers shown to be exerting antimicrobial effect against *methicillin resistant S. aureus* (MRSA), *E. Coli*., and also *C. freudii*. (Figure 1.28) (113)

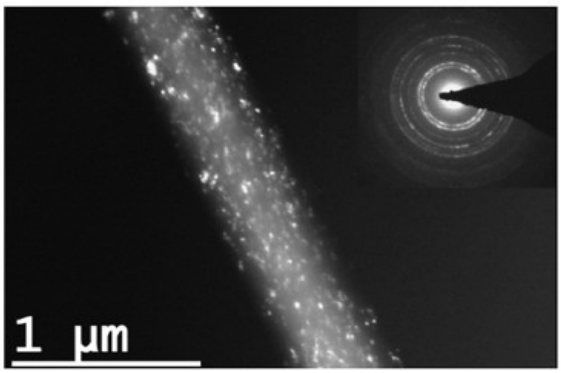

Figure 1-21 TEM image of CA nanofibers loaded with ZnO nanoparticles on its surface. (113)

1.4.2.5 Bioseparation

Aided also with its high surface area/volume ratio, the use of electrospun nanofibers to fix ligands specific to materials of interest can have a successful application in effective separation and purification of biomaterials of interest from fermentation medium. For example, Zhang *et al.* proposed the use of electrospun CA fibers with diethylaminoethyl (DEAE) ligand for binding of bovine serum albumin (BSA). They demonstrated a higher binding capacity of 40 mg/g compared with maximum of 33.5 mg/g shown as cast functionalized membranes. (114)

1.4.2.6 Bioremediation

Pollution and its drawbacks on water are of great concern. It has a direct toxic effect on the marine living organisms. Additionally, it has an indirect effect on the living things drinking from polluted water. It can also affect them when feeding on marine living organisms that were affected by pollution. This will end up with cumulative toxicity with hazardous impacts. The global concern about pollution is driving global efforts to find new solutions and innovative methods to this problem. The use of nanofibers materials is no far from these efforts. For example, Tian *et al*. reported on the use of electrospun CA nanofibers with poly(methacrylic acid) (PMMA) with its COOH groups available sites for adsorption of heavy metals as (copper, mercury and cadmium).(115) Zhou *et al.* also reported on the use of CA electrospun nanofibers with silk fibroin (SF) for heavy metals adsorption. Cu2+ was used as a model for heavy metals. They reported a higher adsorption of the CA/SF nanofbers than any of them alone with a maximum of 22.8 mg of copper/g (of CA/SF). This was considered as a synergistic effect of CA/SF electrospun fibers. (116)

1.5 Citric acid

Another very interesting natural occurring material is citric acid. Lemons, oranges and grapefruits are among the most common citrus fruits that are known to have high content of citric acid. Carl Wilhelm Scheele, was the first one to discover it by crystallization from lemon juice in 1784. (117) Chemically, it is a weak carboxylic acid with three carboxyl groups. (Figure 2.1 c). (118) It has wide range of applications in different fields such as food industry, pharmaceutical industry, cleansing and personal care industry. A very important property of citric acid is its antimicrobial effect. This property makes it heavily used as a safe and effective preservative in pharmaceutical and food industry. (119)

1.5.1 Antimicrobial effect of citric acid

Multiple factors affect the growth of microorganisms such as the pH, temperature, moisture content, nutrients, redox potential and others. A compromise in the optimum conditions of growth leads to inhibition of microbial growth and many compounds that have antimicrobial activities exert their action by affecting these conditions. This applies to citric acid and its group of week organic acids. Their antimicrobial action is postulated to be through the effect on internal pH changes. The affection on the internal pH of the microorganism finally leads to stress response that leads to energy depletion and growth cessation. This can happen through various effects such as membrane disruption (120), stress on intracellular pH homeostasis (121), the accumulation of toxic compounds inside the cell (122) and inhibition of critical metabolic pathways. (123) At low pH, the weak organic acids exist more in its un-dissociated and uncharged form. In this form, the acid can pass through the cell membrane and enters the cell. Once inside, the acid faces the higher pH that is normally present inside the cell. Accordingly, the acid starts to dissociate and transforms to the ionized form with release of anions and protons. Being charged entities, they cannot pass the membrane again and accumulation inside the cell occurs. As a result a disturbance in internal environment occurs, leading to the stress effect finally ending in inhibition of microbial growth. (124)

The antimicrobial effect of citric acid was reported by many researchers. Conner *et al*. reported on the inhibitory effect of citric acid on listeria monocytogenes at pH 4 using trypticase soy yeast extract broth. *(*125) In addition, Brackett *et al*. reported on the antimicrobial effect of citric acid among other acids like lactic and hydrochloric and acetic acids on *Yersinia enterocolitica*. *(*126) On the other hand, the antimicrobial effect of 0.5 % citric acid at pH 4.5 on *Arcobacter butzleri* was reported by Phillips *et al. (*127) At concentration 0.5 % also, citric acid could inhibit the growth of *Aspergillus versicolor* as reported by Reiss *et al*. *(*128) Moreover, Minor and Marth also related the increase of inhibition of *S. aureus* by citric acid with both the increase in its concentration and the decrease in pH. *(*129) Moreover, Fischer *et al.* reported on using 0.75% concentration of citric acid, also on *S. aureus*, and their results revealed the decrease of inoculated concentration of it together with *Salmonella typhimurium, Yersinia enterocolitica and E. coli. (*130) On the other hand, Fungistatic and fungicidal effects of citric acid on *Trichophyton mentagrophyts, Aspergillus fumigatus, Candida albicans and Malassezia furfur* were reported by Hojatollah Shokri.*(*131) Moreover, the causative agent of the medical emergency case of gas gangrene, *Cl. perfringens* was reported to be inhibited by citric acid at concentration of 4 mg/mL as described in the work of Skrivanova *et al. (*132) Furthermore, the effect on spore forming organism of *Bacillus subtilis* together with *Streptococcus suis & E. coli* was studied by Zhihong Gao *et al*. Their results revealed that the MIC of citric acid was 2, 8 and 1.667 on each organism respectively. *(*133)

1.5.2 Citric acid in wound healing

Wound infection is one of the greatest threats to wound proper healing as mentioned before. The need for an effective antimicrobial material to control the wound infection and enhance the wound healing process is of great importance as was also demonstrated before. The trend to use citric acid in wound healing management has attracted a lot of attention recently mainly due to being natural material, with high safety, its existence in high concentrations in edible citrus fruits and more importantly due to its well-known antimicrobial and preservative effects . Some representative examples are discussed below.

1.5.2.1 The mode of action of citric acid in wound healing

The enhancement of wound healing mechanism by citric acid was recently reported. It is postulated to be modulated by the acidic pH created by citric acid that leads to better control of wound infection, modulation of protease activity in addition to enhancement of epithelization and angiogenesis. *(*134)

1.5.2.2 The use of citric acid in wound surgical site infection control

Surgical operations and other invasive interventions are corner stone of healthcare procedures. However, they are accompanied with high risk of infections. These infections are collectively named as healthcare associated infections (HAI). They are of different types such as pneumonia, gastrointestinal infections, urinary tract infections, primary bloodstream infections, surgical site infections and many others. In 2011, a total of 721, 800 case of HIA were reported in USA. About 22 % of these cases (157,500) were classified as surgical site infections (SSI). They were associated with a 3% rate of mortality. It can be defined as "an infection that occurs after surgery in the part of the body where surgery took place (centers for disease control and prevention" CDC"). *(*135)

Nagoba *et al*., studied the use of citric acid for treatment of SSI with major nosocomial (hospital acquired) infectious agents such as *P. aeruginosa*, *S. aureus*, *E. coli*, *Klesbsiella*, *proteus* and *citrobacter*. Samples of 70 patients that are not responding to ordinary used agents were selected for their study. The pus from wounds were cultured and assessed for antimicrobial susceptibility. They reported that MIC range from 0.5- 2.5 mg/mL could effectively inhibit the growth of all isolates. They reported also the results of the application of 3% citric acid to wounds. With a percentage of 98.57 (69 cases out of 70), a complete healing (57 case) or formation of healthy granulation tissue (12 case) that were closed by suturing was reported. *(*136)

1.5.2.3 The use of citric acid with Diabetic patients

Ranked number eight as a cause of death, diabetes mellitus is a great global health concern. With estimates of 171,000,000 worldwide cases in year 2000 and expectancy to reach 366, 000,000 cases by year 2030 one can easily imagine the big threat humans are facing.*(*137*)* For those lucky patients who were not killed by diabetes, still face its hazardous complications. A major concern with the diabetes is the compromised immunity, which brings them to higher risk of wounds complications. Up to 10 % of diabetic patients are at risk of developing diabetic foot ulcer that can develop leading to amputation of lower extremity. *(*138)

B.S Nagoba *et al*, studied the use of citric acid for treatment of this important group. Seven diabetic ulcer patients among other classes were included in the study. Multiple antibiotic resistant *E. coli* was isolated from wounds. They reported that at MIC of 1.5- 2 mg/mL of citric acid, growth inhibition could be achieved. They also reported on the application of 3 % citric acid gel twice daily to the patients. The complete elimination of infectious bacteria and enhancement of healing of all patients were achieved. *(*139)

1.5.2.4 The use of citric acid with Cancer patients

The use of citric acid for treatment of post operative wound of patients suffering from synovial sarcoma of the knee was reported by Basavraj S Nagoba *et al*. A non-responsive to ordinary treatment wound with pus from post operative section was observed. An isolate of antibiotic resistant *S. aureus* was found upon examination. The case was set on 3 % citric acid ointment. Complete healing with 25 applications in 25 days was reported (Figure 1.30). (140)

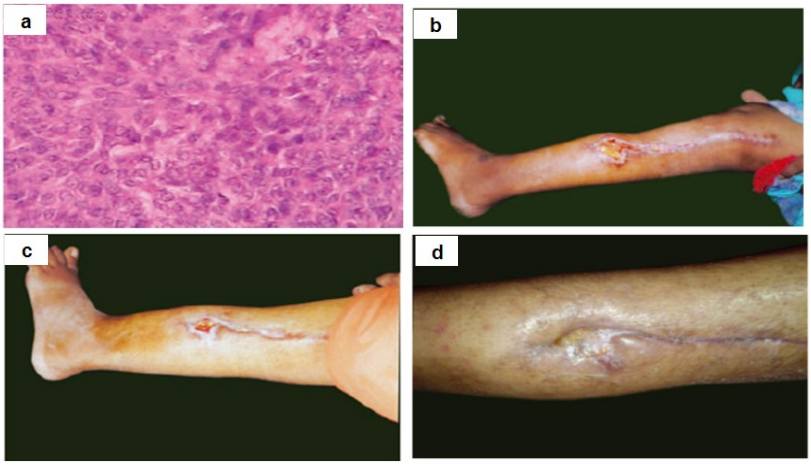

Figure 1-22 a) Monophasic synovial sarcoma under microscope. b) case before c) after 16 applications and d) after 25 applications of citric acid. (140)

1.5.2.5 The use of citric acid with HIV/AIDS patients

Another special group of patients that suffers from immunodeficiency and is at higher risk of wound infection is the HIV/AIDS patients. Basavraj Nagoba- Chandrakala Patil studied the use of citric acid in the treatment of post operative infection of this critical group of patients.

Two cases with HIV/AIDS were studied. In one case, a resistant *E. coli* and in other resistant *P. aeruginosa* and *S. aureus* were isolated. As ordinary agents failed to manage wound effectively, they were subjected to daily 3 % citric acid ointment treatment. They reported the complete healing of the first case by 19 applications of ointments and after 8 days of use for the second case. *(*141)

1.6 Chitosan

Chitosan is another type of natural materials that has interesting properties for wide range of applications and drawing the attention among the scientific community. Chitosan is a polymer obtained by partial deacetylation of chitin using 40-50 % of NaOH. *(*142) Knowing that chitin is a major component of cell walls of fungi and external skeleton of shrimps, crabs and many insects. Chemically it is a polysaccharide polymer of D- glucosamine and N acetyl D glucosamine (See Figure 1.36). Different degrees of acetylation and molecular weights exist and have been reported to greatly affect the properties of the solutions made of it. The solubility of chitosan is a big challenge for its use as it is soluble only in dilute organic acids and not soluble in most common solvents. As a natural material with high biodegradability and biocompatibility, it forms a focal point for many researchers in various applications.*(*143)

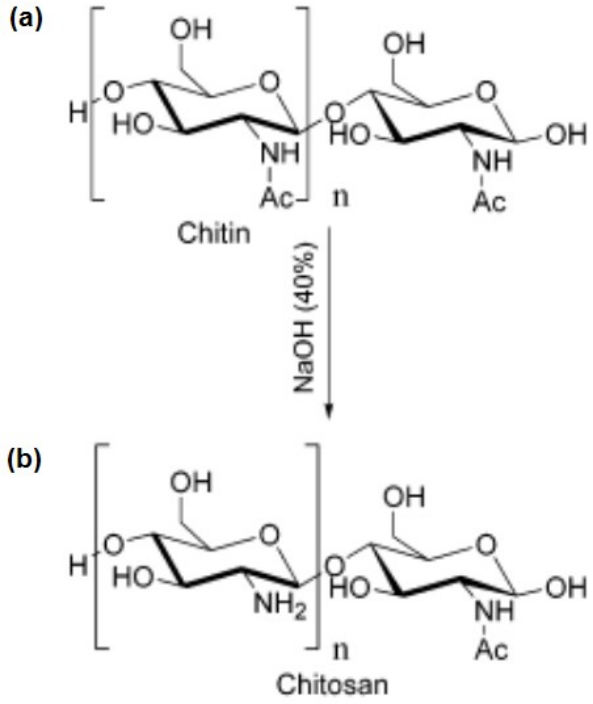

Figure 1-21 Preparation of chitosan from chitin by chemical deacetylation. (143)

1.6.1 Antimicrobial properties of chitosan

The antimicrobial effect of chitosan was reported by many researchers. Higher effectiveness was observed with fungi than with bacteria. A list of MICs of chitosan against different types of bacteria and fungi are shown in tables a and b in Figure 1.37. *(*144)

(a)

fungi	MIC[a] (ppm)
Botrytis cinerea	10
Fusarium oxysporum	100
Drechstera sorokiana	10
Micronectriella nivalis	10
Piricularia oryzae	5000
Rhizoctonia solani	1000
Trichophyton equinum	2500

[a] MIC = minimum growth inhibitory concentration.

(b)

Bacteria	MIC[a] (ppm)
Agrobacterium tumefaciens	100
Bacillus cereus	1000
Corinebacterium michiganence	10
Erwinia sp.	500
Erwinia carotovora subsp.	200
Escherichia coli	20
Klebsiella pneumoniae	700
Micrococcus luteus	20
Pseudomonas fluorescens	500
Staphylococcus aureus	20
Xanthomonas campestris	500

Figure 1-22 Chitosan MIC against list of different types of (a) fungi & (b) bacteria. (144)

1.6.2 Biomedical applications of Chitosan nanofibers

Chitin and chitosan were extensively used in biomedical applications. For example, chitosan has been used in tissue engineering,(145) wound dressing (146), drug delivery (147), biosensors, (148) and filtration applications (149).

1.6.3 Use of chitosan in wound dressing

The effect of microbial infection on delayed wound healing and the enhancement of healing time by proper control of it was described earlier. Tashiro *et al.* described the antimicrobial effect of quaternary ammonium derivatives of chitosan (QCS). Their antimicrobial results were attributed to an effect on the cell membranes of microorganisms *(*150). In addition, Ignatova *et al.* reported on the preparation of electrospun mats of QCS with PVP and PVA. The fibers were found to have a growth inhibiting effect on both Gram negative and Gram positive bacteria. *(*151) On the other hand, Zhou *et al.* also prepared and studied the use of carboxyethyl chitosan and PVA nanofibers in wound healing. They reported on the enhancement of growth of the used mouse

fibroblast cells (L929) and the biocompatibility of the formed fibers as there was no toxicity. *(*152) On other hand, nanofibers made from chitosan and collagen had an enhancing effect on wound healing as reported in the work of Chen *et al*. *(*153.)

Chitosan nanofibers were also reported to have potential use in burns such as the work carried out by Kossovich *et al*. *(*154) In their work, it was attributed to the nanofibers capability to absorb the exudates and protect the site from infection. In addition, Cai *et al.* also used electrospun chitosan together with silk fibroin for burns healing. They reported the enhancement of murine fibroblast cells attachment and proliferation. *(*155)

1.7 Addition of antimicrobial effect on Cellulose & Cotton fabrics

1.7.1 With citric acid:

Sandra Bischof *et al*. reported on the modification of cotton textiles with citric acid to benefit from its known antimicrobial effect against nosocomial infections(See Figure 1.38). This was carried out by impregnation of textile material in a solution of citric acid and sodium hypophosphite monohydrate(SHM). After that, a drying using conventional or microwave heating was performed. The material was assessed for acquired antibacterial effect against MRSA, *S. aureus* and *P. aeruginosa*. They reported a significant antibacterial effect against the tested bacteria. Based on their results, they suggested the use of the treated material for disposable as well as reusable fabrics in controlling nosocomial infection. *(*156)

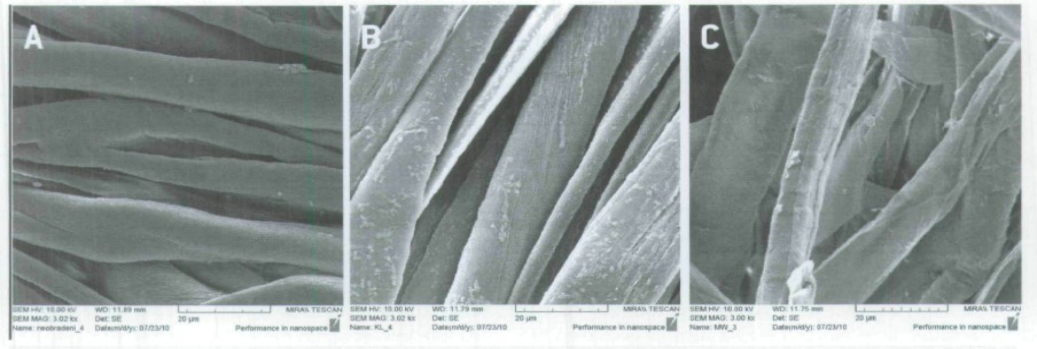

Figure 1-23 A) Fabrics without treatment. B) Fabrics treated with citric acid and SHM. C) treated fabrics after 10 times washing. (156)

1.7.2 With Chitosan

Tavaria *et al*. also reported on the modification of cotton material by adding chitosan to benefit from its antimicrobial effect. Impregnation of textile material with chitosan solution was done. This was followed by drying using conventional heating. The testing for antimicrobial effect was performed using isolates of *Staphylococci* from volunteers. They reported an observed antimicrobial effect of chitosan treated fabrics on some of the strains used. Based on their results, they proposed effective and selective treated fabrics against skin infections. *(*157)

Chapter 2 **Materials and Methods**

Chapter. 2 Materials and Methods

2.1 Materials

The following materials were purchased Cellulose

Acetate (CA) (85%), Citric acid (Cit) (99 %) (LOBACHEIME, India), Chitosan (CS) medium weight (Sigma, Netherlands), acetone (98.5%) (piochem, Egypt), acetic acid (99.5 %) (LOBACHEIME, India). The chemical structures of the solvents and the materials used are shown in Figure 2.1.

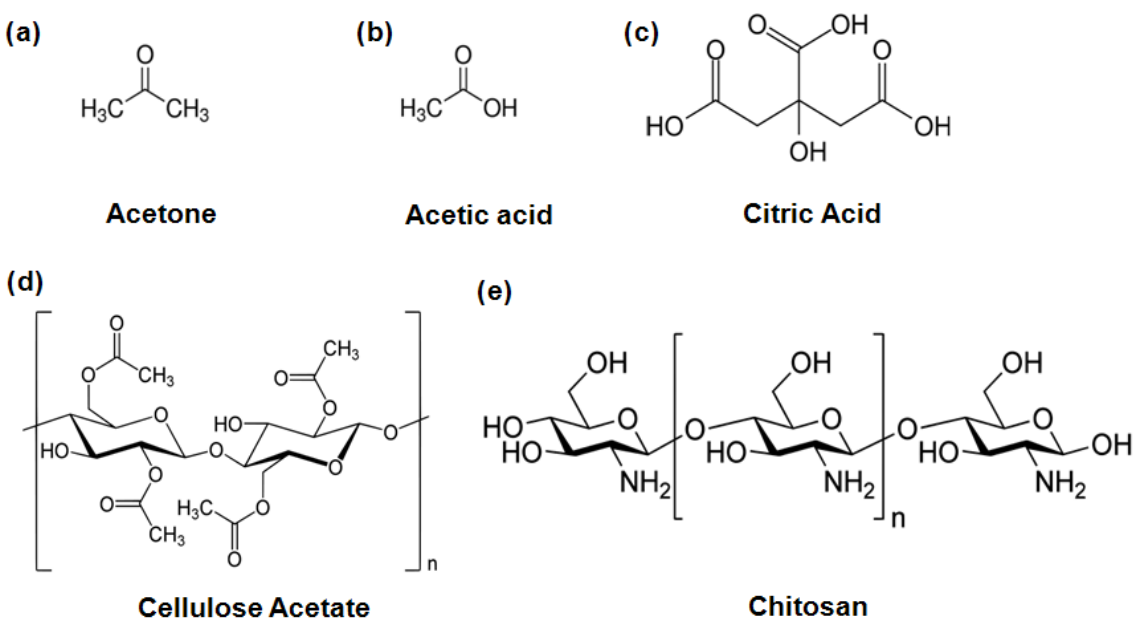

Figure 2-1 Chemical structures of used chemicals & solvents (117, 84, 142)

General scheme for work

The samples were prepared by dissolving the required amount of materials in specified solvents as illustrated in Table 2.1. The samples solutions were then fed into the syringe and the solution flow rate was adjusted to carry out electrospining of the solutions after optimizing the applied voltage to obtain nanofibers. This was followed by characterization of the formed nanofibers (if any). The characterization included SEM for confirmation of nanofibers formation and for the analysis of their morphology & size. The electrospun nanofibers were also examined by FT-IR for chemical composition analysis of possible chemical interactions. Selected electrospun nanofibers that were free of beads were then tested for their antimicrobial activity against E. coli and S. Aureus bacteria.

2.2. Solutions preparation for electrospining

Table 2.1 illustrates the samples composition used in this study.

Solutions preparation for electrospinning for CA & CA-CIT nanofibers:

The following solutions were prepared for electrospinning

Table 2-1 Solutions preparation for electrospinning of CA and CA-CIT

Sample	Material/weight	Solvent/ volume
1	CA/ 5 g	Acetone / 95 mL
2	CA/ 5 g mixed with CIT/ 10 g	Acetone/ 85 mL

Solutions preparation for electrospinning for other CA based composites:

Different sample solutions of CA/ CS composites were prepared as shown in Table 2.2

Table 2-2 Solutions prepaaration for other CA based composites

Sample	Solution A		Solution B		Mixing ratio (A : B)
	Material/weight	Solvent/volume	Material/weight	Solvent/volume	
3	**CA/ 10 g**	**Acetone 95 mL**	**CS/ 0.1 g**	**60% Acetic acid/49.9 (fill to 50 mL)**	**1:1**
4	**CA/ 7.5 g**	**Acetone 92.5 mL**	**CS/ 0.15 g**	60% Acetic acid/ 49.85 (fill to 50 mL)	**2:1**
5	**CA/ 10 g mixed with CIT/ 20 g**	**Acetone 70 mL**	**CS/ 0.1 g**	60% Acetic acid /49.9 (fill to 50 ml)	**1:1**
6	**CA/ 7.5 g mixed with CIT/ 15 g**	**Acetone 77.5 mL**	**CS/ 0.15 g**	60% Acetic acid /49.85 (fill to 50 mL)	**2:1**

2.3 Electrospinning of prepared solutions

2.3.1 Electrospinning of CA alone

2.3.1.1 Effect of voltage experiments

5 % solution of CA in acetone was prepared as described in table 2.1. The flow rate was set at 5 ml/hr & tip - collector distance was set at 5 cm. Variation of KV was then performed for electrospinning process. The used voltages were 10, 12.5, 15 & 17.5 KV.

2.3.1.2 Effect of flow rate experiments

5 % solution of CA in acetone was prepared as described in table 2.1. The Voltage was set at 15 KV & tip - collector distance was set at 5 cm. Variation of flow rate was then performed for electrospinning process. The used flow rates were 3, 5 & 7 ml/hr.

2.3.1.3 Effect of flow rate experiments

5 % solution of CA in acetone was prepared as described in table 2.1. The Voltage was set at 15 KV & flow rate was set at 5 cm. Variation of tip – collector distance was then performed for electrospinning process. The used tip – collector distance were 3, 5 & 7 cm.

2.3.2 Electrospinning of CA – CIT mixtures

A solution containing 5% CA & 10 CIT in acetone was prepared as described in table 2.1. The Voltage was then set at 15 KV, flow rate was set at 5 ml/hr & tip - collector distance was set at 5 cm.

2.3.3 Electrospinning of CA –CS & CA/CIT/CS mixtures

For CA-CS mixture a solution containing 5% CA & 0.1% CS in acetone/60 % acetic acid mixture & for CA-CS-CIT mixture a solution containing 5% CA, 10 % CIT & 0.1% CS in acetone/60 % acetic acid mixture were prepared as described in table 2.2. The Voltage was then set at 15 KV, flow rate was set at 5 ml/hr & tip - collector distance was set at 5 cm.

2.3 Characterization techniques of nanofibers

The nanofibers obtained by electrospining of various mixtures were characterized for the morphology & fiber size using scanning electron microscopy (SEM) (FESEM, Leo Supra 55 – Zeiss Inc., Germany). To verify the composition and determine possible interactions of electrospun materials, Fourier Transform Infrared (FT-IR) spectroscopy (Nicolet 380-Thermo Scientific) was used. To assess the antimicrobial effect of the electrospun fibers, the effect on growth of the broth culture of gram –ve microorganism *(E. coli*) & gram +ve microorganism (*S. aureus*) was determined.

2.3.1 Scanning Electron Microscopy (SEM)

In order to have images at the nanoscale resolution of the formed nanofibers, an optical system of very high resolution power and magnification is needed. In ordinary microscopy, the resolution is limited in one factor by the wavelength (λ) used. The shorter the wavelength, the higher resolution could be obtained. In ordinary light microscope, the wavelength is in the range of 400- 700 nm. However, if electrons are used instead of light, a much shorter wavelength is obtained. Accordingly, a greater resolution could be obtained and hence a higher resolution of the electron microscopy could be achieved. The standard components and function of SEM consist of an 1) electron gun: The source of electron emission that emits electrons that pass through 2) a set of magnetic "lenses" that act as condenser lenses on the generated electron beam to focus it, followed by a terminal one that acts as objective lens controlling and directing it as required over the sample that is located in 3) sample chamber. As the electron beam falls onto the sample, variable reactions occur. Some of the surface atoms of material will acquire energy from the fallen electrons and emit their own electrons which will be called secondary electrons. These electrons will be collected by a special detector called 4) The Secondary electron detector (SED). Other electrons of the fallen beam would just reflect from sample. These are called Back Scattered Electrons which will be collected and detected by special detector called 5) Back Scattered Electrons detector. The last reaction would come from reaction with atoms that'll generate X- Ray that's detected by 6) X-ray detector. The data obtained from the Secondary electron detector SED are most indicative of the surface structure and topography of sample. Those obtained from the other detectors are more indicative and useful on the nature and type of

material itself. The data is gathered in raster scan pattern and is sent for 7) computer analysis and presented on 8) monitor that shows the image of the sample. (158) Figure 2.3 shows the SEM setup.

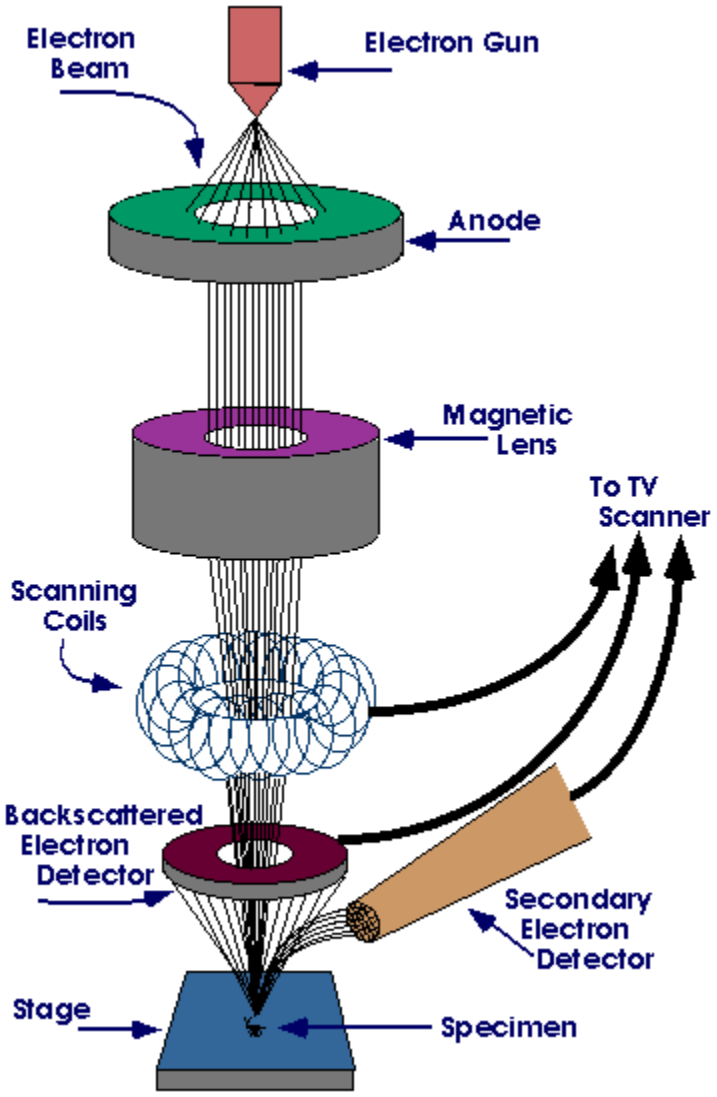

Figure 2-2 A diagram illustrating the main components of SEM (158)

2.3.3 Fourier Transform Infrared (FT-IR) Spectroscopy

The FT-IR stands for Fourier Transform Infrared Spectroscopy. As the name implies, it is an IR spectroscopy. However, it differs from ordinary IR in that it doesn't use a "monochromatic single wave length" each time for the whole spectrum of testing, but rather multiple wavelengths. In IR spectroscopy the molecule of the sample absorbs energy of specific frequency (i.e. wavelength) that alters its vibration state energy from ground to excited state. As this is bond specific, it gives information about the structure of the sample being analyzed. The amount of energy is also an indication of the amount of matter, i.e. quantitative analysis of the material can be done as well. For the FT-IR to perform multiple wavelengths testing simultaneous, it first generates a "composite" wave that interacts with the material, then "decomposes" it back to the original waves through a computerized mathematical method of Fourier Transform and hence its name is generated. With the aid of this simultaneous multiple wavelengths analysis, shorter time as well as more interaction and hence more data about the material is obtained.

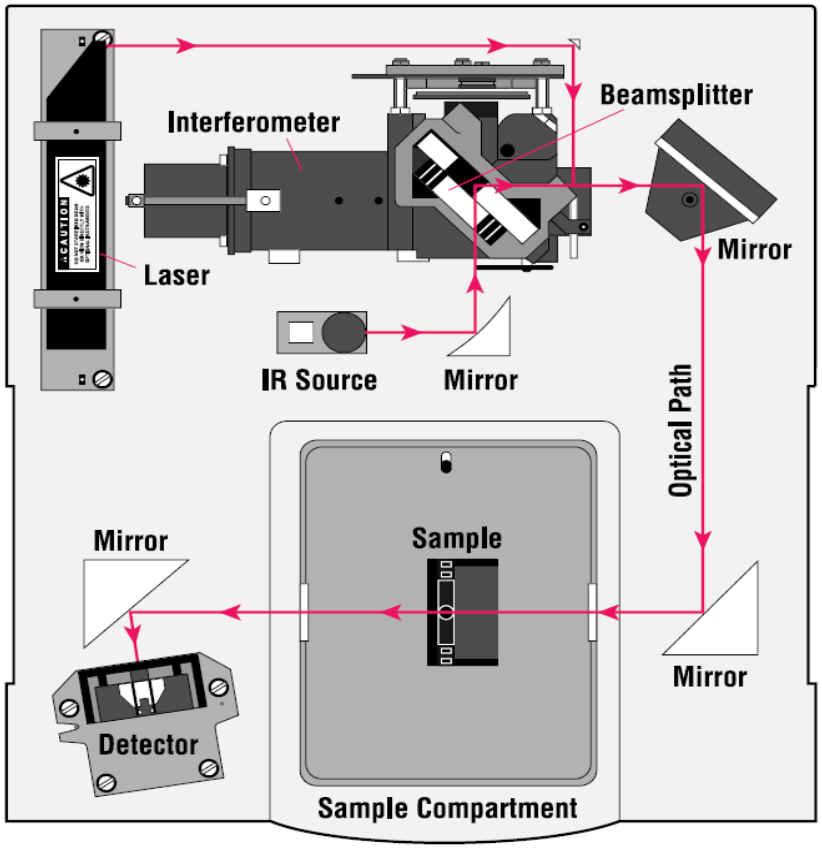

Figure 2-3 A diagram illustrating the main components of FT-IR (160)

As shown in Figure 2.4, the standard setup of the FT-IR consists of: 1) IR source that emits an IR waves into 2) Interferometer, which is the main difference between ordinary IR & FTIR setup. It consists of a beam splitter that "splits" the beam into 2 mirrors, a fixed one and a moving one that moves far and close to the splitter. The beams are reflected back from the 2 mirrors to reunite again on the splitter. If considering a monochromatic light, based on the difference of the distance cut between the 2 beams they might have variable interferences when reunite. The first interference is to superimpose having exactly crests over crests & troughs over troughs to have a maximum constructive interference and this occurs if only the two mirrors are at the same distance which is called Zero path difference (ZPD). The second one will happen when moving the mirror is at distance 1/2 (λ) and accordingly there will be a path difference between the two incidents beams, that'll bring crests of one over troughs of the other & vise versa, leading to a maximum destructive interference to occur. The last interference is the resultant of variables between them. If one considers the input of multiple wavelengths at the same time, at the "ZPD", all wavelengths will superimpose and have their maximum constructive interference leading to very high interaction as a peak (P). However, being having different (λ), each one will react differently in relative to the mirror distance and the overall will be too much lower interaction in all other distances of the mirror (Figure 2.4). The new wave (P) generated "composed" from the interaction of different wavelengths is the one used as the scanning wave that will pass to 3) Sample chamber where the interaction occurs with the sample and then interactions results to 4) detector. The data is sent to the 5) computer where it makes Fourier Transform to decompose the results of the composed wave (P) to its forming waves to draw a spectrum of them all at once that is displayed on 6) a monitor. (159)

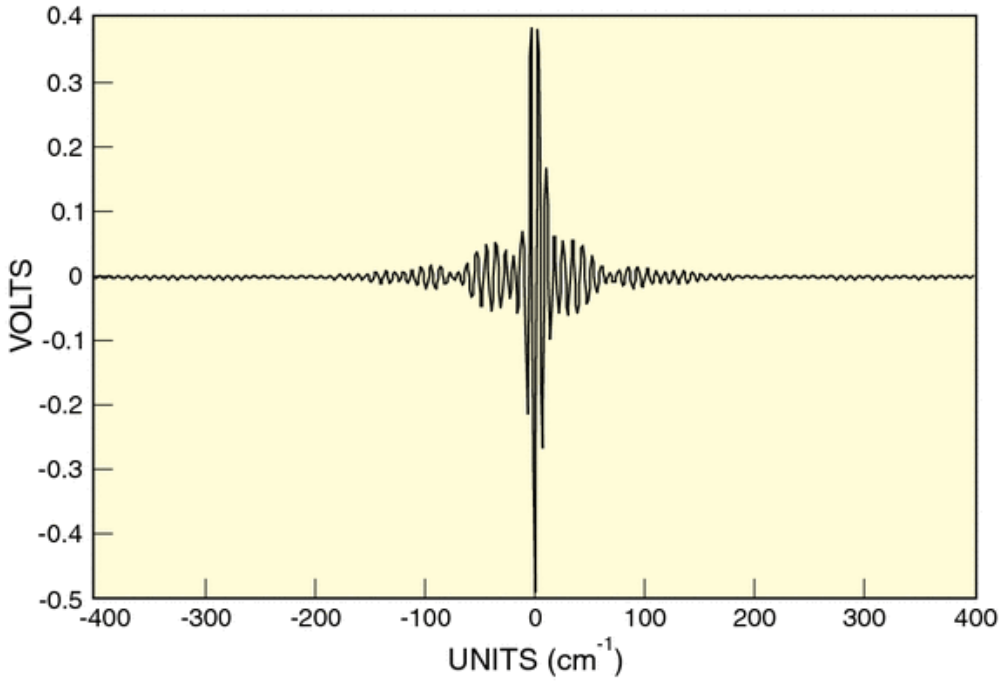

Figure 2-4 A diagram showing the output value in volts of the waves (Y axis) at different distances of the 2 mirrors (x axis), as it is obvious from diagram at zero path difference (ZPD) the highest peak is obtained and less values are obtained at other distances. The wave at ZPD nominated as P is so composed of the interaction of all wavelengths, and is used for sample analysis. (161)

2.3.4 Sample preparation for characterization

2.3.4.1 Scanning Electron Microscopy (SEM)

The samples for SEM were cut into small discs, and put by the aid of forceps on the samples sites then placed stage. Image J analysis software was then used for the analysis of the fibers sizes.

2.3.4.3 FT-IR Spectroscopy

Liquid samples were prepared by sandwiching a drop of sample between 2 NaCl plates to obtain a thin film in between. For solid samples, a small amount(2%) of the sample was mixed with

KBr pellets to obtain homogenous mixture. Part of the mixture was then placed into one bolt and screwed with the other one to have a thin film in between both of them ready for analysis.

2.4 Antimicrobial tests of the formed electrospun nanofibers

In order to determine the antimicrobial activities of the formed electrospun nanofibers, testing the effect of the nanofibers on the growth of microorganisms was performed.

2.4.1 Testing method

2.4.1.1 Bacterial Inoculum preparation

Fresh cultures of *E. coli* & *S. aureus* were prepared using muller hinton broth and incubated at 35 ± 2.5 ºC for 18 hrs. Working culture of the fresh culture of bacteria was then used for the antibacterial assessment.

2.4.1.2. Determination of the Antimicrobial Activity

The samples under test (table 2.1) were added to the bacterial suspensions. The initial count & absorption of bacterial suspension were determined. The bacterial suspensions and the samples were incubated at 35 ± 2.5ºC for 48 hrs with continuous agitation to ensure good contact between samples and suspension. (162)

The absorption as well as the bacterial count after 24 hrs & 48 hrs of exposure was determined. The bacterial count was determined using duplicates samples of the plate count technique after serial dilution of the initial suspension.

Chapter 3 **Results and Discussion**

Chapter. 3. Results and Discussion

This Chapter will present the results obtained in optimization of the electrospinning technique in the fabrication of CA nanofibers. Theses optimum conditions were then used to fabricate CA-CIT composite nanofibers. The results obtained for CA-CIT nanofibers fabrication and their full morphological and spectroscopic characterization is discussed after the optimization part. Next section describes the results obtained during the preparation of other composites namely CA with CS (CA-CS) and CA with CIT and CS (CA-CIT-CS).

3.1 Fabrication & characterization of electrospun CA nanofibers

The fabrication of CA nanofibers was performed using a solution of 5 % of CA in acetone. In order to assess the optimum conditions, a variation of the critical process parameters was made sequentially as will be discussed below in details.

Electrospining parameters effect on the fabrication of CA:

In this section, the effect of variable parameters of electrospininng process and their effect on the fabrication of CA nanofibers is discussed. These factors are summarized below:

3.1.1 Effect of solvent

3.1.2 Effect of applied voltage

3.1. 3 Effect of solution flow rate

3.1. 4 Effect of spinneret tip to the collector distance

3.1.1 Effect of solvent

The solvent choice is very important step in the electrospinning of CA. It has a great effect on the morphology of the resultant electrospun fibers. Single solvent and multiple solvents system prepared in various ratios have been reported. For example, the effect of various types of solvent systems was studied by Tungprapa et al. (163) Their study involved the use of acetone, methanol, pyridine, formic acid, chloroform, dimethylformamide (DMF) and DCM as single solvent systems. For the multiple solvent systems, they studied mixtures of acetone with DCM, methanol with DCM and methanol with chloroform as binary systems. Using acetone and mixtures of acetone with isopropanol and Dimethylacetamide (DMAc), fibers of ribbon like and others of cylindrical morphologies were obtained respectively as shown by the work of Rodriguez et al. (164) The effect of ternary mixture systems on the electrospun CA fibers were also studied. For example mixtures of acetone, DMF and trifluroethanol was studied by Ma & Ramakrishna. (165)

In our research work, three different solvent systems were used in the preparation of CA solution for electrospinning experiments. Namely (A) acetone, (B) acetic acid, and (C) a mixture of acetone with 60 % acetic acid were used. The effect of each system on the fabrication of CA nanofibers by electrospinning is described below:

3.1.1.1 Electrospining using acetone

Acetone is well known for its volatility, which is required for the electrospining process in order to obtain good nanofibers as discussed in the introduction section before. It is also well known for its capability of dissolving CA. Many of the research work on electrospining CA solutions was carried out accordingly using acetone as a solvent in the current study. (86, 163, 164, 165). Additionally, it is a readily available solvent that's produced in too large scale production. Its low price is another important factor for its use in order to obtain a final product with a reasonable price.

Chemically, it belongs to and considered as the simplest form of ketone group organic compounds. It is characterized of being a colorless, highly volatile and highly flammable solvent.

It is miscible with water, and acts as a solvent for many materials. More importantly, it is capable of dissolving citric acid as well. However, chitosan couldn't be dissolved in acetone.

The CA was dissolved in acetone for electrospinning the solution. A sheet of CA nanofibers was observed on the plate collector (aluminum foil). Figure 3.1 shows SEM images of the obtained electrospun CA nanofibers.

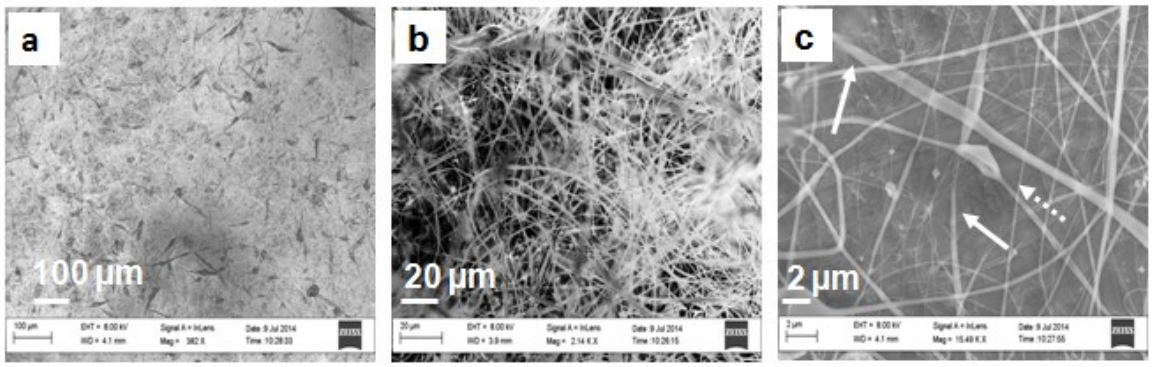

Figure 3-1 a), b & c) SEM images of electrospun CA nanofibers in acetone at different magnifications. Solid arrows refer to nanofiber, and dotted arrows refer to beads

3.1.1.2 Electrospining using acetic acid

Acetic acid was also used in electrospining experiments. It is capable of dissolving CA. Moreover, CIT also was found to be soluble in acetic acid. Additionally, dilute acetic acid can dissolve chitosan. Chemically, it belongs to and considered to be the second simplest form of carboxylic acids group of organic compounds. It is also miscible in water. It is characterized of being colorless, with a characteristic odour. In our trial to find a system that can dissolve both materials (CA and CS), and to be at the same time suitable for electrospining, acetic acid was initially used for the preparation of electrospun CA nanofibers. However, upon performing the electrospinning experiment, no nanofibers could be obtained with it even with variable process parameters, and spherical features were formed. (Figure 3.2)

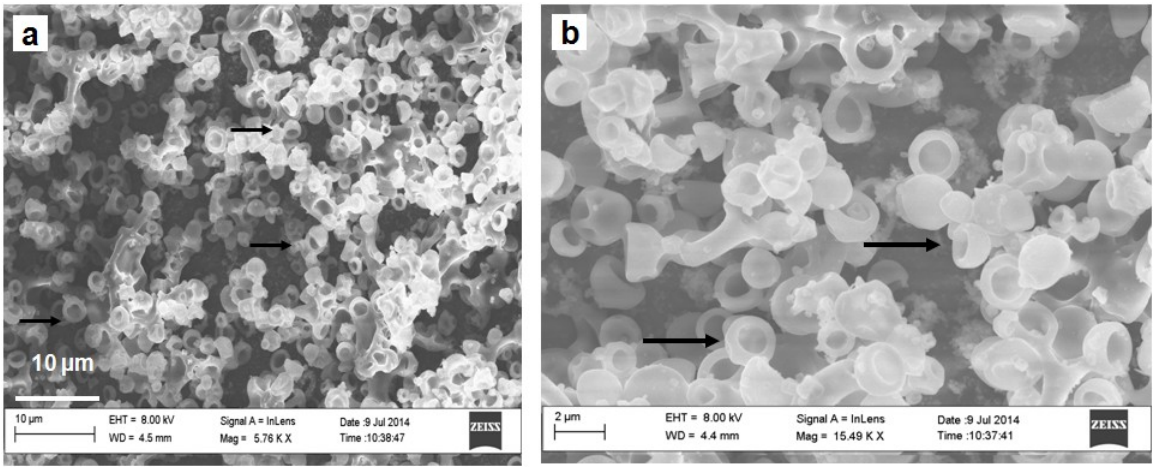

Figure 3-2 SEM image (a, large scale), and (b, magnified image) showing spherical structures (marked with arrows) of CA in acetic acid rather than nanofibers.

3.1.1.3 Electrospining using acetone/ acetic acid mixture

Based on the previous experiments, and to solve the issue of poor solubility of CS in acetone together with the poor electrospinability of CA in acetic acid and its poor solubility in water, a mixed solvent system of dissolving CA in acetone was prepared, then partial mixing of it with 60 % acetic acid in 1:1 and 2:1 ratios were prepared. Electrospinning was then performed using these new solutions. A film was observed only with 2:1 ratio and under SEM, nanofibers could be detected, with some beads within the mesh structure as shown in Figure 3.3.

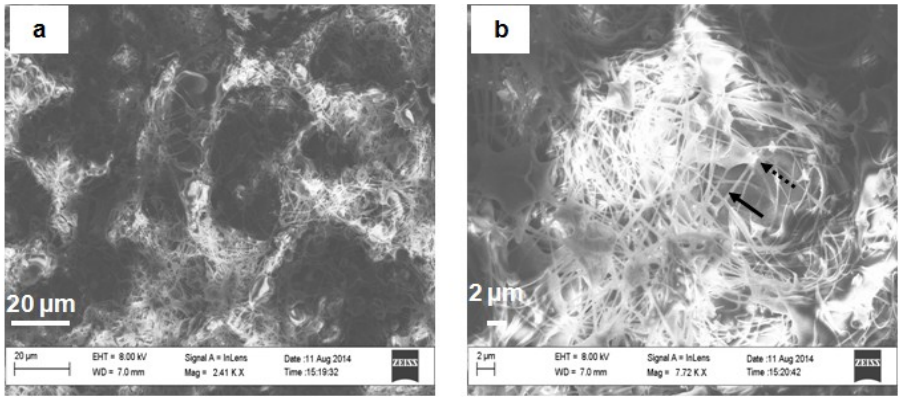

Figure 3-3 (a and b) SEM images of electrospun nanofibers of 2:1 mixture of CA in acetone with 60% acetic acid with different magnification. Solid arrows refere to nanofiber, and dotted arrows refer to beads

From the previous results, we found that the best nanofibers could be obtained using acetone as a solvent system for CA. We postulated that the system could work the same with a mixture of CA and CIT as both are soluble in acetone. However, in case of CS, we expected that the system would not work because CS is not soluble in acetone. The other option was to dissolve CA in 60 % acetic acid, which is the suitable solvent for CS. However, we couldn't obtain nanofibers from this system and instead nanospheres were observed rather than nanofibers. The variation of process parameters did not allow us to obtain better form of nanofibers.

Table 3-1 Properties of acetone & acetic acid.

Property	Boiling point	Viscosity	Surface Tension	Dipole moment
Acetone	56 °C	0.295 cP	23.70	2.91 D
Acetic acid	118 to 119 °C	1.22 cP	27.60	1.74 D
Water	100 °C	1 cP	71.97	1.85 D

By comparing the various properties of acetone and acetic acid (Table 3.1) a possible explanation could be proposed. Initially, the results obtained are consistent with those obtained by Santi Tungprapa *et al.* (163) on studying the effect of solvent on electrospinning of CA in single solvent systems of formic acid "very close to acetic acid", dimethylformamide (DMF), dichloromethane (DCM), methanol, pyridine and chloroform. They described the formed nanostructures as" discrete beads" similar to what we obtained (Figure 3.2). Again, the results would highlight the importance of solvent properties of viscosity, surface tension and dipole moment as was reported by the same group and also by the work on Polystyrene (PS) by Jarusuwannapoom *et al.* (166) and Pattamaprom *et al.* (167) A consensus between all results that a reasonable high dipole moment and low surface tension and viscosity are required for successful electrospining leading to fiber formation. Acetone has higher dipole moment, lower surface tension and lower viscosity than acetic acid.

In this regard, we should analyze the various factors affecting the fate of the electrospun solution till it reaches the plate collector. As shown in (Figure 3.4), these factors can be external, such as applied voltage of the electric field and the mechanical force exerted by the syringe pump, which determines the polymer solution's flow rate. Internal factors on the other hand, also play an important role either directly or indirectly. For example, the dipole moment of the solvent

molecule is expected to affect the degree to which the solution is affected by the applied voltage. If the dipole moment is higher, larger effect by the applied voltage can be expected. The other intrinsic factors include surface tension and viscosity. Obviously, these form resistance to the external factors and to the stretching and moving triggered by them (158,159).

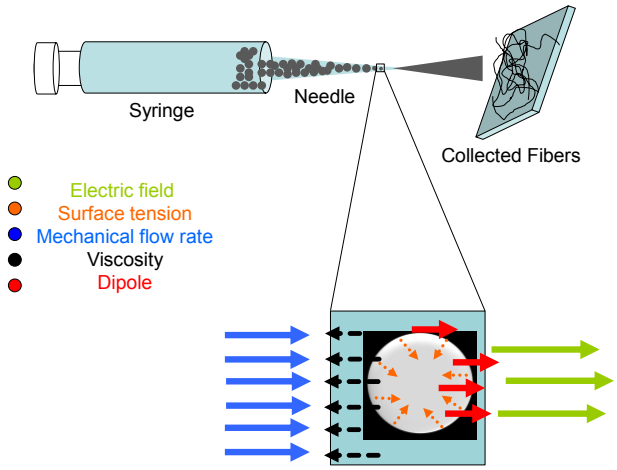

Figure 3-4 Factors and forces acting on a solution when electrospun. The resultant sum of all of these factors determines the fate of the solution. Some factors are external such as applied voltage of electric field and mechanical flow rate, while others are intrinsic such viscosity and surface tension.

As acetic acid has higher viscosity, it has higher resistance to get moved by the electric field and by the syringe pump as well. With its higher surface tension, it has higher tendency to be deposited on the plate collector as droplets, spherical form rather than being stretched into fibers with the aid of electric field. Moreover, with its higher boiling point, it wouldn't vaporize as fast as required and therefore would stay with the polymer longer time affecting its properties. As a result, spherical droplets rather than fibers are obtained. Even when we tried to optimize the different electrospinning parameters such as applied voltage, solution flow rate and tip to collector distance, the same results were observed.

On the other hand, acetone has lower viscosity and lower surface tension as well. Accordingly, it has fewer tendencies to be deposited as droplets and is more affected intrinsically to get stretched into fibers. Also as it has higher dipole moment than acetic acid, it can be affected more by the

applied voltage. Additionally, its boiling point is low and fast enough to get vaporized leaving the polymer to solidify and being collected as fibers on the plate collector. However, it is worth mentioning that the low boiling point and as reported with other studies (Jaeger *et al.* (168) and Liu *et al.* (169)) had a drawback of frequent clogging of the polymer solution at the needle tip. Frequent stopping in collection and cleaning the tip was necessary to have a thick fiber film on the plate collector covered with aluminum foil.

For the mixture solvent, consisting of acetone and 60% acetic acid in water, only with the ratio of 2:1 nanofibers again could be obtained. The 1:1 ratio, however didn't yield any fibers and the same results as with acetic acid alone was obtained. From the effects illustrated of both acetone and acetic acid discussed above, we can postulate that only when acetone has a higher reasonable ratio (2:1 in our case), nanofibers could be obtained.

Other process parameters such as the flow rate, needle to collector distance in addition to the applied voltage, were found to affect the fiber shape and size distribution as described in the work of Konwarth et al. (170) and also by Theopisti and Charalabos (171)

The thickness of the formed fibers was reported to increase with the increase in humidity as described by De Vrieze et al. They also addressed the effect of temperature on the fibers' thickness. (172).

The effects of other parameters; the applied voltage, solution flow rate and tip- collector distance are discussed in next sections.

3.2. 2 Effect of voltage

In order to assess the effect of voltage on the fabrication of CA nanofibers, electrospun at different voltages was performed. Voltages used were in the range of, 10, 12.5, 15 and 17.5 Kv (Figure 3.5 and Figure 3.6).

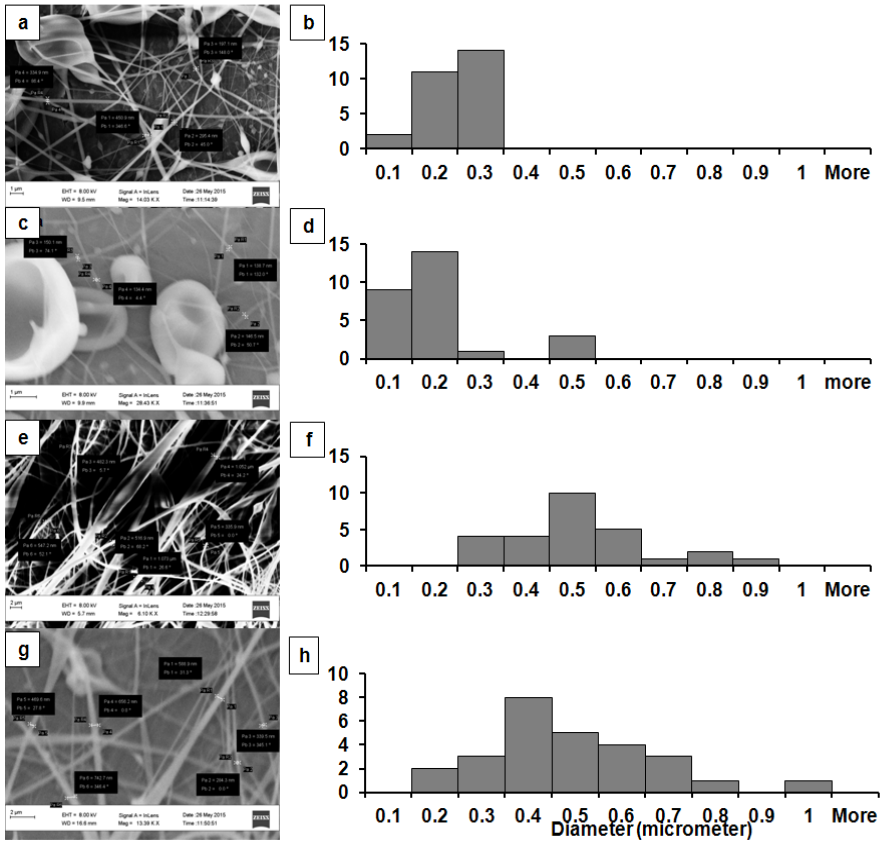

Figure 3-5 SEM images of CA nanofibers and corresponding fiber diameter histogram showing the effect of voltage on the CA fiber thickness: a) , b) at 10 kv, c), d) at 12.5 kv, e), f) at 15 kv and g), h) at 17.5 kv, respectively.

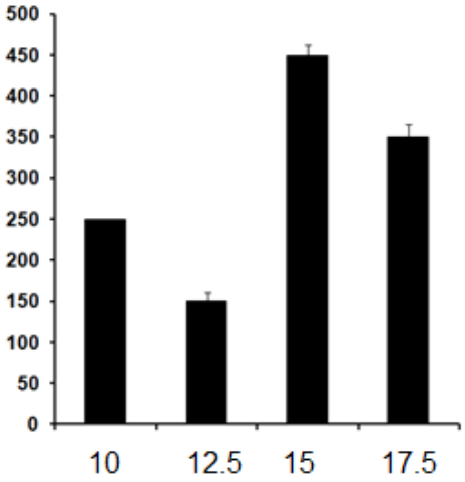

Figure 3-6 Distribution of the average thickness of the obtained CA electrospun nanofibers at different applied voltage. (Data based on the mean of the median)

Table 3-2 Effect of voltage on CA fiber, beads formation and fibers thickness

Applied voltage	Nanofibers formation	Beads formation	Fiber Thickness
10	Yes	High	100 to 300 nm
12.5	Yes	High	100 – 200 nm
15	Yes	Too low	200 to 900 nm
17.5	Yes	Low	100- 800 nm

Based on the above mentioned results, the best uniform and bead free electrospun CA nanofibers were obtained with 15 kv applied voltage. Although at all applied voltages, nanofibers could be obtained, however, when lower voltages were applied (10 and 12.5 Kv), dominating beads in the electrospun nanofibers were observed. The beads where almost undetectable and reached the minimum when 15 kv was applied. On the other hand, when the applied voltage was raised to 17.5 kv, the beads where observed again which indicates that the 15 Kv is the optimum voltage to form uniform and bead free CA nanofibers.

As shown before in Figure 3.4, we have demonstrated the equilibrium of the multiple factors affecting the polymer solution to reach optimum conditions for formation of electrospun CA nanofibers. Too low and also relatively high applied voltage led to more beads formation (Table 3.2). If a too low applied voltage was used, non-efficient continuous breaking of surface tension occurred. A variation between stretching into fibers and the tendency to be in droplet form could exist. This leads to the formation of both nanofibers, when enough accumulation of energy exists to stretch and break the surface tension and also to bead formation when the applied voltage together with the mechanical power of the syringe pump can overcome the gravitational force to move the polymer solution in spherical droplets rather than stretching it into fibers. Higher voltage above the optimum range also led to higher bead formation. Although less than that with low voltage, but still observed. This again indicates an optimum range around 15 kv where nanofibers with minimal beads could be obtained.

Not only the presence and absence of beads that was affected by the applied voltage, but also the fiber thickness was affected too. As shown in (Table 3.2), the minimum thickness range was observed when 12.5 Kv applied and the thicker nanofibers were obtained with 15 kv. An

expected result of the nanofiber thickness relationship to the applied voltage can be postulated as the higher the applied voltage, the thinner the formed nanofiber as discussed before. However, the relationship is not that straight forward in our case (Figure 3.6).

This could be attributed to another very important factor which is related to the beads formation. When heavy beads were formed, a lot of the mass that should be stretched into fibers and giving it its thickness, was aggregated in a form of beads, leaving less material to get stretched, and accordingly, leading to thinner fibers. As best distributed material and lowest bead formation occurred, the nanofiber obtained with 15 kv was the thickest. Moreover, the fibers obtained at17.5 Kv had the second lowest number of beads and had the second thickest fibers too. The fibers obtained at both 10 and 12.5 Kv had the highest number of beads and thinnest fibers. However, when excluding the beads formation factor by grouping them into high beads and low beads, the results in each group again align with the known previously discussed effect of the applied voltage on the fiber's thickness. For those having SEM images showing heavy beads, as with the case of 10 and 12.5 Kv, the fibers were thinner when higher voltage was applied i.e. in case of 12.5 Kv which was thinner than the case with 10 Kv. Also in those having low beads formation, the higher the voltage the thinner the fibers i.e. in case of 17.5 Kv which was thinner than the case with 15 Kv.

3.2.3 Effect of solution flow rate

In order to assess the effect of flow rate on the fabrication of CA nanofibers, electrospinning at different solution flow rates was performed. The solution flow rates used were, 3mL/hr, 5mL/hr and 7 mL/hr (Figure 3.7, 3.8 and Table 3.3).

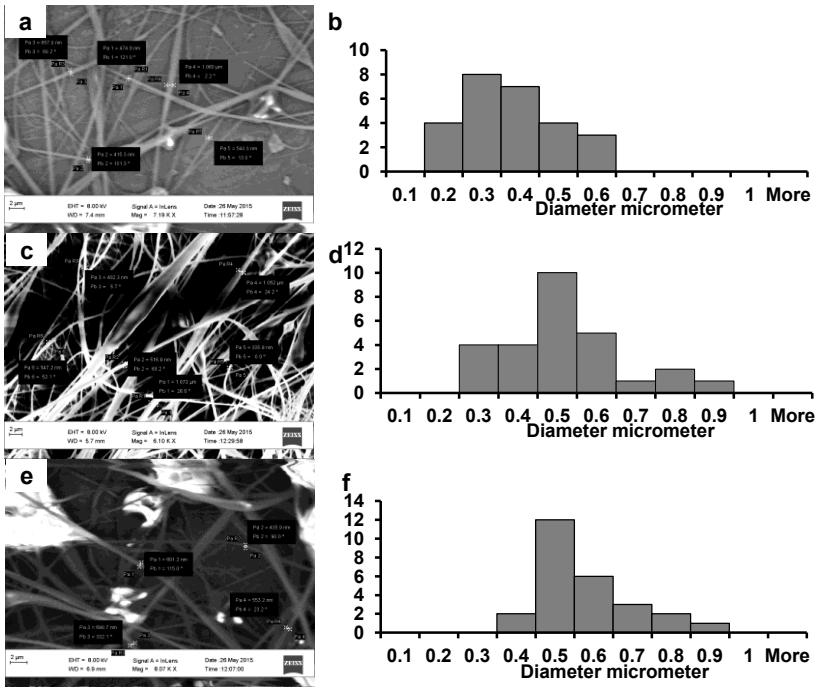

Figure 3-7 SEM images of CA nanofibers and corresponding fiber diameter histogram showing the effect of solution flow rate on the fiber thickness: a), b) at 3 mL/ hr ,c),d) 5mL/hr and e, f) 7 mL/hr.

Table 3-3 Effect of solution flow rate on fiber, beads formation and CA fibers thickness

Flow rate	Nanofibers formation	Beads formation	Fiber Thickness
3 mL/hr	Yes	Medium	100 to 600 nm
5 mL/ hr	Yes	Too low	200 to 900 nm
7 mL/ hr	Yes	High	300 to 900 nm

From the above mentioned results, we found that the best CA electrospun nanofibers were obtained at a solution flow rate of 5 mL/ hr where the lowest beads were observed (Figure 3.7c and d). A relatively low beads where also observed upon using a solution flow rate of 3 mL/hr (Figure 3.7 a and b) in comparison with those obtained at 7 mL/hr (Figure 3.7 e and f) which showed the highest in terms of beads formation.

As discussed earlier in the introduction, the solution flow rate has an effect on the beads formation and the thickness of the formed electrospun fibers. The higher the solution flow rate, the higher the tendency of the formation of beads and the thicker the fibers. The high solution flow rate makes more solution available at the needle tip; accordingly, more solution is exposed to the applied voltage leading to thicker fibers. The same suggestion could be applied to the formation of beads as more solution was transferred at once leading to droplet passage and beads formation (Table 3.3).

A comparison between the low solution flow rate of 3 mL/ hr, optimum flow rate of 5mL/hr and the high flow rate 7 mL/ hr, showed that by increasing the solution flow rate, the nanofibers got thicker and the tendency of the formation of beads was increased. Flow rates 5 mL/hr and the 7 mL/ hr have led to the formation of fibers with almost the same thickness, although it was expected that the flow rate of 7 mL/hr would lead to the formation of thicker fibers. However, as previously discussed under the section of effect of voltage, the direct relationship was valid when the beads were excluded. As the flow rate of 7 mL/hr led to fibers with higher beads, thinner fibers than expected were formed. They were in the same range as nanofibers formed with lower flow rate of 5 ml/hr. However, both of the flow rates were thicker than the slow rate of 3 mL/hr.

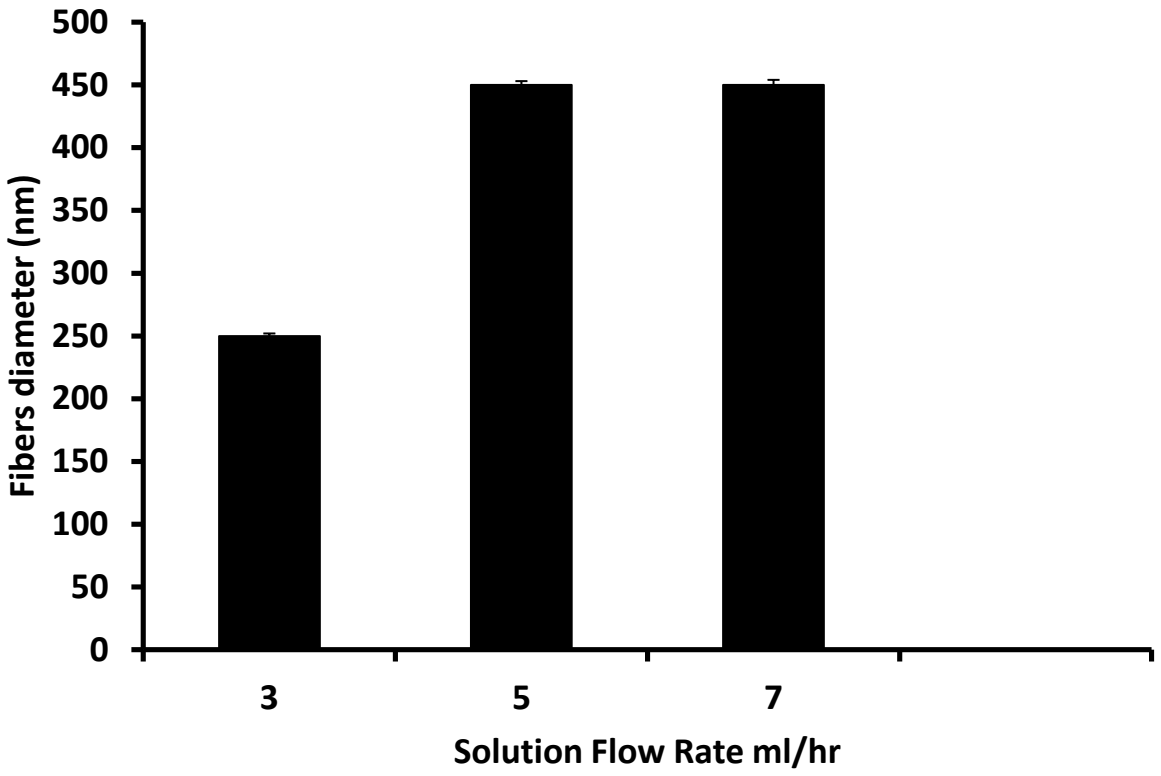

Figure 3-8 Distribution of average thickness of obtained CA nanofibers with various solution flow rates. (Data based on the mean of the median)

3.2.4 Effect of tip to collector distance

In order to assess the effect of the distance between the needle tip to plate collector on the fabrication of CA nanofibers, electrospining experiments at different distances were performed. The distances used were adjusted to 3, 5 and 7 cm. Figure 3. 9 shows SEM images and their corresponding fiber diameter histograms of CA electrospun nanofibers that were collected at 3, 5, and 7 cm, respectively.

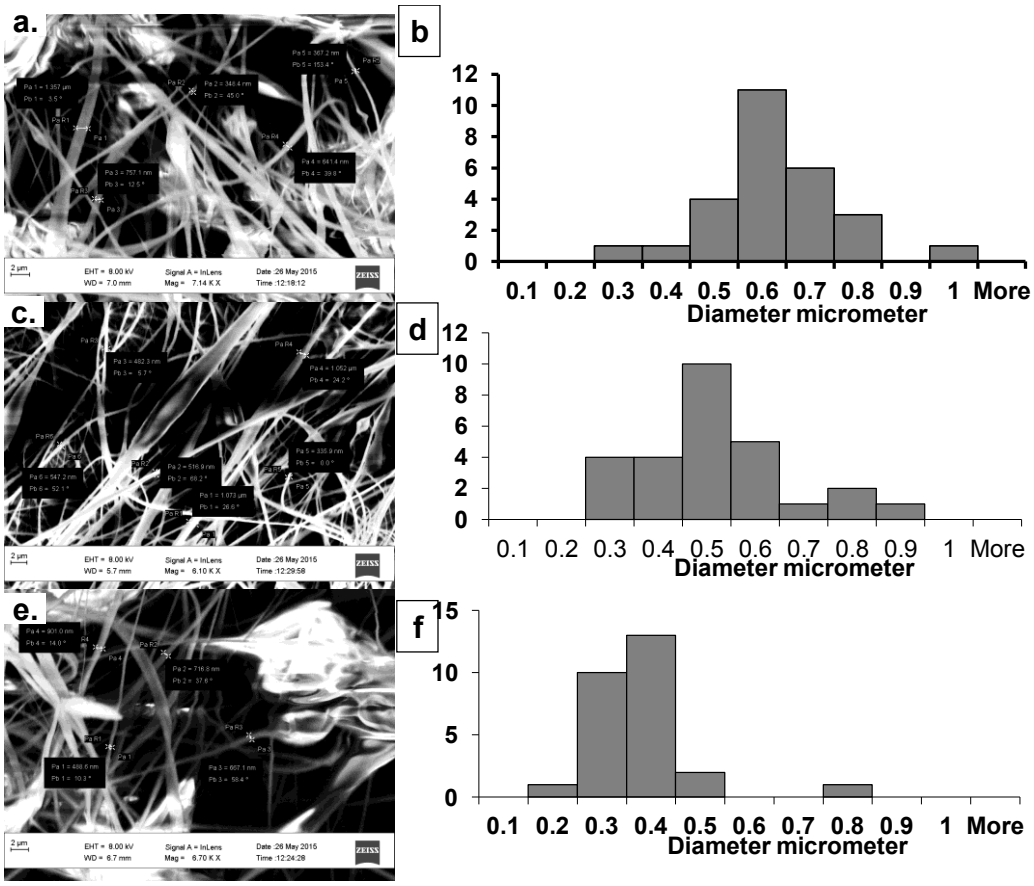

Figure 3-9 SEM images of CA electrospun nanofibers and corresponding fiber diameter histograms showing the effect of tip to collector distance on the fiber thickness. The fibers were collected at (a, b) 3 cm; (c, d) 5 cm and (e, f) 7 cm.

Table 3.4 summarizes the effect of the distance between the tip to the plate collector on the morphology of the CA electrospun nanofibers that are collected at 3, 5, and 7 cm distances.

Table 3-4 Effect of tip - collector distance on the fiber, beads formation and fibers thickness

Distance	Nanofibers formation	Beads formation	Fiber Thickness
3 cm	Yes	High	200 to 800 nm
5 cm	Yes	Too low	200 to 900 nm
7 cm	Yes	High	100 to 500 nm

From the above results, we found that the best CA electrospun nanofibers were obtained at 5 cm distance from the tip to the plate collector where the lowest beads were observed. The other two distances, 3 and 7 cm, respectively, led to more beads formation in comparison to the 5 cm.

As discussed earlier, the tip to collector distance has an effect on the thickness of the formed nanofiber. In this regard, the larger the distance is, the thinner the formed fibers will be. This can be due to stretching the same amount of solution over larger distance. Accordingly, a thinner fiber is obtained.

The diameter comparison between CA nanofibers obtained at different distances shows that by increasing the distance, the nanofibers get thinner as shown in (Figure 3.10).

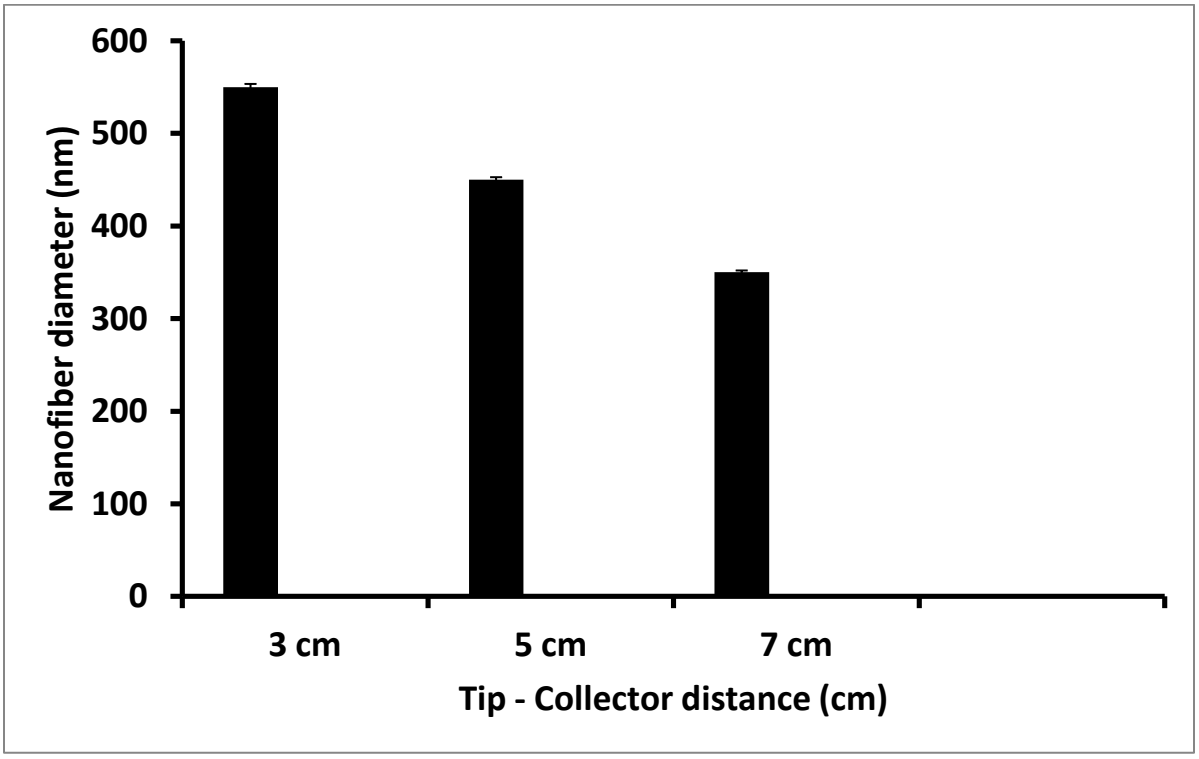

Figure 3-10 Distribution of average thickness of obtained CA nanofibers with various tip to collector distance. (Data based on the mean of the median)

3.2 Electrospinning and Characterization of CA-CIT composite nanofibers:

3.2.1 SEM and morphological analysis of the formed CA-CIT nanofiers:

As discussed earlier, the antibacterial effect of CIT is well known. Its enhancing effect on wound healing was also demonstrated in the introduction chapter. As an approach to add these interesting properties to the CA nanofibers, a composite nanofiber of CA together with CIT was fabricated. The fabrication of CA with CIT nanofibers, was performed using a solution of 5 % of CA & 10 % citric acid (sample 2 in Table 2.1). As both materials are soluble in acetone, it was used and no issue of solvent system existed. Based on previously discussed study performed on the CA nanofibers alone, the optimum conditions based on the results were used which are the use of acetone as the solvent, 15 Kv as the applied voltage, 5 mL/ hr as the flow rate & 5 cm as the tip to collector distance. The formed nanofibers were then characterized by SEM and later by FT-IR to prove the chemical composition & possible interactions. Finally, to assess the antibacterial effect of the formed nanofibers, the antibacterial study was performed and the results are discussed in section 3.4.

Based on the SEM images obtained (shown in Figure 3.11), the nanofibers of CA- CIT, interestingly, appeared with no beads. The film was characterized being a dense network of nanofibers. The thickness varied between 100-700 nm.

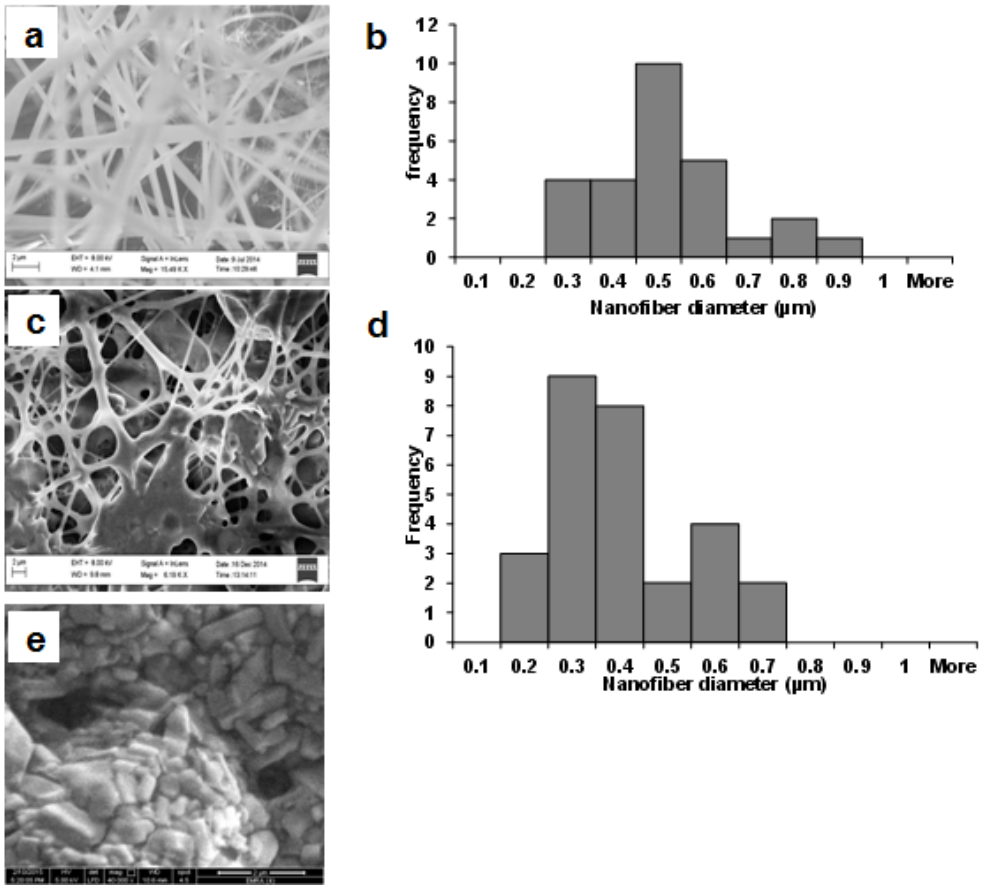

Figure 3-11a) SEM image of electrospun CA nanofibers, b) CA nanofiber size distribution histogram c) SEM image of electrospun CA-CIT nanofibers, d) CA-CIT nanofiber size distribution histogram, and e) SEM image of CIT solution after exposure to electrospinning conditions.

Some observations are obvious from the SEM images in Figure 3.11. The first observation is the complete absence of beads in CA-CIT nanofibers in Figure 3.11c in comparison to CA alone in Figure 3.11a. The second observation is that the formed CA-CIT nanofibers are more uniform in size distribution and thinner than those of CA alone as shown in Figure 3.11d and c, respectively. The third observation is a collection of thick material at the intersections of the nanofibers as can be seen in Figure 3.11c. CIT solution did not form electrospun nanofibers, but instead formed aggregates as shown in Figure 3.11e.

The absence of beads

As stated earlier, the solution of CA at the optimum electrospinning conditions could form nanofibers with minimal beads. However, it was obvious that even this minimal number of beads completely disappeared with the addition of CIT to the CA solution. In order to explain this observation, we have to track the possible changes that led to this improvement. With the addition of CIT to the CA solution, two changes were expected. The first is the increase in conductivity of the solution due to the addition of the conductive material of CIT. The second effect is the increase in solution viscosity by the effect of the added CIT material.

If we consider the first parameter, conductivity, we have mentioned before that the increase in solution conductivity enhances the effect of the applied voltage leading to better spinablity. This will accordingly lead to formation of better fibers with no beads as observed.

The second change that can lead to better nanofiber formation without beads is the increase in solutes mass and concentration by addition of CIT. The addition of CIT would lead to increasing the viscosity of the solution. The viscosity acts against the flow rate thus aiming to resist it and slow it the flow of the solution down. Accordingly, increasing the flow rate leads to increasing the beads formation as discussed in the introduction section, it is then logic to find a decrease in the beads formation while decreasing the solution flow rate due to the increase in viscosity.

The net result is a "slowing down" effect that represses the formation of beads and allows better exposure to the applied voltage which is already enhanced as an effect caused by the increased conductivity of the solution and better spinnability with no beads is finally obtained.

Presence of thick material at fibers intersections

As mentioned before from the SEM images in Figure 3.11, that the CA-CIT nanofibers obtained were without beads and were thinner than those of CA alone. (Table 3.5). It was also mentioned that the SEM images showed a mass of material at the intersections of the formed nanofibers. In this section we'll discuss the possible explanations for these observations.

At First, we need to assess the possible mechanisms of fiber formation of the CA-CIT composite mixture. Two possibilities exist; (i) a formation of new chemical entity by chemical interaction

from which the nanofibers are formed. (ii) Formation of CA nanofibers as a backbone to which CIT molecules are bonded or deposited on top.

Table 3-5 Fiber , beads formation and fibers thickness in electrospun CA & CA-CIT

Composition	Nanofibers formation	Beads formation	Fiber Thickness
CA	Yes	Too low	200 to 900 nm
CA-CIT	Yes	No beads	100 to 700 nm

The formation of new chemical entity has too little probability. Revising the chemical structure of both compounds could help (the chemical structures of each material is shown in Figure 2.1). Theoretically, CIT is an acid with three free carboxylic (-COOH) groups and one free hydroxyl (-OH) group. These COOH groups could in principle react with the free OH group of CA to form an ester bond. However, practically it is not likely to happen.

With a simple look at the chemical structure of both compounds (CA and CIT), one can clearly see the large size of the compounds especially that of CA. It is easily observed that the free OH group of the CA molecule is surrounded with the two groups of acetate from the two sides. The other direction is completely blocked with the two acetates plus the ether linkage of the two molecules of the polymer. On the other hand, by looking at the CIT and its large size and multiple branching and functional groups, it is clearly understood that a steric hindrance effect is prevalent and there is a too little possibility – even impossible- for a chemical intermolecular CA-CIT interaction to occur. This was also proved by the FT- IR spectrum of the formed nanofibers. The FT- IR didn't show significant change suggesting the formation of the new ester bond (Figure 3.13).

Accordingly, no new molecule is formed and the observed nanofibers are most likely formed from CA to which CIT bonded or deposited. Clearly, the compound which forms the nanofibers is CA alone and not the CIT. It is worth mentioning that CIT alone is not spinnable and could not form nanofibers on its own as shown in Figure 3.11e and when spinned with other materials as will be illustrated in next sections. Moreover, it is clear that the behavior of CIT when exposed to electrospining conditions is to form a dense mass over the electrospun area (Figure 3.12). This brings in the possibility of the formation of CA nanofiber over which CIT is deposited. This

postulation explains also the other important observations of the formation of dense network and the deposition of thick material at the fibers intersections which is greatly similar to CIT when electrospinned. Additionally, it was clear physically, that the material once exposed to water, that an integer film instantaneously formed and separated from the collection foil. This wasn't the case when CA alone was used.

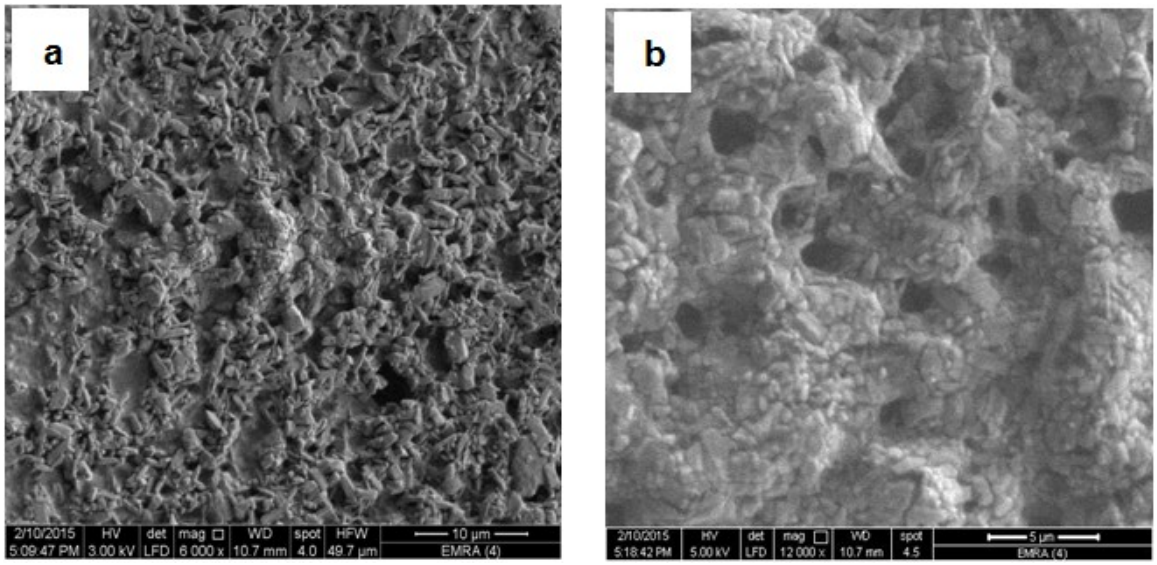

Figure 3-12 SEM image of CIT solution in acetone when subjected to electrospinning conditions showing clumps of mass

Thus, we can suggest that CA nanofibers are formed over which CIT is deposited and gets solidified as solvent evaporates, resulting in holding the nanofibers together with the mass at the fiber intersection points as shown in Figure 3.11c.

Another very important scenario for this film formation, in addition to the deposition of CIT at the fiber intersections, is the formation of CA nanofiber backbone to which the CIT is bonded by hydrogen bonding. This postulation will be discussed in detail under the FT-IR analysis in following section.

3.2.2 FT-IR analysis of the formed CA-CIT nanofibers

In order to prove the chemical structure of the used materials and to assess any possible intermolecular interactions, FT-IR was performed. The FT-IR of CA alone, CIT alone and the CA-CIT nanofibers are discussed below in details.

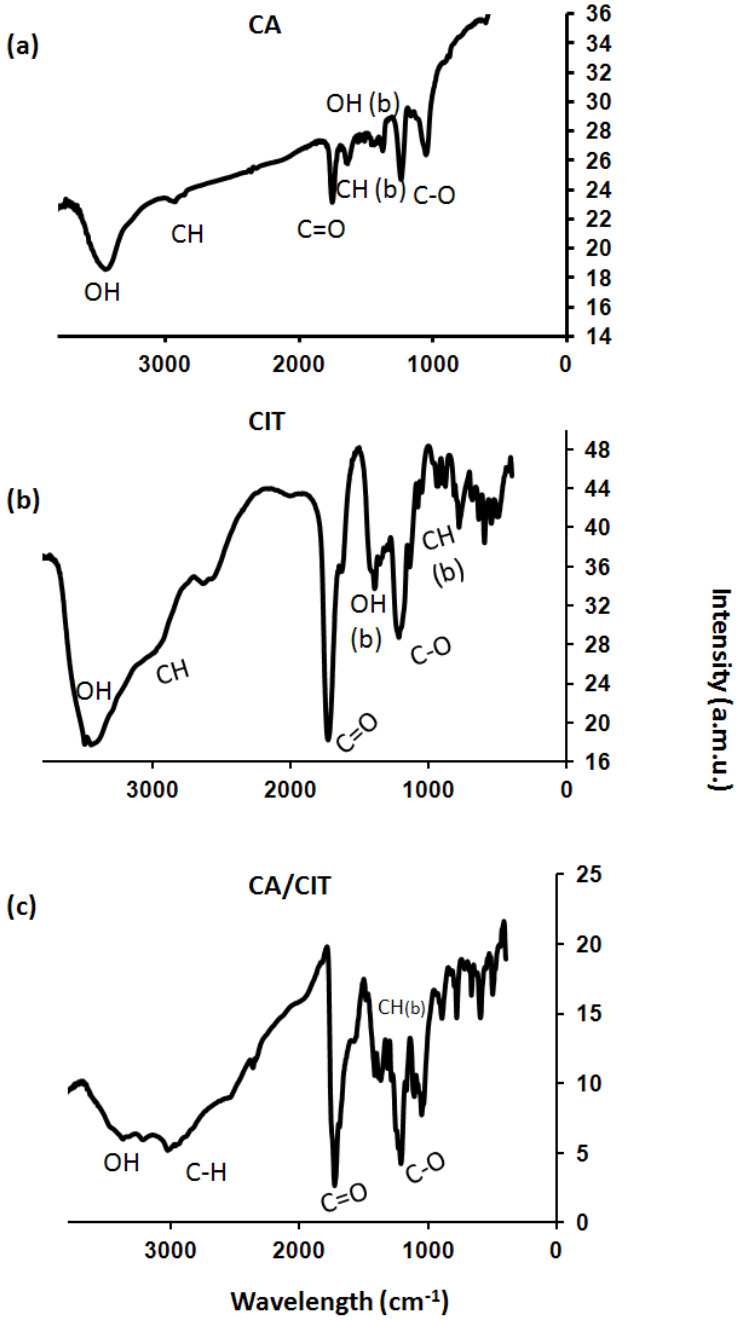

Figure 3-13 FT-IR analysis spectra of a) Electrospun CA, b) CIT and c) Electrospun CA-CIT.

FT- IR of CA alone

In reference to the chemical structure and FT- IR spectrum of CA shown in (Figure 3.13 a), one can observe the very characteristic peak of the ester carbonyl group stretching at 1740cm^{-1}. The left hand shift to higher energy of 1740 cm^{-1} instead of 1720 cm^{-1} is most probably due to increased double bond character of the C=O of the ester over the normal ketone group. This can be attributed to the O atom that causes an inductive electron withdrawal and so more electrons exist at this point leading to the double bond character and so requiring higher energy for bond excitation demonstrated by the left shift. In addition, the ester bond is proofed more with the two characteristic peaks of its OH group stretching; one peak appearing at 1050 cm^{-1} (representing the single bond of CH_2 - O) and another peak appearing at 1230 cm^{-1} (corresponds to of O-C=O). The later one increased energy is attributed also to the same effect as described with the ester carbonyl. A close absorption at 1159 cm^{-1} comes from the ether bonds stretching, the external (the polymer bond) and the internal one (the cyclic bond). Another characteristic strong peak of the stretching of secondary alcohol free OH group is also clear at around 3500 cm^{-1}. At around 3000 cm^{-1}, another peak of the aliphatic C-H stretching is also obvious while the peaks of the bending appear at 1450 cm^{-1} and 1370 cm^{-1}. Below 1000 cm^{-1} are considered the compound fingerprint. (173)

FT- IR of CIT alone

By careful analysis of the FT-IR spectrum of CIT (Figure 3.3 b), the very characteristic peak of carbonyl group stretching appears at 1720 cm^{-1}. It is also clear that there is a very high intensity of the peak as three groups exist in molecule. The peak of stretching the C-O of the OH group of the tertiary alcohol appears at 1150 cm^{-1} while the characteristic strong stretching peak of the OH group itself is observed at around 3500 cm^{-1}. At around 3000 cm^{-1}, the peak of aliphatic C-H stretching is also obvious while the peak of the bending appears at 1450 cm^{-1}. Below 1000 cm^{-1} are considered the compound fingerprint. (173)

FT-IR of CA - CIT electrospun nanofiber

As appears from the spectrum (Fig. 3.3 c), at 1720 cm^{-1} the stretching of the carbonyl group of the ester and COOH of CA and CIT respectively appear. The peaks of the stretching of the C-O representing the ester OH groups of CA appear also at 1050 cm^{-1} and 1220 cm^{-1}. While that of

tertiary alcohol of CIT appears at 1110 cm^{-1}, and another one at 1159 cm^{-1} comes from the ether bonds. A very interesting and significant broad peak appears between 3300 cm^{-1} and 3500 cm^{-1} representing the stretching of OH groups and overlapping with the peak of the aliphatic C-H stretching (at ~3000 cm^{-1}). The peak of the C- H bending appears at 1420 cm^{-1} and 1370 cm^{-1}. Below 1000 cm^{-1} are considered the compound fingerprint. (173)

Based on the above mentioned analysis, we have three important observations to consider. First is the increase in the intensity of the C=O and C-O peaks in comparison to the CA FT-IR alone. This could be attributed to the contribution from the CIT common groups with CA which are the carbonyl and C-O of the OH groups.

Yet the most important observation regards the large broadening of the OH group which signifies a hydrogen bonding effect. (173)

The importance of this observation is that it postulates a cross-linking observation that may also be explained by the formation of this hydrogen bond. As the CIT has two terminal COOH groups, these can make it acting as a "bridge" linking together two chains of CA polymer together. Some of the proposed configurations of this cross-linking are illustrated in (Figure. 3.4). This also matches with what we found in the formation of the intact film that separates from the collection foil by exposure to water.

From the previous results and discussion, we suggest that the two scenarios took place. i.e. part of the CIT is physically deposited on the formed nanofibers and acted as " cement material" and part of it formed hydrogen bonding with CA and cross-linking the CA nanofibers together. This postulate covers all the observations obtained from both physical characteristics of the formed nanofibers film together with the obtained SEM images and FT- IR results.

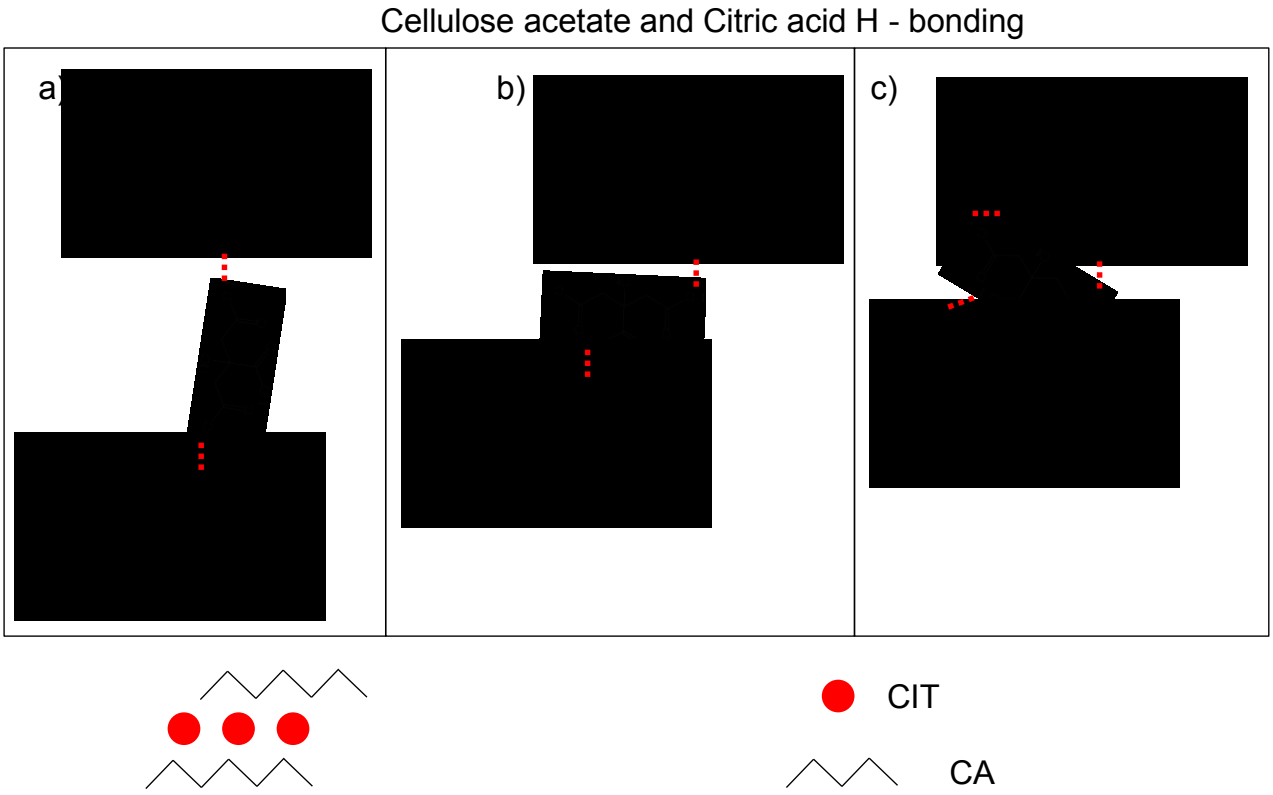

Figure 3-14 Cross - linking of two chains of CA with CIT via intermolecular hydrogen bonding (represented by dotted lines). (a) the CIT molecule is titlted perpindicular to the CA horizontal axes, (b) the CIT molecule is parallel to the CA molecular axes, and (c) the CIT molecule is tilted with an angle with repsect to the CA molecular axes.

3.3 Electrospinning and SEM Characterization of other CA based composite nanofibers

As mentioned before, the antibacterial effect of Chitosan (CS) is well known. As another approach to add these antibacterial properties to the CA nanofiber, preliminary trials to fabricate other CA composites with CS only (section 3.3.1) and mixture of CS, & CIT (section 3.3.2) are presented respectively. The FT- IR analysis of these composites was performed too and the results are presented in (section 3.3.3).

3.3.1 Electrospinning and SEM Characterization CA/CS composite nanofibers:

We had two challenges in this attempt. The first challenge we met was to have a common solvent system to both of the used compounds. The second was to successfully obtain nanofibers from this solvent.

For the first challenge of solubility, it was difficult because solubility of CS is very limited and only could be dissolved in dilute acids with water. It is insoluble in common organic solvents, including acetone which we used for the main polymer forming CA nanofiber. On the other hand, CA is not soluble in water. In order to overcome this challenge, separate solutions of CA in acetone were mixed in different ratios with solution of CS in 60 % acetic acid. By this method, we could bring both polymers in the same solvent system without precipitation and overcome the first challenge of solubility.

The second challenge was the spinnability of the mixture solution. As discussed before under the effect of solvent on the electrospinning of CA solution, it is soluble in acetic acid, however, no nanofibers could be obtained from this solvent system (Figure 3.2). We used the same approach in solving the solubility challenge to solve the spinnability challenge by using a mixture of CA in acetone with 60 % acetic acid. Again, as previously shown in (Figure 3.3), nanofibers could be obtained using this solvent system. Accordingly, we proposed that this system and its mixing way will be capable of forming nanofibers if CS is added to solution. However, no nanofibers could be formed even by varying electrospining parameters (Figure 3. 15).

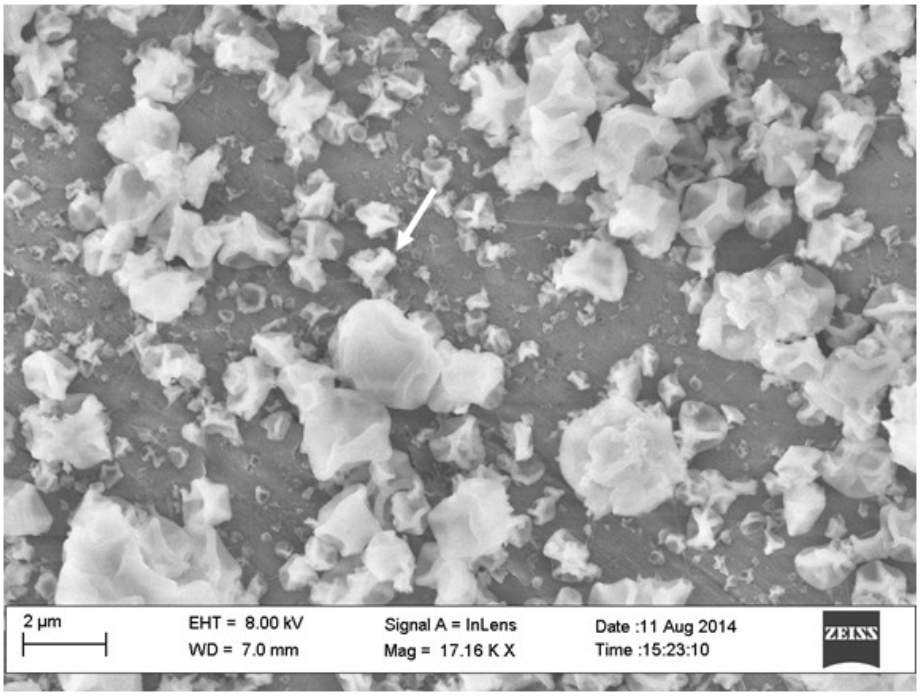

Figure 3-15 Electrospun CA/CS SEM image. Arrow indicates aggregated features (clumps) rather than fibers. Electrospinning parameters used are 15 kv, 5 ml/hr and 5 cm distance.

As we've mentioned before, no nanofibers could be obtained using CA/CS solution. Only aggregated features (clumps) were found. We were expecting that as system worked for nanofiber formation when CA alone was used, that the addition of CS won't affect the spinnability and the nanofibers would form. However, this did not happen. A clear observation during CA/CS solution preparation was the significant increase in its viscosity. It is very characteristic property of CS that its solutions have high viscosity. Both solutions of CS, alone in acetic acid, or when mixed with CA in acetone were viscous. As mentioned before, (Figure 3.8) the viscosity is one of the resistant forces acting against the spinnability of the polymer solution by the effect of the applied voltage. As the viscosity increases beyond the optimum limit it affects the spinnability negatively and this was the case with CA + CS solutions.

Another reason that may be the cause for this weak spinnability of the CA/CS solution after the addition of CS can be attributed to its electrical property. To get dissolved in the dilute acid solvent, CS should be in its positively ionized form by the effect of the acidic medium on the NH_2 groups (Figure 2.1)

Due to this electrical property, negative (acetic) and positive (CS) molecules exist with each other. This would lead to binding and aggregation in clumps or aggregated forms resisting the spinnability of CA under the effect of applied voltage. These aggregates are observed in the SEM shown in (Figure 3.15).

Another indirect effect is the electric behavior of the solutions that can play a role in this resistance of spinnability of the solution. It is logic to think that if the solution molecules are similarly charged, they will be more affected by the applied voltage. The opposite is right with the existence of oppositely charged molecules in the same solution. In this case, some of them will act against the effect of the applied voltage and hence it'll have lowered effect on solution and so lower spinnability is expected.

As a result of the increased viscosity of the system, tendency to form aggregates due to the different electric properties of existing molecules and the decrease in the effect by the applied voltage for the same reason, the polymers formed aggregated features (clumps) instead of nanofibers as shown in the SEM image. This observation was found with both mixtures of 1:1 & 2:1. Changing in the electrosinning parameters didn't enable us to fabricate nanofibers. As a conclusion, no nanofibers could be obtained by mixing CA & CS and only aggregated features were formed.

3.3.2 Electrospinning and SEM Characterization of CA-CIT-CS composite nanofibers:

As we mentioned before, both CIT and CS have very interesting properties related to antibacterial effect and if these properties could be added to the CA nanofibers through electrospinning, this could have good application in medical field as well other fields. We could obtain better nanofibers with the addition of CIT, however, that was not the case with CS when used with CA alone. We proposed that the addition to the improved CA nanofibers by CIT could overcome the non spinnability resulting from the addition of CS. So, we tried to fabricate nanofibers from the mixture of CA, CIT & CS.

Similar to the previous solubility challenge, we used a common solvent system for all the materials. CA and CIT were dissolved in acetone. CS was dissolved in 60% acetic acid. Then mixtures of 1:1 & 2:1 (v/v%) were prepared and subjected to electrospinning. However, no nanofibers could be obtained also by this system (Figure 3.16).

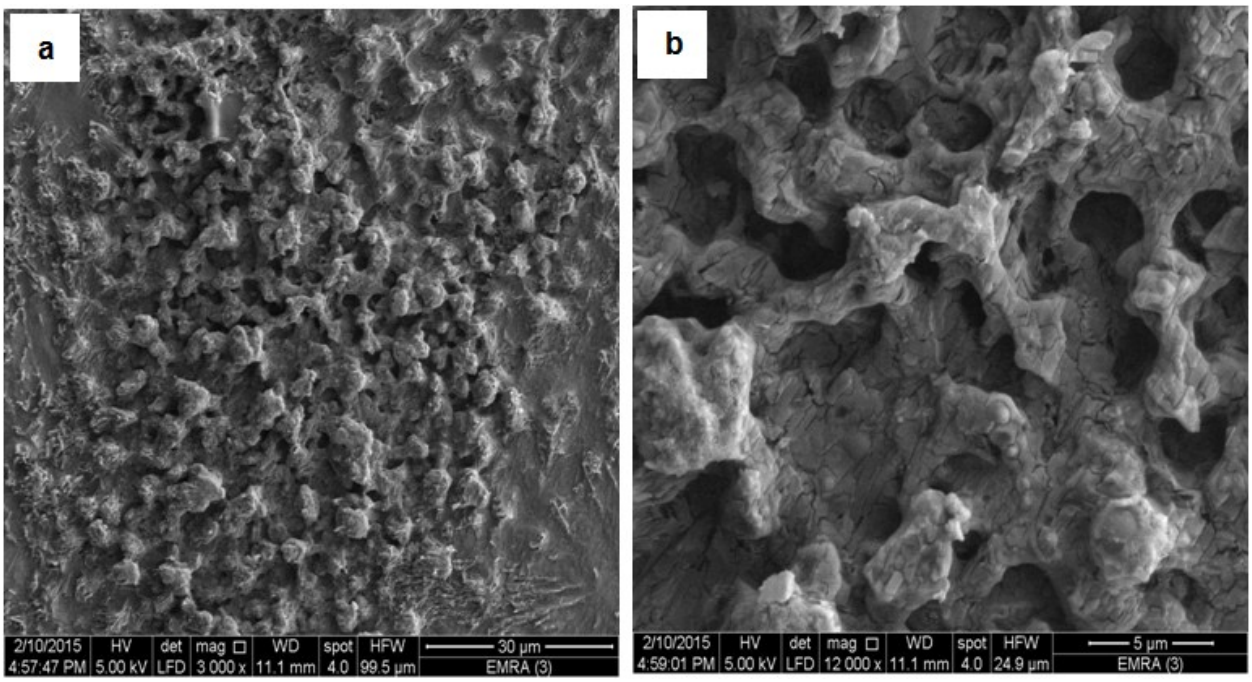

Figure 3-16 SEM images of electrospining CA-CIT-CS solution at different scales. No nanofibers were formed, and instead aggregated clumps are observed. Electrospinning parameters used are 15 kv, 5 mL/hr and 5 cm distance.

In order to understand the formed nanostructures, we need to revise both the CA-CS nanofibers alone & those formed. It is also useful to have a look on the shape of CIT alone when electrospining was performed on them (Figure 3.17).

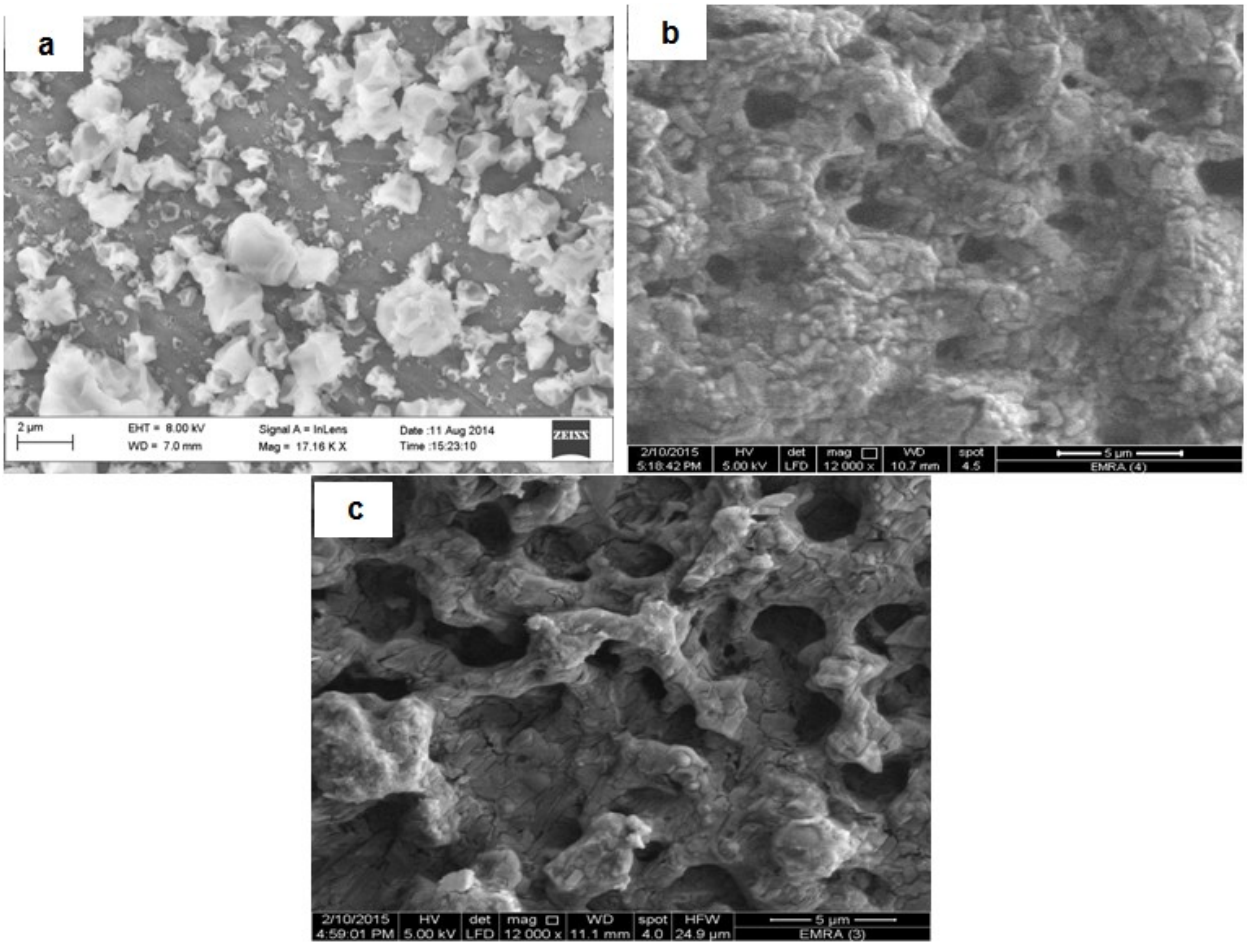

Figure 3-17 SEM images of a) CA- CS, b) CIT alone and c) CA, CS, CIT mixture when electrospinning was performed on them. Electrospinning parameters used are 15 kv, 5 ml/hr and 5 cm distance.

From the above images, we can clearly observe that Figure 3.17 C is just the sum of A & B. In other words, the formed nanostructure from CA – CS were just covered by the CIT that forms a thick layer above them. Accordingly, the same nanostructures formed when CA/ CS used alone are again formed and no nanofibers were formed. The CIT addition didn't lead to nanofibers formation; however it just led to thick deposition over the formed aggregated nanostructures.

Both mixing ratios 1:1 & 2:1 didn't form nanofibers and also the variation of the electrospinnning conditions didn't lead to any nanofibers.

As the same reasons under CA - CS to explain the formed aggregated features rather than fiber form still exist, accordingly the same justification can be applied here too. For example, the viscosity of the formed mixture is still out of the optimum limit and even may increase with the addition of extra mass of CIT. The second reason which is the tendency for aggregate formation by CS because of its opposite charges to the existing molecules still here too. Even it is expected to increase with the addition of CIT as extra negatively ionized molecules were added. In other words CS will not form aggregates with only acetic acid, it'll form aggregates with CIT too. Therefore, the addition of CIT to this mixture didn't lead to improvement in nanofibers formation.

The CIT addition here as mentioned before is proposed to just form a thick layer over the formed nanostructures. As appears from (Figure 3.17) and as discussed before under the CA/ CIT nanofibers, the CIT alone when subjected to electrospinning conditions forms a thick mass over the collection foil. The same thing happened here too and it was deposited over the formed nanostuctures. This again reinforces what we have mentioned in discussion in the CA/CIT nanofibers. As we mentioned there, the CA formed the nanofibers, over which CIT was deposited. When deposition occurred at intersections they were held together forming the thick mass under SEM.

As a conclusion from the previous discussion and figures, no nanofibers were formed from the composite solution of CA- CIT – CS. The variation in the mixing ratios and the variation in the electrospining parameters didn't lead to nanofibers formation. What was formed is the same aggregated nanostructures described under CA/CS electrospinning with the deposition of a thick mass of CIT over it.

3.3.3 FT- IR results of Cellulose Acetate-based Composite Electrospun Nanofibers

FT- IR of CS alone

At first we will have a look over the spectrum & chemical structure of CS before the mixture (Figure 3.18a). All peaks were in agreement with previous reports on the FT-IR spectrum of CS alone. A peak between 3300 and 3500cm^{-1} represents the stretching of both the hydroxyl group and the amino group. As the absorption of the OH is stronger than that of secondary amine, the latter peak mostly masked or covered by the O-H one. Additionally, their C-O and C-N bonds stretching peaks appear at around 1080 cm^{-1}. At 2880 cm^{-1} the peak of the aliphatic C-H group stretching and that of binding appears at 1450 cm^{-1}. At around 1600 cm^{-1} a medium peak of the NH bending also appears. (173)

FT-IR of CA-CS electrospun nanofibers

We performed FT- IR analysis on the electrospun nanofibers of CA-CS to prove the chemical structure of the formed nanofibers and to assess the possibility of any chemical interaction that might have occured. As appears from the spectrum (Figure 3.18b), at 1740 cm^{-1} the stretching peak of the carbonyl group of the ester of CA appears. The peaks of the C-O representing the ester hydroxyl groups stretching of CA appear also at 1050 cm^{-1} and 1220 cm^{-1}. At 1050 cm^{-1} also it is expected that the C-N group stretching peak of CS to be at this point. Close to it at 1159 cm^{-1} another peak appears which comes from the ether bonds stretching. Between 3300 cm^{-1} and 3500 cm^{-1} the peak appears representing the hydroxyl groups and amino group. At around 2850 cm^{-1}, another peak of the C-H aliphatic stretching is also obvious while the peak of the bending appears at 1430 cm^{-1} and 1370 cm^{-1}. The N-H bending of chitosan also appears at around 1600 cm^{-1}. Below 1000 cm^{-1} are considered the compound fingerprint. *(*173)

As appears from the spectrum and in contrast to the spectra of CA CIT, we have an important observation regards the absence of big broadening of the hydroxyl group which signifies no hydrogen bonding effect. (173)

FT- IR results of electrospun CA-CIT-CS nanofibers

To prove the chemical entity and possible chemical interactions, FT-IR on the CA-CIT-CS subjected to electrospinning was performed (Figure 3.18c).

As appears from the spectrum (Figure 3.18 c), at 1740 cm^{-1} a peak representing stretching of carbonyl groups both of the ester of CA and the carboxyl group of CIT appear. The peaks of the C-O stretching representing the ester hydroxyl groups of CA appear also at 1050 cm^{-1} and 1220 cm^{-1}. At 1080 cm^{-1} also it is expected that the C-N group bending peak of CS to be at this point. Close to it at 1140 cm^{-1} another peak appears which comes from stretching of the ether bonds. Between 3300 cm^{-1} and 3500 cm^{-1} a too strong, a broad peak appears representing the hydroxyl groups (from CA, CIT & CS) and amino group (of CS). At around 2850 cm^{-1}, another peak of the aliphatic C-H stretching is also obvious while the peak of the bending appears at 1430 cm^{-1} and that of at 1370 cm^{-1}. The N-H bending of CS also appears at around 1600 cm^{-1}. Below 1000 cm^{-1} are considered the compound fingerprint. (173)

As the spectrum illustrates, no major changes in the spectrum of CS, CA/CS and CA/CS/CIT were observed. Also as discussed before, we think that no interaction took place between the various component molecules. This as described before, in the section 3.1.1. , was because of the steric hindrance effect.

Slight increase in the intensity o the carbonyl group peak due to contribution from CIT was observed. There is a slight increase in the width of the hydroxyl group peak suggesting a hydrogen bonding formation; however it is less than that observed with the CA/ CIT spectra. We postulate a small degree – if any- of cross-linking to occur accordingly.

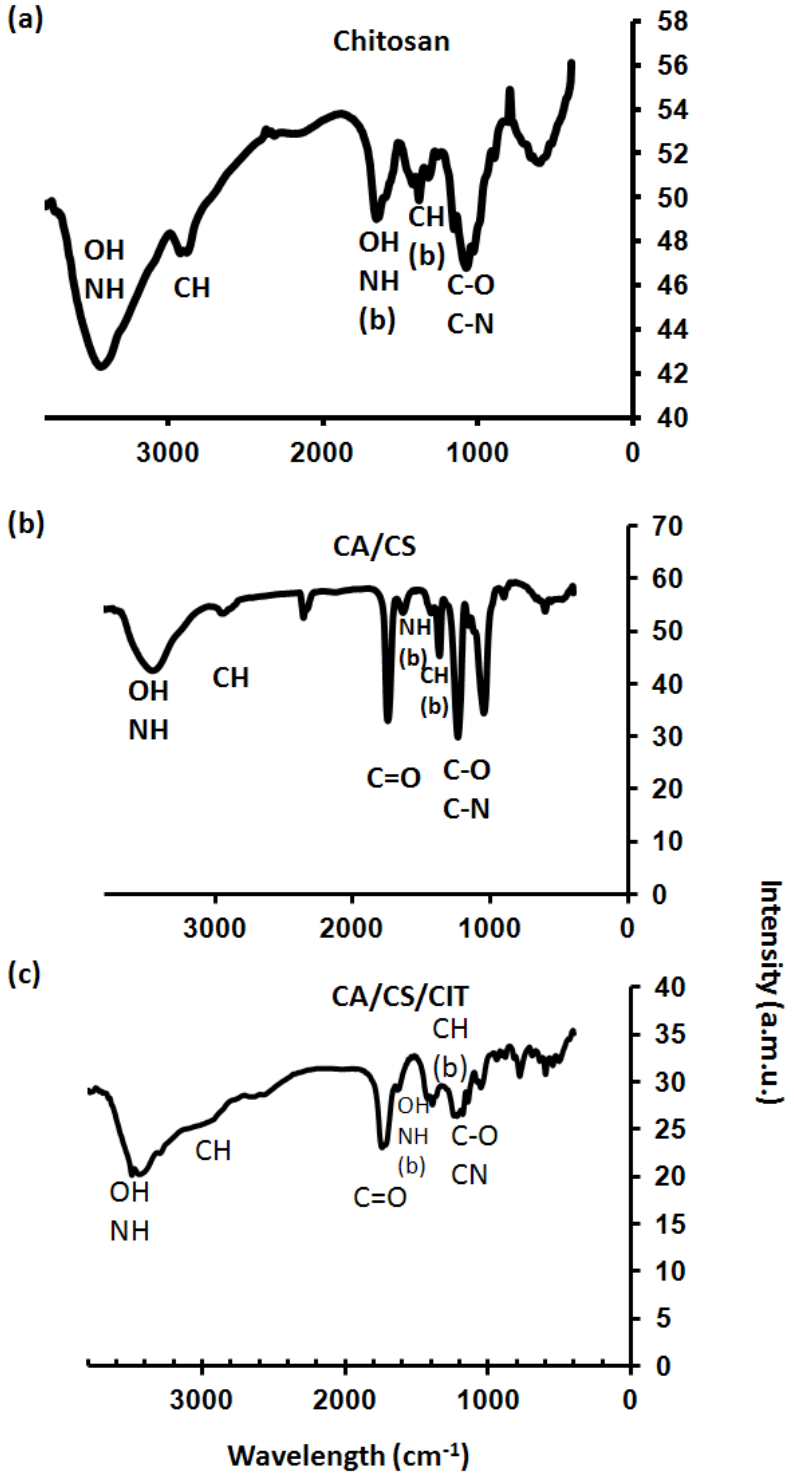

Figure 3-18 FT-IR spectrum of (a) chitosan, (b) CA-CS nanofibers, (c) CA-CIT-CS.

In addition, the loose nature, powder form of the electrospinned material on collection foil suggests that no cross-linking occurred in opposite to the observation with the CA/CIT.

Also regarding the formation of the clumps structures, we exclude that it was formed due to chemical interaction leading to cyclic closure and formation of clumps structures instead of fiber one. As these structures were formed with CA only in acetic acid, so it suggests a physical rather than chemical reason for formation. Reasons such as solution viscosity, conductivity or dipole moment as discussed before are the causes of this structure formation rather than chemical interaction. In other words, if this spherical structures are due to chemical interactions between CA & CS, they shouldn't have appeared with CA when electrospun alone in acetic acid. It is also not expected to be a result of interaction between CA and acetic acid for many reasons. First, the acetic acid is a component of Cellulose acetate. The only possible effect can be mild hydrolysis of the CA to cellulose and acetic acid. Giving the excess mass of acetic acid, as it is used as solvent, the chemical equilibrium favors the reformation of the ester which is again cellulose acetate. Also the FT –IR results of electrospun CA / acetic didn't show any change from the structure of CA alone. Another reason for excluding that Cellulose acetate – acetic acid chemical interaction is the reason for the formation of this spherical structure is that we could fabricate nanofibers from CA when acetone and acetic acid were used as solvent system. If it was due to chemical rather than physical interactions, it should have formed the same clumps structures rather than nanofibers, which is not the case.

As a conclusion, nanofibers could be prepared with CA & CA-CIT while no nanofibers could be obtained from CA/CS, with or without addition of CIT and even with variation of solution ratios & electrospinning parameters. This is attributed to increased physical & electrical changes in the electrospinning solution out of optimum conditions to be electrospun rather than chemical interactions. CIT could improve the nanofibers formed from electrospinning of CA, but didn't do so much when CA was electrospun with CS. In all cases, CIT formed a thick mass over the electrospining material adding a very interesting cross-linking property to CA nanofibers but without great value to it again when electrospun with CS.

3.4 Antibacterial activity assessment of formed nanofibers

In order to assess the effect of electrospun nanofibers on the growth of microorganisms, antibacterial activity study was performed on the formed nanofibers. We choose *E.coli* as a representative to gram negative bacteria while *S. aureus* was used as a representative to gram positive bacteria. The samples tested are displayed in Table 3.6. As no nanofibers were formed from CS mixtures, we excluded them from the antibacterial study and only those of CA-CIT compared to CA alone was studied. Additionally, the samples in their solution form before spinning was tested to compare to electrospun nanofibers and to study if the conversion of the material to the nanoscale would change their antimicrobial properties.

However, all the samples dissolved in acetone including pure acetone solution showed no bacterial growth. In this context, no significant difference of bacterial growth between pure acetone samples and other samples that were dissolved in acetone was observed. This is mainly because acetone is known for its cytotoxicity mediated by its effect on the cell membranes (174-175). Accordingly, the results of these samples aren't displayed and only those of nanofibers are discussed

A preliminary study using seed agar plate technique was performed to assess the antibacterial activity. However, no significant change was observed when compared to negative control. Accordingly, testing in broth medium was used instead. As a guide reference to the testing method, we adopted the ASTM testing standard E1249 "Standard Test Method for Determining the Antimicrobial Activity of Antimicrobial Agents Under Dynamic Contact Conditions".(162) The scope of this standard is the testing of antibacterial treated fibers and fabrics which matches our scope of work.

As it is required and expected that the antimicrobial exerts its effect while bound to the fibers, ensuring good contact between the antibacterial agent in fiber and the challenging microorganism is critical. Accordingly, the test method adopts continuous agitation of the sample under test in a suspension of the bacteria in use.

A comparison between the fibers of added antibacterial "the term treated is used by standard" to those without the added antibacterial agent is done. A blank sample of microorganism without

both tested materials is run in parallel as a negative control. Citric acid alone also was added to other bacterial cultures in parallel as positive control. The evaluation is based on the difference in growth reduction of tested samples to assess the antibacterial activity.

Table 3-6 list of samples used in the antibacterial activity testing

Sample no.	Sample description	Remarks
A	Cellulose acetate (CA)/acetone solution	Sample negative control
B	Cellulose acetate with citric acid (CA-CIT)/ acetone solution	Sample
C	Citric acid /acetone solution	Sample Positive control of antimicrobial agent
D	Acetone solution	Solvent Negative control
E	Electrospun Cellulose acetate (CA)	Fiber without antimicrobial agent "untreated"
F	Electrospun Cellulose acetate with citric acid (CA-CIT)	Fiber with antimicrobial agent "treated"
G	Citric acid powder	Positive control of antimicrobial agent
N1	*S. aureus*	Negative control
N2	*E. coli*	Negative control

Results of antibacterial activity:

The absorption & count of the bacterial suspensions with the samples at zero time, after 24 and 48 hrs of incubation and contact with samples are shown in table 3.7 and (Figure 3.19) for *S. aureus*, and in table 3.8 and (Figure 3.20) for *E. coli*, respectively.

Table 3-7 Absorption and bacterial count of *S. aureus* suspension at zero time, 24 and 48 hrs. N1 is the negative control

Sample	Zero time		24 hrs		48 hrs	
	ABS	**Count (CFU)**	**ABS**	**Count (CFU)**	**ABS**	**Count (CFU)**
A	0.092	1.1×10^8	0.137	1.64×10^8	0.195	2.34×10^8
B	0.096	1.15×10^8	0.111	1.33×10^8	0.141	1.69×10^8
C	0.076	9.1×10^7	0.107	1.28×10^8	0.17	2.04×10^8
N1	0.091	1.09×10^8	1.277	1.53×10^9	2.564	3.08×10^9

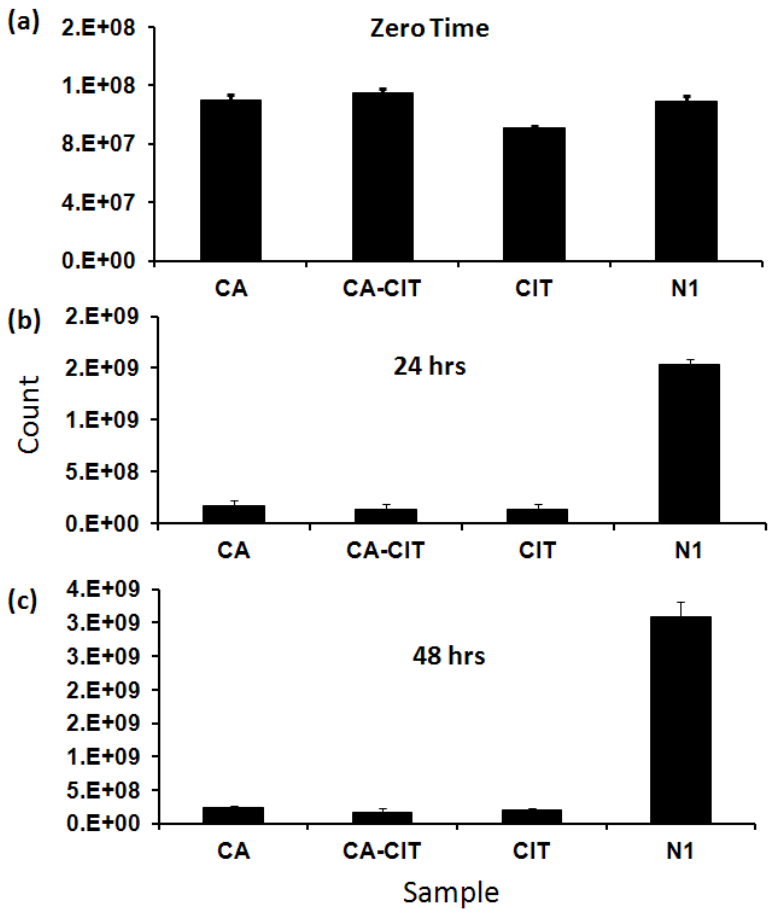

Figure 3-19 *S. aureus* culture count (Y-axis) with each material (X-axis) at (a) zero time, (b) after 24 and (c) after 48 hrs., respectively.

Table 3-8 Absorption & count of *E. coli* suspension at zero time, 24 & 48 hrs

Sample	Zero time		24 hrs		48 hrs	
	ABS	Count (CFU)	ABS	Count(CFU)	ABS	Count (CFU)
A	0.091	1.09×10^8	0.158	1.9×10^8	0.201	2.41×10^8
B	0.108	1.3×10^8	0.137	1.64×10^8	0.165	1.98×10^8
C	0.082	$9.8\ 10^7$	0.123	1.48×10^8	0.173	2.08×10^8
N2	0.088	1.06×10^8	1.298	1.56×10^9	2.341	2.81×10^9

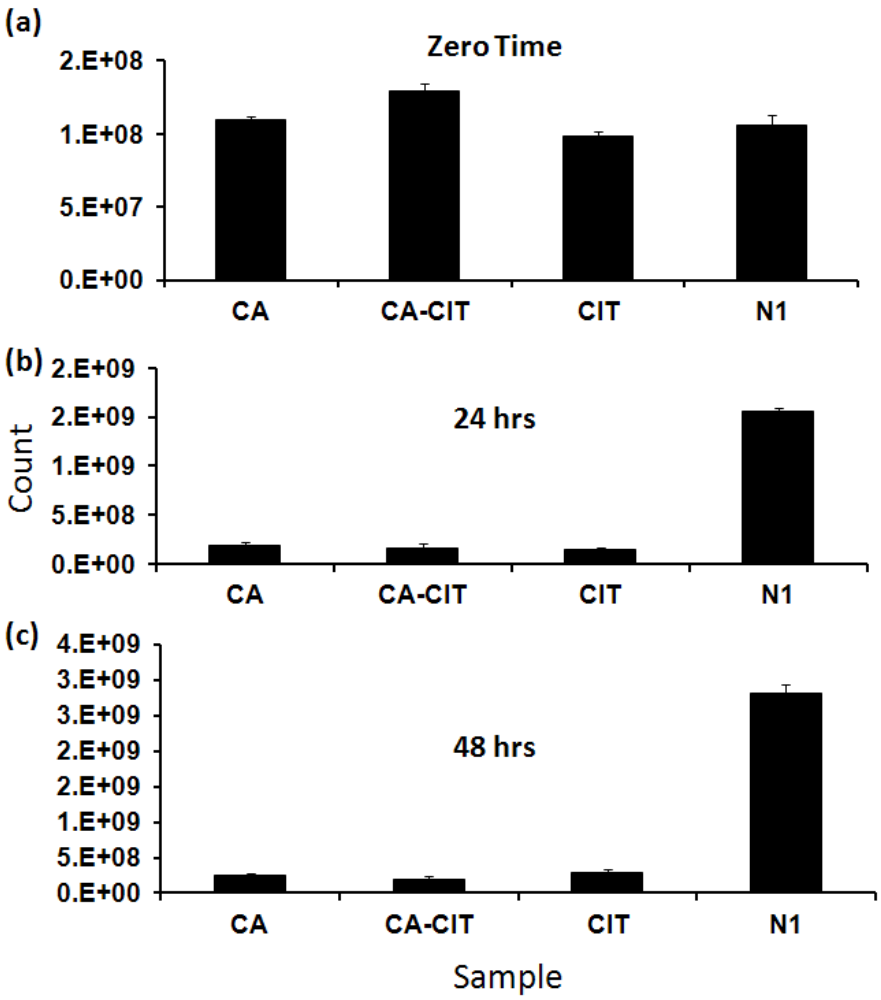

Figure 3-20 *E.coli* culture count (y-axis) with each material (x-axis) at (a) zero time, (b) after 24 and (c) after 48 hrs., respectively.

The above mentioned bacterial growth results indicate that none of the tested samples has shown complete antibacterial activities (i.e. zero growth). In fact, all the materials have shown bacterial growth but with different (%) of the growth. This Growth % can be calculated as follows (equation 3.1):

Growth % = (Count at time b / Count at time a) x 100

Equation 3-1 calculation of the growth %

So, for example, the bacterial growth of N1 (*S.aureus*) increased from 1.09 x 10^8 to 1.53 x 10^9, which is equivalent to an 11.4 % increase in the bacterial growth, after 24 hrs of incubation. Moreover, the bacterial growth has further increased to 3.08 x 10^9, which is equivalent to 13.4% (compared to the values obtained at zero time) and 2 % (compared to the values obtained after 24hrs of incubation).

Upon careful examination and comparison between each sample and its respective % increase in the bacterial growth (i.e. growth %), we can observe that the bacterial growth of Sample A (CA) increased from 1.1 x 10^8 at zero time to only 1.64 x 10^8 after 24 hrs which is 1.5 % increase in the growth %. While the growth % after 48 hours reached only 2.34 x 10^8 which accounts for a total increase in the growth % of about 3 % from the initial value and extra 1.5 % from that obtained after 24 hours.

A very important note here is the relative growth % (equation 3.2) between the increase in growth of the sample of CA and that of the N1 culture alone. From zero time to 24 hrs, the increase of CA was only 1.5 % in comparison to 10 % increase observed with the culture alone in absence of CA.

By simple calculation:

$$\text{Relative Growth \%} = (S / NC) \times 100$$

Where S: sample reading
NC: negative control reading

Equation 3-2 calculation of the relative growth %

We can observe that the relative growth % of CA to N1 %= 1.5/ 10 x100= 15 %.
In other words it has 85 % less growth % than that observed with N1 alone when calculated as shown in equation 3.3.

$$\text{Relative Growth reduction \%} = 100 - \text{Relative growth \%}$$

Equation 3-3 calculation of the relative growth reduction %

This result suggests that the nanofiber negatively affects the growth rate of the bacteria and accordingly is supposed to show antibacterial activity.

The same thing applies for other samples of CA-CIT & CIT when their growth % is compared to the growth % of N1. The results for the growth %, relative growth % and relative growth reduction % are shown in table 3.9 & 3.10 respectively.

Table 3-9 Count Growth % of *S. aureus* at intervals from zero time- 24 hours, 24 - 48 hours and the overall zero – 48 hours

Sample	**0-24**	**24- 48 hrs**	**0-48 hrs**
	Growth %	**Growth %**	**Growth %**
A	1.5 %	1.46 %	2.1 %
B	1.13 %	1.27 %	1.46 %
C	1.4%	1.5%	2.1%
N1	14%	2%	28%

Table 3-10 Relative Growth % of *S. aureus* overall zero – 48 hours comparison between the samples and negative control N1

Sample	**Relative Growth %**	**Relative Growth reduction %**
A	7.5 %	92.5 %
B	5 %	95 %
C	7.5 %	92.5 %
N1	100 %	0%

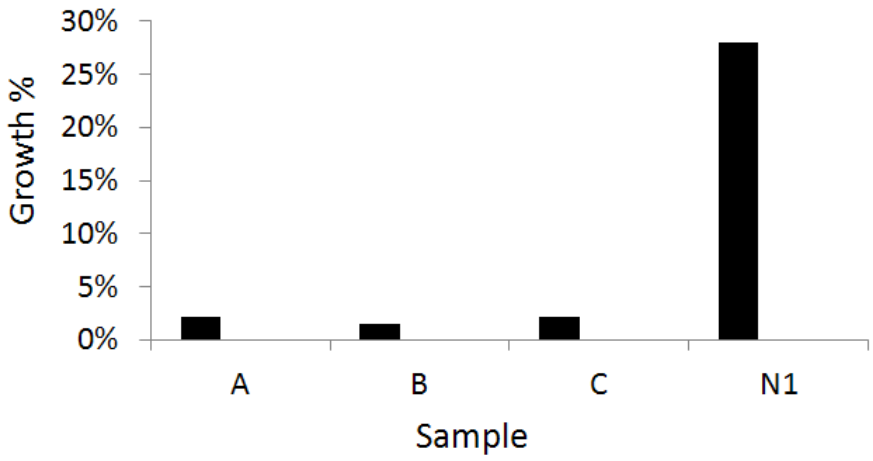

Figure 3-21 *S. aureus* culture growth rate from 0-48 hours of different samples.

Cultures of *E. Coli* also show similar results with all tested samples. For example, the bacterial count of N2 increased from 1.06 x 10^8 to 1.56 x 10^9, which is equivalent to a 14.7 % increase in the bacterial growth %, after 24 hrs of incubation. Moreover, the bacterial count has further increased to 2.81 x 10^9, which is equivalent to 26.5 % growth % (compared to the values obtained at zero time) and 1.8 % (compared to the values obtained after 24hrs of incubation). When comparing this to the growth % of other samples, and calculating the relative growth % as described in equation 3.1 and 3.2, we can observe great reduction in the growth %. The results of the growth % and relative growth % are demonstrated in tables 3.11 and 3.12. These results also suggest an antibacterial effect exerted by the fibers. (Figure 3.22)

Table 3-11 Count Growth % of *E.Coli* at intervals from zero time- 24 hours, 24 - 48 hours and the overall zero – 48 hours

Sample	0-24	24- 48 hrs	0-48 hrs
	Growth %	Growth %	Growth %
A	1.7 %	1.2%	2.2%
B	1.2%	1.2%	1.5%
C	1.5%	1.4%	2.1 %
N2	14.7%	1.8%	26.5%

Table 3-12 Growth rate % of *S. aureus* overall zero – 48 hours comparison between the samples and negative control N2

Sample	Growth %	Growth reduction %
A	8.3 %	91.7 %
B	5 .6 %	94.4 %
C	8 %	92 %
N2	100 %	0%

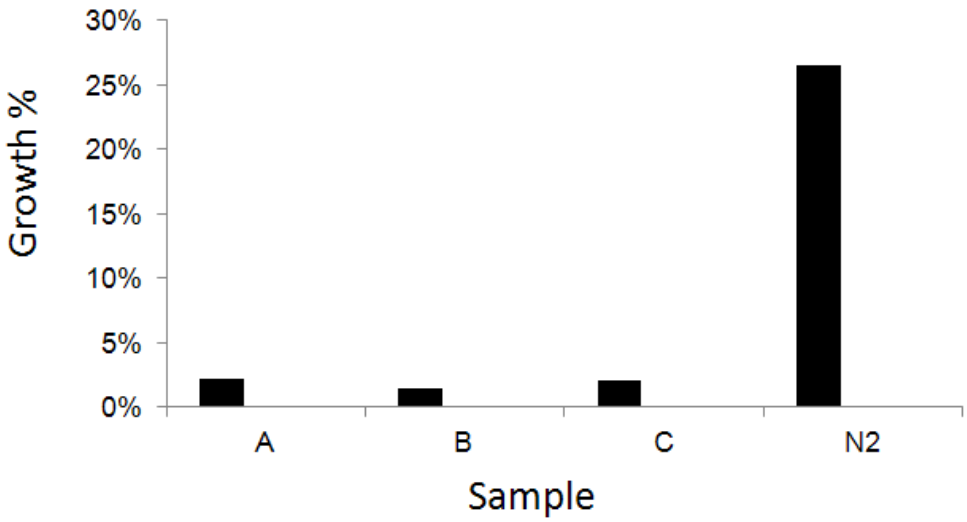

Figure 3-22 *E.Coli* culture growth rate from 0-48 hours of different samples.

As appears from the results above, the growth % of both types of bacteria was affected with the presence of electrospun nanofibers in comparison to the growth % of the negative control suspension suggesting that all the material have an antibacterial activity with respect to the negative control.

We can observe that at zero time, the only material that showed growth inhibitory effect was the free form positive control of CIT. The direct action by addition of the acid is accompanied by

lowering of the pH of the solution which most probably resulted in the injury to the bacterial cells.

After 24 hrs, all the materials showed a growth inhibiting effect on the growth % of the bacteria in comparison to the negative control. The highest effect was observed with CA-CIT (around 92 % on *S.aureus & E.coli*). The next was the CIT alone with relative growth reduction % of 90 % and the least was observed with CA alone with relative growth reduction % about 88%.

After 48 hrs, all the samples were keeping their growth inhibitory effect, too. The highest effect came from CA-CIT also with (94.5 % vs 93.3 % on *S.aureus* and 92.6 % vs 92.3 % on *E.coli*). Note that CA and CIT alone showed almost the same effect of 92 %.

From the above mentioned results, we can observe that all the materials have a significant antibacterial effect on the growth of the bacterial suspensions in comparison to the negative control.

Another very important question to answer is "does the addition of an antibacterial agent to nanofibers improve the antibacterial activity of the nanofiber?". In order to answer this question, we need to assess the antibacterial effect of CA- CIT in comparison to the effect exerted by the CA alone where it is this time used as a negative control. Again, the relative growth percent is calculated as mentioned in equation 3.2 but using the readings of CA only as a negative control instead of the bacterial suspension alone.

Table 3-13 Count Relative Growth % for CA-CIT versus CA alone of at intervals from zero time- 24 hours and the overall zero – 48 hours

Sample	**0-24**	**0-48 hrs**
	Growth %	**Growth %**
S. aureus	75 %	69.5 %
E.coli	70 %	68 %

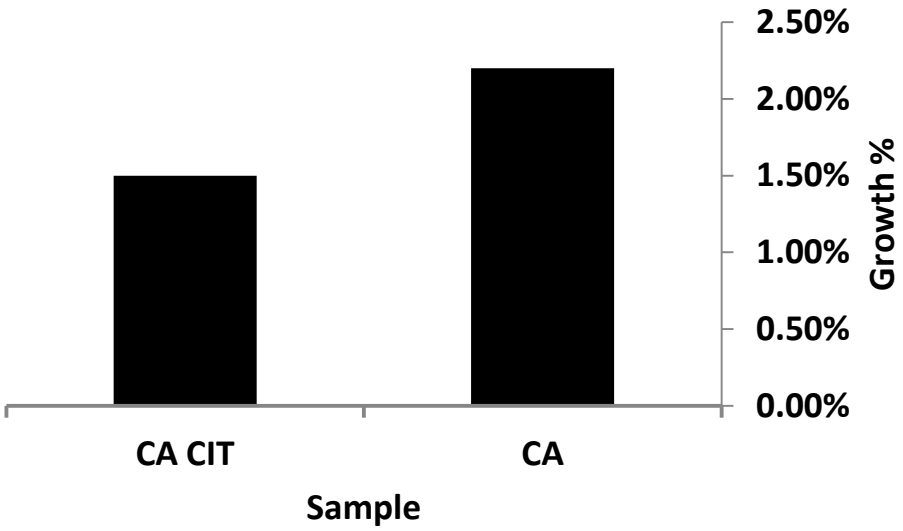

Figure 3-23 Growth rate % of *E.coli* overall zero – 48 hours comparison between the CA vs CA/CIT samples

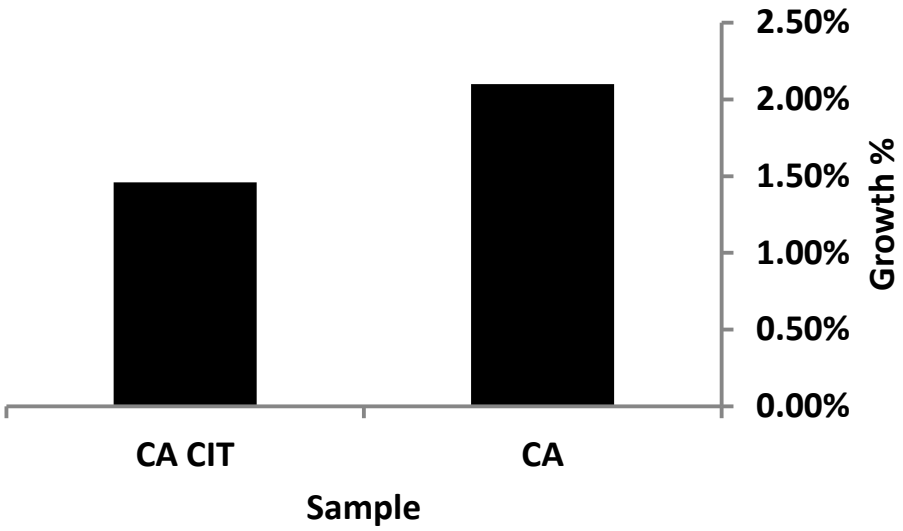

Figure 3-24 Growth rate % of *S. aureus* overall zero – 48 hours comparison between the CA vs CA/CIT samples

We can observe from the results CA-CIT has higher antibacterial effect than CA alone. The addition of CIT clearly added an antibacterial effect to the fabricated nanofiber. This result is logical due to the known antibacterial effect of CIT. It is likely that the addition of an antibacterial agent such as CIT to the mixture solution has led to electrospun nanofibers which

most probably carry (surface deposition) CIT (as proved before with the FT-IR results) and that the antibacterial effect of CIT is maintained and not negatively affected by the electrospinning.

Not only CA-CIT was higher in antibacterial effect than CA alone, but amazingly it has higher effect than CIT alone. These results can be approached in two ways. The first is that CIT has higher effect in nanoform more than the normal particle size. As discussed earlier, CIT exerts its effect after it passes through the cell membrane and dissociates inside it. The dissociation disrupts the internal environment in the cell finally impairing its function. A close contact between the acid molecule and the cells is so required. As the availability of the acid in the medium increases, the action is expected to increase too. As the material decreases in size, its contact surface area increases too (Figure 3.25). This allows the particle to be more in contact with bacteria in comparison to the normal scale. Accordingly, it can have higher effect at the same or even lower concentration.

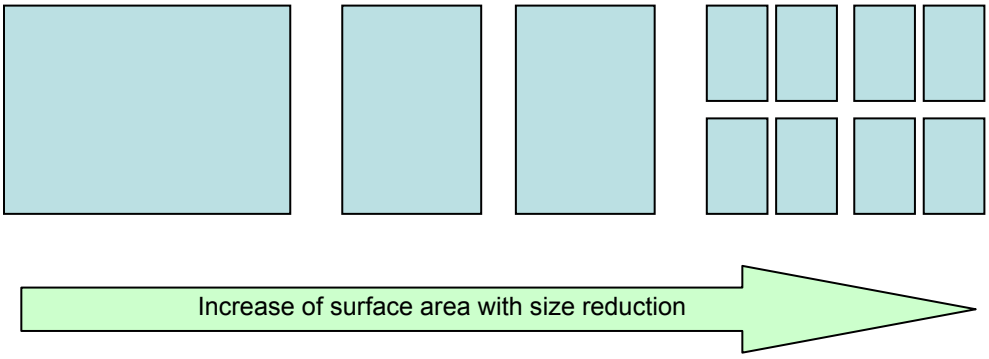

Figure 3-25 The increase of the material surface area with decrease in its size

The second approach suggests that a synergistic effect of the CA-CIT over any one of them alone and this will take us to another important observation is that amazingly, CA nanofibers alone had an antibacterial effect.

At zero time no effect or even negative impact is observed with CA nanofibers. However, after 24 hrs and 48 hrs, it showed great reduction on the growth% of bacterial suspensions in comparison to the negative control. As per our knowledge through literature review, CA has not

been reported for its antibacterial activity. Also, the samples carried out on solution form didn't show significant difference from the solvent alone confirming it has no effect.

CA has too large polymer size making it practically impossible to enter the cell and exert an intracellular antibacterial action. In addition, it exists in the ester form and almost no active functional groups exist such as carboxylic acid group that allows it to exert an extracellular antibacterial effect. Accordingly, we did not expect it would have an antibacterial effect. However, it showed to have.

In order to explain the new observation, we need to tackle the changes that can happen to it by changing its form into nanoform. The change into nanoform would not reduce the molecular size; hence it is still practically impossible to exert an intracellular effect. Chemical structure also will not change upon transforming it into nanoscale and accordingly, no new groups would exert an antibacterial action. So what might explain this observation? As mentioned before, it is well known that one of the major changes on material by transforming into nanoscale is the huge increase in surface area. (Figure 3.25)

As the surface area increases, adsorption affinity of species increases too. A known application to this is the use of electrospun CA nanofibers (especially after surface modification) in membranes and the accompanied adsorption of heavy metals as well as others. The same concept can be used here. The increase in the surface area would lead to high adsorption of nutrients and other vital materials from the growth medium. This would act as a" competitor" on the nutrients material available for existing bacteria and hence would affect its growth rate. A similar concept is adopted physiologically, were the bacterial normal flora competes with pathogenic ones and so plays an immunity rule. The competition proposed is not only on nutrients of the medium, space occupation is another field of competition. Although supposed to have less impact than effect on nutrients, the space occupied by the nanofibers, decreases the available space for bacteria and hence decreases its growth.

The absence of effect at zero time is accordingly logical as it doesn’t affect the environment at once, but after time. As the increase in the adsorption and surface area are accompanied with the change of CA into nanoscale fibers, accordingly we propose that the observed antibacterial effect is attributed to the nanoscale transformation of the material.

Accordingly, the fabrication of the material in the nanoscale form has an effect on the materials. In one turn, an increase in antibacterial effect is shown from CA-CIT more than the positive control itself (CIT). This can be explained as an increase in the activity of both materials with a synergistic effect.

Comparative study of the effect of materials on gram positive & gram negative bacteria

Based on the obtained results, we have demonstrated that the formed nanofibers have an antibacterial effect that is enhanced by being in the nanoform and is time dependant as it relates to the gradual release of CIT from the CA nanofiber network. In this section we want to investigate the specificity, i.e. if the antibacterial effect varies with the type of bacteria between gram positive and gram negative.

Table 3-14 Relative growth reduction % on *E. coli and S. aureus* suspensions 0-48 hours interval

Sample	**Relative Growth reduction %**	
	S. aureus	*E.Coli*
A	92.5 %	91.7 %
B	95 %	94.4 %
C	92.5 %	92 %

It is clear from the results that all of samples had an effect on both types of bacteria. It is also clear that they have slightly higher effect on *S. aureus* relative to *E.coli*. It is worth mentioning that the high efficacy on S. aureus is especially of great value. This is because a known group of resistant *S. aureus*, which is *Methicillin resistant s. aureus* (MRSA), is one of the major challenges in infection and wound control specially that is related to nosocomial infections. If this material CA- CIT will have a good efficacy against this group of bacteria, it'll so have a great application in its control.

Chapter 4 **Conclusion and Future Perspectives**

Chapter 4. Conclusion and Future perspectives

As a conclusion, based on results, CA- CIT nanofibers could be fabricated using electrospinning. The formed nanofibers were tested for their morphological aspects using SEM. The chemical composition was confirmed using FT-IR. They were then tested for their antimicrobial effect against gram positive and gram negative microorganisms. The antimicrobial testing demonstrated a significant antimicrobial effect relative to negative control. The electrospun nanofiber of CA CIT has an observable antibacterial effect and the effect exhibited is higher than that of the electrospun CA nanofiber alone or CIT alone used here as positive control. These results accordingly suggest and enforce the postulation of having an electrospun nanofiber with antibacterial property through the integration of antimicrobial agent.

We propose this innovative composite nanofiber with these properties as a novel material that can be used in wound dressings and in many other applications. The antimicrobial effect is important part as discussed early in the introduction chapter. We have highlighted too in the same chapter the rule of citric acid in wound healing. Based on these theoretical bases together with the practical part which was the scope of this research work to fabricate and test for the antimicrobial properties of the formed nanofibers, we propose that this material can be efficient in enhancing the wound healing management.

The materials used are natural or derived from natural materials that all are readily available and with high known safety for use with human being which is a very important advantage of this composite. Additionally, their economic value adds an extra advantage to this innovative composite over other innovative approaches in developing nowadays. This advantage is achieving an efficient tool in a reasonable price that can be used with largest number of patients without economic constrain. This is too important in developing countries such as in Egypt.

Future work can include the clinical testing of the fabricated materials to assess the outcome of the use of the material on wound management.

Further research on the use of this material for other applications beside wound can include, but not limited to, the use of this material in filtration media, food packaging material, medical & hygienic clothing and furniture.

References

1. *The top 10 causes of death, WHO fact sheets, http://www.who.int/mediacentre/factsheets/fs310/en/ last update, May 2014, Last accessed 29th Dec. 2015*
2. *Hutchinson J (1992). The Wound Programme. Centre for Medical Education: Dundee*
3. *Percival JN. 2002. Classification of wounds and their management. Surgery 20:114–117.*
4. *Harding KG, Morris HL, Patel GK. 2002. Science, medicine and the future: Healing chronic wounds. Br Med J 324:160–163.*
5. *Bolton L, van Rijswijk L. 1991. Wound dressings:Meeting clinical and biological needs. Dermatol Nurs 3:146–161.*
6. *Krasner D, Kennedy KL, Rolstad BS, Roma AW. 1993. The ABCs of wound care dressings. Wound Manag 66:68–69.*
7. *Singer AJ, Taira BR, Lee CC, Soroff HS. Thermal burns. In: Marx JA, ed. Rosen's Emergency Medicine: Concepts and Clinical Practice. 7th ed. Philadelphia, Pa: Mosby Elsevier; 2009:chap 6*
8. *Cuzzell JZ. The new RYB color code. Am J Nurs. 1988;88:1342–1346 infection. (n.d.) Dorland's Medical Dictionary for Health Consumers. (2007)*
9. *European Wound Management Association (EWMA). Position Document: Identifying criteria for wound infection. London: MEP Ltd, 2005.*
10. *James, William D.; Berger, Timothy G.; et al. (2006). Andrews' Diseases of the Skin: clinical Dermatology. Saunders Elsevier. p. 269.*
11. *Centers for Disease Control and Prevention, Healthcare-associated Infections (HAIs), Pseudomonas aeruginosa in Healthcare Settings*
12. *http://www.cdc.gov/hai/organisms/pseudomonas.html, last updated May 2014, last accessed 29th Dec 2015.*
13. *Stukalov O1, Korenevsky A, Beveridge TJ, Dutcher JR., Use of atomic force microscopy and transmission electron microscopy for correlative studies of bacterial capsules. Appl Environ Microbiol. 2008 Sep;74(17):5457-65. doi: 1128/AEM.02075-07. Epub 2008 Jul 7*
14. *Naylor, C.E., Eaton, J.T., Howells, A., Justin, N., Moss, D.S., Titball, R.W., Basak, A.K. Structure of the key toxin in gas gangrene. Nat.Struct.Biol. v5 pp.738-746 , 1998.*
15. *Diagnosis and misdiagnosis of necrotizing soft tissue infections: three case reports. Cases J 2008, 1:252. doi: 10.1186/1757-1626-1-252*
16. *Schultz GS. 1999. Molecular regulation of wound healing. In: Bryant RA, editor. Acute and chronic wounds: Nursing management. 2nd edition. St. Louis, MO: Mosby. pp 413–429.*
17. *Misra A, Nanchahal J. 2003. Use of gauze soaked in povidone iodine for dressing acute wounds. Plast Reconstr Surg 111:2105–2107.*

18. *Hudspith J, Rayatt S. 2004. ABC of burns; first aid and treatment of minor burns. Br Med J 328:1487– 1489.*

19. *Liao ZJ, Huan JN, Lv GZ, Shou YM, Wang ZY. 2006. Multi-centre clinical study of the effect of silver nitrate ointment on the partial thickness.*

20. *McEvoy GK, ed. Bethesda, MD: Bacitracin, AHFS drug information 2004. American Society of Health-System Pharmacists; 2004:3305-6*

21. *Purner SK, Babu M. 2000. Collagen based dressings- A review. Burns 26:54–62.*

22. *van Rijswijk L. 2006. Ingredient-based wound dressing classification: A paradigm shift that is passe´ and in need of replacement. J Wound Care 15:11–14.*

23. *Queen D, Orsted H, Sanada H, Sussman G. 2004. A dressing history. Int Wound J 1:59–77.*

24. *British Pharmacopoiea Monograph 1988. Cotton Conforming Bandage BP.*

25. *British Pharmacopoiea Monograph 1988. Polyamide and Cellulose Contour Bandage, Knitted BP.*

26. *Dealey C. 1993. Role of hydrocolloids in wound management. Br J Nurs 2:358–362.*

27. *Thomas S, Loveless PA. 1997. A comparative study of twelve hydrocolloid dressings. World Wide Wounds 1:1–12.*

28. *Thomas S. 1992. Hydrocolloids. J Wound Care 1: 27–30.*

29. *Hoekstra MJ, Hermans MH, Richters CD, Dutrieux RP. 2002. A histological comparison of acute inflammatory responses with a hydrofibre or tulle gauze dressing. J Wound Care 11:113– 117.*

30. *Lay-Flurrie K. 2004. The properties of hydrogel dressings and their impact on wound healing. Prof Nurse 19:269–273.*

31. *Wichterle O, Lim D. 1960. Hydrophilic gels for biological use. Nature 185:117–118.*

32. *Moody A. 2006. Use of a hydrogel dressing for management of a painful ulcer. Br J Comm Nurs 11:S12–S17.*

33. *Martin L, Wilson CG, Koosha F, Tetley L, Gray AI, Senel S, Uchegbu IF. 2002. The release of model macromolecules may be controlled by the hydrophobicity of palmitoyl glycol chitosan hydrogels. J Control Release 80:87–100.*

34. *Joshua S. Boateng, Kerrh H. Matthews, Howard N.E. Stevens, Gillan M. Eccleston. Wound Healing Dressings and Drug Delivery Systems: A Review, Wiley InterScience DOI 10.1002/jps.21210*

35. *DuoDERM® CGF® Control Gel Formula Dressing Package Insert, ConvaTec Division of E.R. Squibb & Sons, L.L.C.*

36. *Nancy Morgan, Calcium alginate, Wound Care Education Institute (WCEI), copyright 2012*

37. *Seaweed, Synthetic natural polymers http://www.snpinc.com/chemical-products/alginates.*

38. *Schmidt RJ, Turner TD. 1986. Calcium alginate dressings. Pharm J 236:578.*

39. *Doyle JW, Roth T, Smith M. 1996. Effects of calcium alginate on cellular wound healing processes modelled in vitro. J Biomed Mater Res 32: 561–568.*

40. *Thomas A, Harding KG, Moore K. 2000. Alginates from wound dressings activate human macrophages to secrete tumour necrosis factor-a. Biomaterials 21:1797–1802.*

41. *Lansdown AB. 2002. Calcium: A potential central regulator in wound healing in the skin. Wound Repair Regen 10:271–285.*

42. *Gilchrist T, Martin AM. 1983. Wound treatment with Sorbsan—An Alginate fibre dressing. Biomaterials 4:317–320.*

43. *Agren MS. 1996. Four alginate dressings in the treatment of partial thickness wounds: A comparative study. J Plast Surg 49:129–134.*

44. *O'Meara S, Callum N, Majid M, Sheldon T. 2000. Systematic reviews of wound care management (3)antimicrobial agents for chronic wounds (4) diabetic foot ulceration. Health Technol Assess 4:1–237.*

45. *Nelson EA, O'Meara S, Craig D, Iglesias C, Golder S, Dalton J, Claxton K, Bell-Syer SE, Jude E, Dowson C, Gadsby R, O'Hare P, Powell J. 2006. A series of systematic reviews to inform a decision analysis for sampling treating infected diabetic foot ulcers. Health Technol Assess 10:1–221.*

46. *Harihara Y, Konishi T, Kobayashi H, Furushima K, Ito K, Noie T, Nara S, Tanimura K. 2006. Effects of applying povidone-iodine just before skin closure. Dermatology 212:53–57.*

47. *Dijke P, Iwata KK. 1989. Growth factors for wound healing. Biotechnology 7:793–798.*

48. *Wallace E. 1994. Feeding the wound: Nutrition and wound healing. Br J Nurs 3:662–667.*

49. *Komarcevic A. 2000. The modern approach to wound treatment. Med Pregl 53:363–368.*

50. *Mann A, Niekisch K, Schirmacher P, Blessing M. 2006. Granulocyte-macrophage colony-stimulating factor is essential for normal wound healing. J Investig Dermatol Symp Proc 11:87–92.*

51. *Linda M. 1991. Nutritional biochemistry and metabolism with clinical applications. 2nd edition. East Norwalk, CT: Appleton & Lange.*

52. *Osieki H. 1995. Nutrients in profile. 2nd edition. Kelvin Grove, Queensland: Bioconcepts.*

53. *Nanoscience, size and scale, http://nanotechnology.wmwikis.net/Lesson+3+Size+and+Scale, last accessed 29th Dec. 2015.*

54. *Ploschner, M., et al., (2012) Bidirectional optical sorting of gold nanoparticles. Nano Lett. 2012 Apr 11;12(4):1923-7. doi: 10.1021/nl204378r.*

55. *Olubayode Ero-Phillips, et al., (2012) Tailoring Crystallinity of Electrospun Plla Fibres by Control of Electrospinning Parameters. Polymers 2012, 4(3), 1331-1348*
56. *Thomas S. Miller, et al., (2012) Electrochemistry at carbon nanotube forests: sidewalls and closed ends allow fast electron transfer, Chem. Commun., 2012,48, 7435-7437*
57. *Takuya Tsuzuki, (2009) Commercial scale production of inorganic nanoparticles, International Journal of Nanotechnology (IJNT), Vol. 6, No. 5/6, 2009*
58. *Guozhong Cao, Ying Wang, (2011) Nanostructures and Nanomaterials: Synthesis, Properties, and Applications, Volume 2 of World scientific series in nanoscience and nanotechnology, World Scientific, 2011, ISBN 9814322504, 9789814322508*
59. *Thomas Tsakalakos, Ilya A. Ovid'ko, Asuri K. Vasudevan (2003) Nanostructures: Synthesis, Functional Properties and Applications, Volume 128 of NATO science series: Mathematics, physics, and chemistry, ISSN 1568-2609*
60. *Xinyu Zhang, et al., (2004), Nanofibers of polyaniline synthesized by interfacial polymerization, Synthetic Metals, Volume 145, Issue 1, 27 August 2004, Pages 23–29*
61. *Christoper J. Ellison, et al., (2007), Melt blown nanofibers: Fiber diameter distributions and onset of fiber breakup, Polymer 48 (2007) 3306e3316*
62. *Eliton S. Medeiros , et al.,(2009), Solution blow spinning: A new method to produce micro- and nanofibers from polymer solutions, Journal of Applied Polymer Science Volume 113, Issue 4, pages 2322–2330, 15 August 2009*
63. *Aguiar MR, et al., (2009), Synthesis of carbon nanotubes and nanofibers by thermal CVD on SiO2 and Al2O3 support layers. J Nanosci Nanotechnol. 2009 Jul;9(7):4143-50.*
64. *Yongwen Wang , et al.,(2009), Template Synthesis of Carbon Nanofibers Containing Linear Mesocage Arrays, Nanoscale Research Letters 2010, 5:913-916*
65. *Xiangwu Zhang, et al., (2014), Centrifugal Spinning: An Alternative Approach to Fabricate Nanofibers at High Speed and Low Cost, Polymer Reviews 2014 Volume 54, Issue 4 :677-701*
66. *Jun-Seo Park, (2010), Electrospinning and its applications, 2010 Adv. Nat. Sci: Nanosci. Nanotechnol. 1 043002*
67. *Dario Pisignano, (2013), Polymer Nanofibers: Building Blocks for Nanotechnology, 2013, Issue 29 of RSC nanoscience and nanotechnology, ISSN 1757-7136*
68. *V. Thavasi, (2008), Electrospun nanofibers in energy and environmental applications, Energy Environ. Sci., 2008, 1, 205-221*
69. *Thandavamoorthy Subbiah, et al., (2004), Electrospinning of Nanofibers, Journal of Applied Polymer Science, Vol. 96, 557–569 (2005)*
70. *Megelski, S., Stephens, et al., (2002) Micro- and Nanostructured Surface Morphology on Electrospun Polymer Fibers. Macromolecules, 35, 8456-8466.*

71. *Buchko, C.J., et al., (1999) Processing and microstructural characterization of porous biocompatible protein polymer thin films, Polymer., 40, 7397-7407, 1999.*

72. *Li, Zhenyu , et al., Effects of Working Parameters on Electrospinning, One-Dimensional nanostructures Electrospinning Technique and Unique Nanofibers, Springer Science & Business Media, 2013, ISBN 3642364276, 9783642364273*

73. *Didem Rodoplu, et al., (2012) Effects of Electrospinning Setup and Process Parameters on Nanofiber Morphology Intended for the Modification of Quartz Crystal Microbalance Surfaces, Journal of Engineered Fibers and Fabrics 118 Volume 7, Issue 2 – 2012*

74. *Baumgarten PK (1971) Electrostatic spinning of acrylic microfibers. J Colloid Interface Sci 36:71–79*

75. *Casper CL, et al., (2004) Controlling surface morphology of electrospun polystyrene fibers: Effect of humidity and molecular weight in the electrospinning process. Macromolecules 37(2):573–578.*

76. *Dietzel, J. M., et al., (2001) Controlled Deposition of Electrospun Poly(Ethylene Oxide) Fibers. Polymer 2001, 42, 8163–8170*

77. *Doshi, J., and Reneker, D. H., (1995) Electrospinning Process and Applications of Electrospun Fibers, J. Electrostatics 35, 151 (1995)*

78. *Ümran Özkoç, et al., (2011) Effect of Concentration on Polyacrylonitrile (PAN) Nanofibers, Journal of Materials Science and Engineering 5 (2011) 277-280*

79. *Zong XH, et al., (2002) Structure and process relationship of electrospun bioabsorbable nanofiber membranes. Polymer, July 2002; 43(16):4403–4412.*

80. *Huang C, et al., (2006) Electrospun polymer nanofibres with small diameters. Nanotechnology 17(6):1558–1563.*

81. *Keun Hyung Lee, et al., (2002) Influence of a mixing solvent with tetrahydrofuran and N,N-dimethylformamide on electrospun poly(vinyl chloride) nonwoven mats*

82. *Ji-Hong Chai, et al., (2013) Electrospinning preparation and electrical and biological properties of ferrocene/poly(vinylpyrrolidone) composite nanofibers, Beilstein J Nanotechnol. 2013; 4: 189–197*

83. *Nishiyama, Yoshiharu; et al., (2002). "Crystal Structure and Hydrogen-Bonding System in Cellulose Iβ from Synchrotron X-ray and Neutron Fiber Diffraction". J. Am. Chem. Soc 124 (31): 9074–82*

84. *Weitao Zhou, et al., (2011) Studies of Electrospun Cellulose Acetate Nanofibrous Membranes, The Open Materials Science Journal, 2011, 5, 51-55*

85. *Klemm, Dieter; et al., (2005). "Cellulose: Fascinating Biopolymer and Sustainable Raw Material". Angew. Chem. Int. Ed. Vol 44 Issue 22, 3358–3393*

86. *Zhang L and Hsieh Y-L (2008), 'Ultra-fine cellulose acetate/poly(ethylene oxide) bicomponent fibres', Carbohydrate Polymers, 71, 196–207.*

87. *Castillo-Ortega MM, et al., (2010) Fibrousmembranes of cellulose acetate and poly(vinyl pyrrolidone) by electrospinning method: preparation and characterization. J Appl Polym Sci 2010;116(4):1873–8.*

88. *Tang C, et al., (2008) Cocontinuous cellulose acetate/polyurethane composite nanofiber fabricated through electrospinning. Polym Eng Sci 2008;48(7):1296–*

303.

89. *Zhou W, et al., (2011) Electrospun silk fibroin/cellulose acetate blend nanofibres: structure and properties. Iran Polym J 2011; 20(5):389–97.*

90. *Rocktotpal Konwarh, et al., (2013) Electrospun cellulose acetate nanofibers: The present status and gamut of biotechnological applications Biotechnology Advances 31 (2013) 421–437*

91. *Taepaiboon P, et al., (2007). Vitamin-loaded electrospun cellulose acetate*

92. *nanofiber mats as transdermal and dermal therapeutic agents for vitamin A acid and vitamin E. Eur J Pharm Biopharm 2007;67:387.*

92. *Huang XJ, et al., (2011) Immobilization of Candida rugosa lipase on electrospun cellulose nanofiber membrane. J Mol Catal B: Enzym 2011;3–4:95-100.*

93. *Cui W, et al., (2010) Electrospun nanofibrous materials for tissue engineering and drug delivery. Sci Technol Adv Mater 2010;11(014108). [11pp.]*

94. *Kumar CG. A review of transdermal therapeutics system. Review Article Journal der Pharmazie Forschung (Formerly-Recent Advances in Pharmaceutical Science Research) Vol-2 No-1 2013*

95. *Chien YW. Novel drug delivery systems, Vol. 50. NY: Marcel Dekker, New York; 1992.*

96. *Tungprapa S, et al., (2007) Release characteristics of four model drugs from drug-loaded electrospun cellulose acetate fiber mats. Polymer 2007a;48:5030–41.*

97. *Castillo-Ortega MM, et al., (2011) Preparation, characterization and release of amoxicillin from cellulose acetate and poly(vinyl pyrrolidone) coaxial electrospun fibrous membranes. Mat Sci Eng C Mater 2011;31:1772–8.*

98. *Kontogiannopoulos KN, et al., (2011) Electrospun fibermats containing shikonin and derivativeswith potential biomedical applications. Int J Pharm 2011;409(1–2):216–28.*

99. *Liu X, et al., (2012) Antimicrobial electrospun nanofibers of cellulose acetate and polyester urethane composite for wound dressing. J Biomed Mater Res B Appl Biomater 2012;100(6):1556–65.*

100. *Chen L, et al.,(2008) Electrospun cellulose acetate fibers containing chlorhexidine as a bactericide. Polymer 2008; 49(5):1266–75.*

101. *Sun X, et al., (2010) Electrospun composite nanofiber fabrics containing uniformly dispersed antimicrobial agents as an innovative type of polymeric materials with superior antimicrobial efficacy. ACS Appl Mater Interfaces 2010; 2(4): 952–6.*

102. *Miyamoto T, et al., (1989) Tissue biocompatibility of cellulose and its derivatives. J Biomed Mater Res 1989;23:125–33.*

103. *Pajulo O, et al., (1996) cellulose sponge as an implantable matrix: changes in the structure increase the production of granulation tissue. J Biomed Mater Res 1996;32:439–46.*

104. *Bartouilh de Taillac L, et al., (2004) Grafting of RGD peptides to cellulose to enhance human osteoprogenitor cells adhesion and proliferation. Compos Sci*

Technol 2004;64:827–37.

105. *Rodríguez K, et al., (2011) Biomimetic calcium phosphate crystal mineralization on electrospun cellulose-based scaffolds. ACS Appl Mater Interfaces 2011;3:681–9.*

106. *Rubenstein DA, et al., (2010) In vitro biocompatibility of sheath–core cellulose-acetate-based electrospun scaffolds towards endothelial cells and platelets. J Biomater Sci Polym Ed 2010;21(13):1713–36.*

107. *Dragulescu-Andrasi A, et al., Electrospun polysaccharide fiber meshes supporting the chondrogenic differentiation of human bone marrow stromal cells. Abstracts of Papers, 236th ACS National Meeting; 2008. p. CARB-048. [Philadelphia, PA, United States, August 17–21].*

108. *Gouma PI, et al., (2010) Novel bioceramics for bone implants. Cer Eng Sci Proc 2010;30(6):35–44.*

109. *Huang C, et al., (2011) Electrospinning of nanofibres with parallel line surface texture for improvement of nerve cell growth. Soft Matter 2011b;7:10812-7.*

110. *Cakmakci E, et al., (2011) Cell growth on in situ photo-cross-linked electrospun acrylated cellulose acetate butyrate. J Biomater Sci Polym Ed 2011;23(7):887–99.*

111. *Wang X, et al., (2004) Electrostatic assembly of conjugated polymer thin layers on electrospun nanofibrous membranes for biosensors. Nano Lett 2004;4:331–4.*

112. *Son WK, et al., Antimicrobial cellulose acetate nanofibers containing silver nanoparticles. Carbohydr Polym 2006;65:430–4.*

113. *Anitha S, et al., Optical, bactericidal and water repellent properties of electrospun nano-composite membranes of cellulose acetate and ZnO. Carbohydr Polym 2012;87:1065–72.*

114. *Zhang L, et al., (2008) Fabrication and bioseparation studies of adsorptive membranes/felts made from electrospun cellulose acetate nanofibers. J Membr Sci 2008;319(1+2):176–84.*

115. *Tian Y, et al., Electrospun membrane of cellulose acetate for heavy metal ion adsorption in water treatment. Carbohyd Polym 2011;83:743–8.*

116. *Zhou W, et al., Preparation of electrospun silk fibroin/cellulose acetate blend nanofibers and their applications to heavy metal ions adsorption. Fiber Polym 2011a;12(4):431–7.*

117. *Richard Myers, The Basics of Chemistry, Greenwood Publishing Group, 2003, ISBN 0313316643, 9780313316647*

118. *Alexander Apelblat, Properties of Citric Acid and Its Solutions, Springer International Publishing, 05 Dec 2014, pp 13-141, ISBN 978-3-319-11233-6*

119. *Manas R. Swain , et al., Citric Acid: Microbial Production and Applications in Food and Pharmaceutical Industries, Citric Acid: Synthesis, Properties and Applications, Edition: 1, Chapter: 4, Publisher: Nova Science Publisher pp.97-118, ISBN: 978-1-62100-353-3*

120. *Freese, E., et al. (1973) Function of lipophilic, acids as antimicrobial food additives. Nature 241, 321–325.*

121. *Salmond, C.V., et al., (1984) The effect of food preservatives on pH homeostasis in Escherichia coli. J. Gen. Microbiol. 130, 2845–2850*

122. *Eklund, T., (1985). The effect of sorbic acid and esters of para - hydroxybenzoic acid on the proton motive force in Escherichia coli membrane vesicles. J. Gen. Microbiol. 131, 73–76.*

123. *Krebs, H.A., et al., (1983) Studies on the mechanism of the antifungal action of benzoate. Biochem. J. 214, 657–663.*

124. *S. Brul , P. Coote, (1999), Review; Preservative agents in foods Mode of action and microbial resistance mechanisms, International Journal of Food Microbiology 50 (1999) 1–17*

125. *Conner, D. E., et al., (1990) Growth, inhibition and survival of Listeria monocytogenes as affected by acidic conditions. J. Food Prot. 53:652-655*

126. *Brackett, R. E. 1987. Effects of various acids on growth and survival of Yersinia enterocolitica. J. Food Protect. 50:598–601*

127. *Phillips CA, (1999) The effect of citric acid, lactic acid, sodium citrate and sodium lactate, alone and in combination with nisin, on the growth of Arcobacter butzleri, Lett Appl Microbiol. 1999 Dec;29(6):424-8*

128. *Reiss J (1975) Prevention of the formation of mycotoxins in whole wheat bread by citric acid and lactic acid. (Mycotoxins in foodstuffs, Experientia. 1976 Feb 15;32(2):168-9*

129. *Minor, T.E. and Marth, E.H. 1970. Growth of Staphylococcus aureus in acidified pasteurized milk. J. Milk FoodTechnol. 33:516-520 136.*

130. *Fischer, J.R., et al., (1985). Microbiological properties of hard-cooked eggs in a citric acid-based preservation solution. J. Food Prot. 4:252*

131. *H. Shokri, 2011, Evaluation of Inhibitory Effects of Citric and Tartaric Acids and Their Combination on the Growth of Trichophyton mentagrophytes, Aspergillus fumigatus, Candida albicans and Malassezia furfur, World Journal of Zoology 6 (1): 12-15, 2011*

132. *E. SKRIVANOVA, et al., (2006), Susceptibility of Escherichia coli, Salmonella sp. and Clostridium perfringens to organic acids and monolaurin, Veterinarni Medicina, 51, 2006 (3): 81–88*

133. *Zhihong Gao, et al., (2012) Evaluation of different kinds of organic acids and their antibacterial activity in Japanese Apricot fruits, African Journal of Agricultural Research Vol. 7(35), pp. 4911-4918, 11 September, 2012.*

134. *Nagoba BS, et al., (2008) Microbiological, histopathological and clinical changes in chronic wounds after citric acid treatment. J Med Microbiol 2008;57:681–2.*

135. *Magill SS, Edwards JR, Bamberg W, et al. Multistate Point-Prevalence Survey of Health Care–Associated Infections. N Engl J Med 2014;370:1198-208*

136. *Nagoba B, et al., (2011), Citric acid treatment of surgical site infections: a prospective open study, Wound Practice and Research, Volume 19 Number 2 – June 2011*

137. *World Health Organization. Global Health Estimates: Deaths by Cause, Age, Sex and Country, 2000-2012. Geneva, WHO, 2014.*

138. Nalini Singh, et al. , (2005) Preventing Foot Ulcers in Patients With Diabetes AMA. 2005;293(2):217-228. doi:10.1001/jama.293.2.217.

139. B.S. Nagoba, et al., (2008) , A simple and effective approach for the treatment

139 of chronic wound infections caused by multiple antibiotic resistant Escherichia coli, Journal of Hospital Infection (2008) 69, 177-180

140. Basavraj S Nagoba, et al., (2011), Citric acid treatment of postoperative wound in an operated case of synovial sarcoma of the knee, Int Wound J 2011; 8:425–427

141. Basavraj Nagoba, et al.,(2014) Citric acid treatment of post operative wound infections in HIV/AIDS patients, Journal of Tissue Viability (2014) 23, 24-28

142. Han LK, et al., (1999) Reduction in fat storage during chitin chitosan treatment in mice fed a high fat diet. Int J Obes Relat Metab Disord. 1999;23: 174-9

143. Entsar I. Rabea, (2003) Review; Chitosan as Antimicrobial Agent: Applications and Mode of ActionBiomacromolecules. 2003 Nov-Dec;4(6):1457-65.

144. Xiao Fei Liu, et al., (2001), Antibacterial action of chitosan and carboxymethylated chitosan, Journal of Applied Polymer Science Volume 79, Issue 7, pages 1324–1335, 14 February 2001

145. Feng ZQ, Chu X, Huang NP, Wang T, Wang Y, Shi X, et al. The effect of nanofibrous galactosylated chitosan scaffolds on the formation of rat primary hepatocyte aggregates and the maintenance of liver function. Biomaterials 2009;30:2753–63.

146. Chen RN, et al.,(2006) Development of N, O-carboxymethyl chitosan/collagen matrixes as a wound dressing. Biomacromolecules 2006; 7: 1058–64.

147. Prabaharan M, Mano JF. Chitosan-based particles as controlled drug delivery systems. Drug Deliv 2005;12:41–57.

148. Huang XJ, et al., (2007) Preparation and characterization of stable chitosan nanofibrous membrane for lipase immobilization. Eur Polym J 2007;43:3710–8.

149. Desai K, et al., (2009) Nanofibrous chitosan nonwovens for filteration applications. Polymer 2009;50:3661–9.

150. Tashiro T. (2001) Antibacterial and bacterium adsorbing macromolecules. Macromol Mater Eng 2001;286:63–87.

151. Ignatova M, et al., (2007) Novel antibacterial fibers of quaternized chitosan and poly(vinyl pyrrolidine) prepared by electrospinning. Eur Polym J 2007;43: 1112–22.

152. Zhou YS, et al., (2008) Electrospun water-soluble carboxyethyl chitosan/poly(vinyl alcohol) nanofibrous membrane as potential wound dressing for skin regeneration. Biomacromolecules 2008;9:349–54.

153. Chen JP, et al., (2008) Electrospun collagen/chitosan nanofibrous membrane as wound dressing. Colloids Surf A Physicochem Eng Asp 2008b;313–314:183–8.

154. L.Y. Kossovich, et al.,(2010) Electrospun chitosan nanofiber materials as burn dressing IFMBE Proc, 31 (2010), pp. 1212–1214

155. *Z.-X. Cai, et al. (2010) Fabrication of chitosan/silk fibroin composite nanofibers for wound-dressing applications Int J Mol Sci, 11 (2010), pp. 3529–3539*

156. *Bischof Vukušić S, et al., (2011) Cotton textiles modified with citric acid as efficient anti-bacterial agent for prevention of nosocomial infections, Croat Med J. 2011 Feb;52(1):68-75.*

157. *F.K. Tavaria, et al., (2012) Chitosan: antimicrobial action upon staphylococci after impregnation onto cotton fabric, Journal of Applied Microbiology 112, 1034–1041.*

158. *Joshi, M., et al, (2008) Characterization techniques for nanotechnology applications in textiles. Indian J Fibre Text Res, 2008. 9: p. 304-317]*

159. *Berthomieu, C. and R. Hienerwadel, Fourier transform infrared (FTIR) spectroscopy. Photosynthesis research, 2009, 101(2-3): p. 157-170].*

160. *Introduction to Fourier Transform Infrared Spectrometry http://www.thermoscientific.com/en/product/nicolet-is-50-ft-ir-spectrometer.html*

161. *Introduction to FTIR Spectroscopy http://www.newport.com/Introduction-to-FTIR-spectroscopy/405840/1033/content.aspx*

162. *199. ASTM E2149-13a, Standard Test Method for Determining the Antimicrobial Activity of Antimicrobial Agents Under Dynamic Contact Conditions, ASTM International, West Conshohocken, PA, 2013 DOI: 10.1520/E2149*

163. *Santi Tungprapa, et al., (2007) Electrospun cellulose acetate fibers: effect of solvent system on morphology and fiber diameter, Cellulose (2007) 14:563–575*

164. *Rodriguez K, et al., (2012) Electrospinning cellulosic nanofibers for biomedical applications: structure and in vitro biocompatibility. Cellulose 2012;19(5):1583–98.*

165. *Ma Z, Kotaki M, Ramakrishna S (2005) Electrospun cellulose nanofiber as affinity membrane. J Membrane Sci 265:115–123*

166. *Jarusuwannapoom T, et al., (2005) Effect of solvents on electro-spinnability of polystyrene solutions and morphological appearance of resulting electrospun polystyrene fibers. Eur Polym J 41:409–421*

167. *Pattamaprom C, et al., (2006) The influence of solvent properties and functionality on the electrospinnability of polystyrene nanofibers. Macromol Mater Eng 291:840–847*

168. *Jaeger R, et al., (1998) Electrospinning of ultra thin polymer fibers. Macromol Symp 127:141–150*

169. *Liu H, Hsieh YL (2002) Ultrafine fibrous cellulose membranes from electrospinning of cellulose acetate. J Polym Sci—Polym Phys 40:2119–2129*

170. *Konwarh R, et al., (2013) Diameter-tuning of electrospun cellulose acetate fibers: a Box–Behnken design (BBD) study. Carbohydr Polym2013;92(2):1100–6.*

171. *Theopisti C, Charalabos D. (2010) Biodegradable cellulose acetate nanofiber fabrication via electrospinning. J Nanosci Nanotechnol 2010;10(9):6226–33.*

172. *De Vrieze S, et al., (2009) The effect of temperature and humidity on electrospinning. J Mater Sci 2009;44(5): 1357–62.*

173. *John Coates, (2000) Interpretation of Infrared Spectra, A Practical Approach, Encyclopedia of Analytical Chemistry pp. 10815–10837*

174. *Donald M. Pace, Alice Elliott (1962) Effects of Acetone and Phenol on Established Cell Lines Cultivated in Vitro Cancer Res 1962;22:107-112.*

175. *Posokhov YO , Kyrychenko A., (2013) Effect of acetone accumulation on structure and dynamics of lipid membranes studied by molecular dynamics simulations. Comput Biol Chem. 2013 Oct; 46:23-31.*